

JIMMA UNIVERSITY

SCHOOL OF GRADUATE STUDIES

JIMMA INSTITUTE OF TECHNOLOGY

FACULTY OF CIVIL AND ENVIRONMENTAL ENGINEERING

STRUCTURAL ENGINEERING STREAM

Performance Analysis of Steel-Concrete Composite Columns using non-linear analysis.

A Thesis Submitted to School of Graduate Studies of Jimma University in Partial Fulfillment of the Requirements for the Degree of Masters of Science in Structural Engineering.

By Regasa Yadeta Sembeta

July 16, 2021

JIMMA, ETHIOPIA

JIMMA UNIVERSITY
SCHOOL OF GRADUATE STUDIES
JIMMA INSTITUTE OF TECHNOLOGY
FACULTY OF CIVIL AND ENVIROMENTAL ENGINEERING
STRUCTURAL ENGINEERING STREAM

Performance Analysis of Steel-Concrete Composite Columns using non-linear analysis.

A Thesis Submitted to School of Graduate Studies of Jimma University in Partial Fulfillment of the Requirements for the Degree of Masters of Science in Structural Engineering.

By Regasa Yadeta Sembeta

Main Adviser:-Engr. Elmer C. Agon (Asso.Prof.)

Co-Adviser:-Engr.Kefiyalew Zerfu (Asst.Prof.)

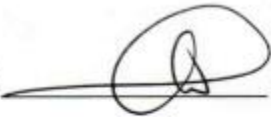

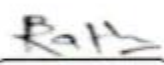

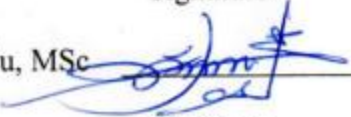
July 16, 2021

JIMMA, ETHIOPIA

JIMMA UNIVERSITY
SCHOOL OF GRADUATE STUDIES
JIMMA INSTITUTE OF TECHNOLOGY
FACULTY OF CIVIL AND ENVIRONMENTAL ENGINEERING
STRUCTURAL ENGINEERING STREAM

As a member of the examining board of the final MSc open defense, we certify that we have read and evaluated the thesis prepared by *Regasa Yadeta Sembeta* entitled: *Performance Analysis of Steel-Concrete Composite Columns using non-linear analysis* and recommended that it be accepted as fulfilling the thesis requirement for the degree of Master of Science in Structural Engineering.

APPROVED BY BOARD OF EXAMINERS

1. Engr. Elmer C. Agon, Asso. Prof.		<u>16 / 07 / 2021</u>
Main advisor	Signature	Date
2. Engr. Kefiyalew Zerfu, Asst. Prof.		<u>16 / 07 / 2021</u>
Co-advisor	Signature	Date
3. Dr. Badrinarayan Ratha, PhD		<u>16 / 07 / 2021</u>
External Examiner	Signature	Date
4. Engr. V. S. Ravi Kumar, MSc		<u>16 / 07 / 2021</u>
Internal Examiner	Signature	Date
5. Engr. Besukal Befekadu, MSc		<u>16 / 07 / 2021</u>
Chairperson	Signature	Date

DECLARATION

I declare that this Thesis entitled “***Performance Analysis of Steel-Concrete Composite Columns using non-linear analysis.***” is my original work and has not been submitted as a requirement for the award of any degree in Jimma University or in any other university. Where ever contribution of others is involved, every effort is made to indicate this clearly, with due reference to the pieces of literature.

Regasa Yadeta Sembeta

Candidate

Signature

Date

As research Adviser, I hereby certify that I have read and evaluated this thesis paper prepared under my guidance, by Regasa Yadeta Sembeta entitled “***Performance Analysis of Steel-Concrete Composite Columns using non-linear analysis.***” and recommend and would be accepted as a fulfilling requirement for the Degree Master of Science in Structural Engineering.

Engr. Elmer C. Agon, (Asso. Prof.)

Advisor

Signature

Date

Engr.Kefiyalew Zerfu (Asst.Prof.)

Co-Advisor

Signature

Date

ABSTRACT

Steel-concrete composite construction has gained wide acceptance worldwide as an alternative than pure steel and pure concrete construction because composite column has both compression and tension resistance. However, this system is a relatively new concept for the construction industry in Ethiopia.

*This study presents the performance of fully encased composite column subjected to axial load and at the same time increase the accuracy of results. The ES EN 2015 code and Eurocode 4 mainly are used codes in this paper. The Performance of steel concrete composite columns presented using tables, graphs and charts from finite element analysis by using ABAQUS software. In order to achieve the goal of the study, a parametric investigation procedure is undertaken, on a series of eighteen (18) samples column with different study parameters. An Independent Variables used are Compressive strength of concretes, Length of column, and Diameter of rebar. A parametric study was conducted using the numerical model to investigate the influences of geometric properties of fully encased composite (FEC) columns. The material quality used for composite columns are C25, C30, C35 and C50 grades, The structural steel encased in concrete adopts the standard British steel section UC152 * 152 * 30, Longitudinal reinforcement bars with diameters(12mm,13mm,14mm and 16mm) and for transverse reinforcement bar(10mm) were used. The nonlinear combined hardening and the concrete damage plasticity (CDP) model were used to define properties of steel and concrete respectively. In the Finite Element Analysis (FEA) C3D8R was used for solid elements and T3D2 was used for reinforcements. The load capacity of the composite columns increased by 6.38% and 5.93% with increasing concrete strengths from C25 to C30 and C35 decreased from 3.50% to 10.20% with increasing column lengths from 600mm to 800mm and 1000mm. The same area effects of longitudinal bars and the confinement effects with different diameter and spacing of transverse longitudinal bars are introduced. As the diameter of longitudinal reinforcement of Composite Column increased from 12mm to 14mm and 16mm the load carrying capacity of composite column is increased from 4.14% to 4.77% respectively.*

Key Words: - *Finite Element, Fully concrete-encased steel section, Axial load Capacity, Concrete strength, Length of column, Diameter of longitudinal reinforcement bar.*

ACKNOWLEDGEMENT

First of all, my heartfelt thanks are extended to Almighty God Allah for his unending helping and Blessings for every success in my life and satisfactory accomplishment of this Thesis. Next, I would to express my deepest gratitude to my main advisor, **Engr.Elmer C. Agon (Asso.Prof)** and my co-advisor **Engr.Kefiyalew Zerfu (Asst.Prof.)** for their continuous support, guidance and encouragement over the past years of my master candidate and thesis performing.

My special heartfelt gratitude goes to my family and friends, for their love, support, and encouragement throughout this research and during the many years of study that preceded it. I also would like to express my thanks to my friend Lelistu Negesa for her technical and practical supports throughout my work.

Also, my deepest gratitude goes to the Ministry of Education (MoE) and Jimma University (JU) to create this beautiful environment for me and have got the chance of this lovely education.

Finally, my special thanks go to Jimma Institute of Technology (JIT) particularly the Structural Engineering Department for facilitating this program which helps me to upgrade my knowledge and profession.

Table of Contents

ABSTRACT	I
ACKNOWLEDGEMENT	II
LIST OF TABLES	V
LIST OF FIGURES	VI
ACCRONYM	VIII
CHAPTER ONE	1
1. INTRODUCTION	1
1.1 Background of the Study	1
1.2 Statement of the Problem	2
1.3 Research Question	3
1.4 Objectives of the Study.....	3
1.5 Significance of the Study.....	4
1.6 Scope of the Study.....	5
CHAPTER TWO	6
2. REVIEW OF RELATED LITERATURE	6
2.1. Background.....	6
2.2. Analysis of Composite Columns According to the Eurocode 4.....	9
2.3. The Simplified Method.....	10
2.4 Analytical and Experimental Investigation of Concrete Encased Composite Columns .	24
CHAPTER THREE	35
3. RESEARCH METHODOLOGY	35
3.1 .General.....	35
3.2 Research Methodology	35
3.3 Study Variables.....	36
3.4 Population and Sampling Method	36
3.5 Sources of Data.....	38
3.6 Data Collection Procedure.....	38
3.7 Model samples and cross sections used in this study Program	38
3.8 Finite element method	39

3.9	Data Presentation and Analysis	40
3.10	Finite Element Modeling of encased composite column.....	41
3.11	Meshing	46
3.12	Interactions and Kinematic Constraints between Components	47
3.13	Boundary Conditions and Loading.....	49
3.14	Material Modeling	50
3.15	Compression properties of concrete	50
3.16	Structural Steel and Reinforcement material modeling.....	57
3.17	PARAMATRIC STUDY	60
CHAPTER FOUR.....		62
RESULTS AND DISCUSSIONS		62
4.1	.General.....	62
4.2	.VALIDATION OF FINITE ELEMENT MODELLING	62
4.3	FEA result for validation	64
4.4	.Results from Analysis.....	66
CHAPTER FIVE		83
CONCLUSIONS AND RECOMMENDATIONS		83
5.1	Conclusions	83
5.2.	Recommendations	84
REFERENCES		85
APPENDICES		88
A.	MATERIAL INPUT DATA SHEET FOR ANALYSIS OF CONTROL AS A SAMPLE. 88	
B.	MODEL OF COLUMN UNDER STUDY	94
C.	OUT PUT OF ANALYSIS	97
D.	ANALIYSIS OUT PUT FROM ABAQUS PROGRAM (SAMPLE).....	99

LIST OF TABLES

Table 2. 1 Imperfection factor (EBCS-EN 1994-1-1: 2013) 13

Table 2. 2 Maximum values of (d/t, h/t and d/t) with f_y in N/mm^2 (EN 1994-1-1, 2015)..... 16

Table 2. 3: Factors β for the determination of moments to second order theory (EN 1994-1-1, 2015) 18

Table 2. 4 :Buckling curves and member imperfections for composite columns (EN 1994-1-1, 2015) 19

Table 3. 1 Sample of independent variables data 37

Table 3. 2 Samples of constant parameters..... 38

Table 3. 3: Various Elements Used in ABAQUS© (ABAQUS, 2014)..... 45

Table 3. 4: Default parameters of CDP model under compound stress..... 57

Table 3. 5: Mechanical properties of the steel sections and Reinforcement Bars used for this study(Lai, Liew and Xiong, 2019)..... 59

Table 3.6 Independent parameters sample data for column analysis..... 61

Table 3. 7:Constant parameters from journal(Lai, Liew and Xiong, 2019) 61

Table 4. 1:-Load -Displacement of concrete strength (C25, C30, C35)..... 71

Table 4. 2: Load Vs. Displacements of Lengths of column..... 73

Table 4. 3: Load verses Displacements of Diameters of longitudinal reinforcement bars 76

Table 4.4.Euivalent area effects of longitudinal bars 79

Table 4.5.Confinement effects of transverse reinforcement bars 82

Table A 1: Compressive behaviors..... 89

Table A 2: Tensile behaviors 90

Table A 3: ABAQUS Compression input..... 91

Table A 4: ABAQUS Tension input..... 91

LIST OF FIGURES

Figure 2. 1 Typical cross sections of composite columns (EN 1994-1-1:2004).....	7
Figure 2. 2: European buckling curve for composite columns (EBCS-EN 1994-1-1: 2013).....	13
Figure 2. 3: Simplified interaction curve and corresponding stress distributions.....	20
Figure 2. 4: Design of column length under axial load and biaxial bending (EN 1994-1-1, 2015)	22
Figure 2. 5:Finite element model of concrete encased steel composite column(Ellobody, Young and Lam, 2011)	32
Figure 2. 6 :REC Column ;(a) plan view ;(b) 3D view and (c) Elevation(Kartheek and Das, 2020)	34
Figure 3. 1 Concrete Column part.....	41
Figure 3. 2 Longitudinal Reinforcement Bar	41
Figure 3. 3.Transverse Reinforcement Bar (Stirrup)	42
Figure 3. 4.Support and Loading Steel Plate	42
Figure 3.5: Structural Steel Section	43
Figure 3. 6: Modeling of Encased Composite Column components In ABAQUS©CAE.	44
Figure 3. 8: Tie Constraints between column and both loading and support plate.....	49
Figure 3. 9: End boundary conditions (fixed support) and loading.	49
Figure 3. 10: Stress-Strain relations for non-linear structural analysis (EBCS EN 1992, 2015)..	52
Figure 3. 11: Stress-Strain relationships for confined concrete (EBCS EN 1992, 2015).....	53
Figure 3. 12: Post failure stress-fracture energy curve. (ABAQUS user Manual, 2014)	54
Figure 3. 13: Terms for Tension Stiffening Model (ABAQUS user Manual, 2014).....	56
Figure 3. 14: Response of concrete to a uniaxial loading condition in compression (ABAQUS Manual, 2014).....	57
Figure 3. 15: ABAQUS input stress-strain curves for reinforcements and steels(Lai, Liew and Xiong, 2019)	59
Figure :3.16 a Dimension details of specimen(Lai, Liew and Xiong, 2019).....	60
Figure 4. 1: Dimensions Details of test specimens(Lai, Liew and Xiong, 2019).....	63
Figure 4. 2: Stress-strain curve of concrete, steel section and reinforcement bars (Lai, Liew and Xiong, 2019)	64

Figure 4. 3: Experiment and FEA Model set up 65

Figure 4. 4: FEA of Experimental for FEC Composite column for validation..... 65

Figure 4. 5: FEA Load-displacement curve Vs. Experimental load-displacement curve..... 66

Figure 4.6.Loads from manual calculation, Experimental load and Load from FEA 69

Figure: 4.7Effects of Concrete Strength 70

Figure 4.8 Result comparisons between concrete strengths Vs Ultimate loads 70

Figure: 4.9.Effects of Column Length 72

Figure 4.10. Result comparison between column lengths Vs ultimate loads 73

Figure: 4.11.Effects of diameter of longitudinal bars 75

Figure 4.12 Comparison between longitudinal reinforcement bar Vs. Ultimate load 75

Figure 4.13 the effects between #8Φ12mm and #4Φ24mm. 77

Figure 4.14.The effects between #8Φ13mm and #4Φ26mm..... 78

Figure 4.15.The effects between #8Φ14mm and #4Φ28mm..... 78

Figure 4.16.Confinement effects of transverse reinforcement bars 81

Figure A. 1: Unconfined concrete input stress-strain curve 89

Figure A. 2: Stress-crack opening relation for uniaxial tension. 90

ACCRONYM

CES	Concrete Encased Steel
CFST	Concrete-Filled Steel Tubes
EBCS	Ethiopian Building Code Standard
ES EN	Ethiopian Standard Euro Norm code
ETB	Ethiopian Birr
FEA	Finite element analysis
FEM	Finite element model
JIT	Jimma Institute of Technology
JU	Jimma University
MoE	Ministry of Education
NAP	Position of Neutral axis
PNA	Plastic Neutral Axis
ULS	Ultimate limit state

LIST OF SYMBOLS

➤ Latin upper case letters

A_a	Cross-sectional area of the structural steel section
A_c	Cross-sectional area of concrete in the compression zone
A_s	Cross-sectional area of reinforcement bars
A_v	Shear area of a structural steel section
C_y	Thickness of concrete cover to the structural steel in the y-direction
C_z	Thickness of concrete cover to the structural steel in the z-direction
E_a	Modulus of elasticity of structural steel
E_{cm}	Secant modulus of elasticity of concrete
$E_{c, eff}$	Effective modulus of elasticity for concrete
E_s	Modulus of elasticity of reinforcing steel
$(EI)_{eff}$	Effective flexural stiffness for calculation of relative slenderness
I_a	Second moment of area of the structural steel section
I_c	Second moment of area of the un-cracked concrete section
I_s	Second moment of area of the reinforcement
K_e	Correction factor to account for a reduced stiffness of concrete due to Cracking
L	Buckling length of the column
M_{Ed}	Design bending moment
$M_{max,Rd}$	Maximum design value of the resistance moment in the compressive normal force
$M_{p,a,Rd}$	Design value of the plastic resistance moment of the structural steel section

$M_{pl,N,Rd}$	Design value of the plastic resistance moment of the composite section taking into account the compressive normal force
$M_{pl,Rd}$	Design value of the plastic resistance moment of the composite section with full shear connection
$M_{pl,y,Rd}$	Design value of the plastic resistance moment about the y-y axis of the composite section with full shear connection
$M_{pl,z,Rd}$	Design value of the plastic resistance moment about the z-z axis of the composite section with full shear connection
M_y	Resultant moment resisted by the section for bending about the y-y axis
M_{ya}	Resultant moment resisted by the structural steel for bending about the y-y axis
M_{yc}	Resultant moment resisted by the concrete for bending about the y-y axis
M_{ys}	Resultant moment resisted by the reinforcement for bending about they-y axis
M_z	Resultant moment resisted by the section for bending about the z-z axis
M_{za}	Resultant moment resisted by the structural steel for bending about the z-z axis
M_{zc}	Resultant moment resisted by the concrete for bending about the z-z axis
M_{zs}	Resultant moment resisted by the reinforcement for bending about the z-z axis
N_a	Resultant axial force carried by the structural steel
N_c	Resultant axial force carried by the concrete
N_{cr}	Elastic critical normal force
$N_{cr,eff}$	Critical normal force for the relevant axis and corresponding to the effective flexural stiffness with the effective length taken as the column length
N_{Ed}	Design value of the applied axial force

$N_{G,Ed}$	Design value of the part of the compressive normal force that is permanent
$N_{pl,Rd}$	Design value of the plastic resistance of the composite section to compressive normal force
$N_{pl,Rk}$	Characteristic value of the plastic resistance of the composite section to compressive normal force
$N_{pm,Rd}$	Design value of the resistance of the concrete to compressive normal force
N_s	Resultant axial force carried by the reinforcements
R_a	Stress resultants of structural steel
R_c	Stress resultants of concrete
$V_{a,Ed}$	Design value of the shear force acting on the structural steel section
$V_{c,Ed}$	Design value of the shear force acting on the reinforced concrete web Encasement
V_{Ed}	Design value of the shear force acting on the composite section
$V_{pl,a,Rd}$	Design value of the plastic resistance of the structural steel section to vertical shear
W_{pa}	Plastic modulus of steel section
W_{pc}	Plastic modulus of concrete in compression zone
W_{ps}	Plastic modulus of reinforcement steel
Z_{max}	Maximum distance from the geometrical center to the outer most fiber of a cross-section

➤ Latin lower case letters

b	Width of the flange of a steel section
c	Neutral axis depth from top most fiber of the cross-section
d	Overall diameter of circular hollow steel section
f_{cd}	Design value of the cylinder compressive strength of concrete
e_y	Concrete cover to the reinforcement in the y-direction
e_z	Concrete cover to the reinforcement in the z-direction
f_{ck}	Characteristic value of the cylinder compressive strength of concrete at 28 days
f_{sd}	Design value for the yield strength of reinforcement
f_{sk}	Characteristic value of the yield strength of reinforcing steel
f_y	Nominal value of the yield strength of structural steel
f_{yd}	Design value for the yield strength of structural steel
h	Depth of the structural steel section
h_n	Depth of the plastic neutral axis from the geometrical center
k	Amplification factor for second-order effects
n	Exponent in stress-strain relation for concrete
r	Ratio of the smaller to the larger end moments; radius of fillet between the flange and web of structural steel section; nonnegative integer
s	nonnegative integer
t	Thickness of circular hollow steel section
t_f	Thickness of a flange of the structural steel section

t_w	Thickness of the web of the structural steel section
w_i	Gauss weights
X_i	Gauss points
Y	Distance from the geometrical center of a cross-section; lever arm
z	Distance from the geometrical center of a cross-section; lever arm

Greek lower case letters

α_{cr}	Factor by which the design loading would have to be increased to cause elastic instability
α_M	Coefficient related to bending of a composite column
β	Equivalent moment factor
γ_a	Partial factor for structural steel
γ_c	Partial factor for concrete
γ_s	Partial factor for reinforcing steel
δ	Structural steel contribution ratio
ϵ_a	Strain in the structural steel
ϵ_c	Compressive strain in the concrete
ϵ_{c2}	Compressive strain in the concrete at reaching the maximum strength
ϵ_{cu2}	Ultimate compressive strain in the concrete
ϵ_s	Strain in the reinforcing steel
ϵ_{sd}	Design yield strain in the reinforcing steel
ϵ_{yd}	Design yield strain in the structural steel

ϵ_{ud}	Ultimate design tensile strain in steel
λ	Relative slenderness
μ	Related moment factor
μ_d	Moment factor related to design for compression and uniaxial bending
μ_{dy}	Factor μ_d for bending about the y-y axis
μ_{dz}	Factor μ_d for bending about the z-z axis
P	Parameter related to reduced design bending resistance accounting for vertical shear
σ_a	Stress in the structural steel
σ_c	Compressive stress in the concrete
σ_s	Stress in the reinforcement
ϕ	Value to determine the reduction factor χ
Φ_t	Creep coefficient
χ	Reduction factor for flexural buckling
ψ	Distance from the neutral axis

CHAPTER ONE

1. INTRODUCTION

1.1 Background of the Study

Steel-concrete composite construction has gained wide acceptance worldwide as an alternative to pure steel and pure concrete construction. Nowadays, steel-concrete composite construction is used to meet the performance and functional requirements of structures.

In recent years, Concrete Encased Steel (CES) Composite columns gains increasing popularity in top-down or basement construction due to its superior structural performance Compared with conventional bare steel columns and reinforced concrete (RC) columns.(Lai, Liew and Xiong, 2019).Composite structures acquire the structural and constructional advantages of both concrete and steel. Concrete has low material costs, good fire resistance, and easy to place. Steel has high ductility, high strength-to-weight, and stiffness-to-weight ratios (Hanswille, 2008). When properly combined, composite construction can yield saving in initial and life-cycle costs. (Kim, 2005)

A steel-concrete composite column is a compression member, comprising either a concrete-encased steel section or a concrete-filled tubular steel section and is generally used as a load-bearing member in a composite framed structure. In a composite column, both the steel and concrete resist the external loading by interacting together through bond and friction. Supplementary reinforcement in the concrete encasement prevents excessive spalling of the concrete both under normal load and fire conditions. The most usual types of composite columns are the concrete filled steel tubes and the partially or fully encased steel profiles. Fully encased composite column (FEC) provides compressive strength, stability, stiffness, improved fire proofing and better corrosion protection.(Rahman, Begum and Ahsan, 2016)

The resistance of a composite column to combined compression and bending is determined using an interaction curve of its cross-section. In a typical interaction curve of a column with a steel section, only the moment resistance undergoes a continuous reduction with an increase in the axial load. However, a short composite column will often exhibit an increase in the moment resistance beyond plastic moment under relatively lower values of axial load. This is because the

compressive axial load prevents concrete cracking and makes the composite cross-section of a short column more effective in the resisting moment.

Several studies have been conducted to investigate the strength of composite column under axial compression, axial compression and bending, axial tension, pure bending, as well as combined compression and bending, which contribute to tell the performance of those columns separately (An and Roeder, 2014). Extensive studies have been conducted to analyze the behavior of concrete filled steel tub under cyclic (Han et al., 2009). Limited studies were found on the performance of CES columns with various structural steel profile, slenderness ratios, and spacing of transverse reinforcement subjected to axial and cyclic loading conditions.

The ES EN code and Eurocode 4 are widely used codes has incorporated simplified methods for analysis of composite columns *using ABAQUS software*. The purpose of this study was to implement and verify the performance of encased composite rectangular fully encased composite column with different concrete compressive strength, lengths and diameters of rebar under an action of axial load by using Finite Element method. The simulation result was used to choose concrete compressive strength which has good performance and lengths of column which undergo good performance for the stated loading condition and additionally used as reference for simulation and practice work in the future.

1.2 Statement of the Problem

The design of composite columns needs accurate knowledge as per codes on behavior of steel and concrete material properties and specifications. Although high-rise construction is being introduced in Ethiopia, the topic of composite structures is often given only a limited consideration up to now. However, they can provide optimal solution in medium to high-rise buildings or large span structures. Several studies have been conducted to investigate the strength of composite column under axial Compression, axial compression and bending, axial tension, pure bending, as well as combined Compression and bending, which contribute to tell the performance of those columns separately (An and Roeder, 2014). Extensive studies have been conducted to analyze the behavior of concrete filled steel tub under cyclic (Han et al., 2009). Limited studies were found on the performance of FEC columns with various structural

concrete compressive strength, lengths and diameter of longitudinal bar subjected to axial loading conditions.

This study aims to perform extensive numerical investigations on CES columns under concentric axial load. Therefore, it is necessary to establish a systematic research by finite element program to examine the structural performance/response of concrete encased steel composite columns subjected to axial loading. By considering this loading condition performance of the column was examined and generates information on the effects of controlling parameters through parametric study using a validated numerical model which can adequately predict the performance/response of encased composite columns.

1.3 Research Question

- ✓ What is the Performance of steel-concrete composite columns of different compressive strength of concrete?
- ✓ What are the effects of different column lengths on the performance analysis of composite columns?
- ✓ What are the effects of different diameter of longitudinal reinforcement bar on analysis the performance of composite columns using ABAQUS software?
- ✓ What are the effects of the same area of longitudinal bars and Confinement effects by the transverse reinforcement bars with different diameter and spacing?

1.4 Objectives of the Study

General objective

The general objective of this study was to assess the Performance of Steel-Concrete Composite Columns using non-linear analysis by ABAQUS/CAE.

Specific objective

- ✓ To assess the Axial Performance of steel-concrete composite columns different compressive strength of concrete.
- ✓ To evaluate the effects of different column lengths on analysis composite columns.
- ✓ To evaluate the effects of different diameter of longitudinal bar on analysis the performance of composite columns using ABAQUS software as per ES EN 2015 Code.

- ✓ To determine the effects of the same area of longitudinal bars and Confinement effects by the transverse reinforcement bars with different diameter and spacing.

1.5 Significance of the Study

The result of this study is used to provide data and information that helps for stake holders in construction industry such as designer, architects, contractors and students to know performance analysis of steel-concrete composite columns as per ES EN code easily for building structure on the capacity of building. Composite column is among the composite structure widely used now a day. These essentially different materials are completely compatible and complementary to each other; they have an ideal combination of strengths with the concrete efficient in compression and the steel in tension. For encased composite column concrete gives corrosion protection and thermal insulation to the steel at elevated temperatures or have good fire resistance and additionally can restrain slender steel sections from local or lateral torsional buckling. Currently different steel profile sections are used as encasement in the design of composite column to get column which have good performance under desired loading condition. This investigation can help the structural designer's community to choose easily the appropriate compressive strength of concrete, length of column and diameter of longitudinal bar for good performance. It can contribute significant input for other researchers for further study. Therefore, this research will help any design companies and /or any researchers to have better understand and estimate of the performance of encased rectangular composite column Sections subjected to axial load and bending in particular for "I" structural steel sections and normal strength concrete With different compressive strengths. This research is believed to aware the students and Ethiopian construction industry by providing an analysis and design of composite columns to know the performances of its which they may miss understand like with/without reinforcement, uniaxial /biaxial, encased/filled and structural advantage of composite column. In addition to the above, this study has a significant value to select appropriate composite columns for the specific location of structures because fully encased composite column has high fire and corrosion resistances. Finally, it helps to minimize the gap for other researchers.

1.6 Scope of the Study

The study covers Performance analysis of fully encased rectangular composite columns and extended to demonstrate the influence of different compressive strength of concrete, length of column and diameter of longitudinal bar on the column performance. This thesis was focusing on FEA program ABAQUS©CAE of square concrete fully encased steel column under axial loading. The proposed procedure to study the performance of axial load and bending moment of different parameters in geometry of the same cross section of composite column is limited to finite element analysis by Abacus/CAE. Furthermore, this study is also limited to the following as per ES EN 2015 code, only normal strength concrete i.e., from C20/25 to C50/60 were considered([EN 1994-1-1, 2015](#)).

CHAPTER TWO

2. REVIEW OF RELATED LITERATURE

2.1. Background

The necessities for large span and high-rise construction with reasonable construction time and cost have made composite structures of steel and concrete construction popular. Among the composite members is a composite column. Until the 1950s, structural steel sections were encased in light weight concrete for fire protection. The steel columns were analyzed and designed as if uncased. It was not until later on that was learned the encasement reduces the buckling length of the steel column and hence the buckling load increases. As a result, empirical methods were developed for calculating the reduced slenderness. This simple approach was not reasonable enough as the encasement also carries its share of axial load and bending moments. After many tests that have been carried out, current practices include the contribution of concrete and reinforcement bars to resistance. In the case of encased sections, the concrete reduces the buckling length of the steel sections and this is also taken into account in (EN 1994-1-1, 2015).

Composite columns are divided into three categories in general (Figure 2.1):

- Concrete encased sections (a)
- Partially concrete-encased sections (b and c)
- Concrete-filled hollow sections (d, e, and f).

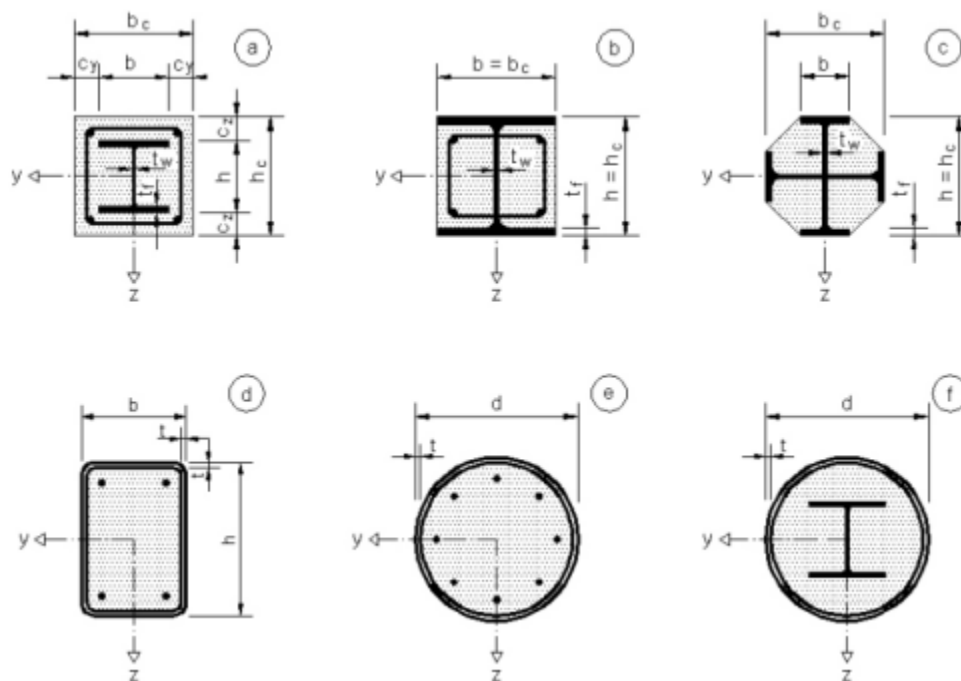


Figure 2. 1 Typical cross sections of composite columns (EN 1994-1-1:2004)

Types of a steel-concrete composite column

- Fully or partially concrete-encased steel section (CES)

They are generally used. The concrete encasement has frequently been taken into consideration as the simplest hearth and corrosion safety for the metal. However, in current years, lateral and now and again longitudinal reinforcement has been brought to the concrete encasement, and the consequent power of the steel and concrete interacting has been used for structural functions. A metallic form, encased in concrete, maybe thought of as reinforcement for the concrete.

The advantage of a concrete encasement is to stiffen the steel section, making it more effective against both local and global buckling. Also, the encasement functions as a fireproofing and corrosion protective from steel sections and reinforcement embedded in concrete. The main disadvantage is that full formwork is required for construction.

- Circular or rectangular/ Square concrete-filled steel tubular section (CFST)

Concrete Filled Steel Tube has been prominent for use as individual section components. The kept solid fill expands the hub load opposition however has little impact on the flexural obstruction. Consequently, it is improbable that these sections would be a decent decision for a minute opposing edge.

In the case of concrete-filled tubes or pipes, the steel section is not protected against fire and corrosion, but no formwork is required. Combinations of concrete-encased and concrete-filled composite columns are common. In concrete-encased composite columns, a reinforcement cage is required to prevent the concrete cover from spalling.

As in other structural components, a composite column must also be designed for the Ultimate Limit State. For structural adequacy, the internal forces and moments resulting from the most unfavorable load combination should not exceed the design resistance of the composite cross-sections. While local buckling of the steel sections may be eliminated, the reduction in the compression resistance of the composite column due to overall buckling should be allowed for, together with the effects of residual stresses and initial imperfections. Moreover, the second-order effects in slender columns as well as the effect of creep and shrinkage of concrete under long-term loading must be considered, if they are significant. The reduction in flexural stiffness due to cracking of the concrete in the tension area should also be considered.

The method of design suggested in this study largely follows EC4, which incorporates the latest research on composite construction. Isolated symmetric columns having uniform cross-sections in braced or non-sway frames may be designed by the Simplified design method described in the next section. This method also adopts the European buckling curves for steel columns as the basis of column design. It is formulated in such a way that only hand calculation is required in practical design. This method cannot be applied to sway columns.

This study will deal with the design of steel-concrete composite columns subjected to both axial load and bending. To design a composite column under combined compression and bending, it is first isolated from the framework, and the end moments that result from the analysis of the system as a whole are taken to act on the column under consideration. Internal moments and

forces within the column length are determined from the structural consideration of end moments, axial and transverse loads. For each axis of symmetry, the buckling resistance to compression is first checked with the relevant non-dimensional slenderness of the composite column. Thereafter the moment resistance of the composite cross-section is checked in the presence of applied moment about each axis, e.g. x-x and y-y axis, with the relevant non-dimensional slenderness values of the composite column.

For the design of a composite column under combined compression and bi-axial bending, the axial resistance of the column in the presence of bending moment for each axis has to be evaluated separately. Thereafter the moment resistance of the composite column is checked in the presence of applied moment about each axis, with the relevant non-dimensional slenderness of the composite column. Imperfections have to be considered only for that axis along which failure is more likely. If it is not evident which plane is more critical, checks should be made for both axes.

Composite columns have the following advantages over reinforced concrete columns and steel columns:

- High load capacity with small cross-section and economical material use
- Increased stiffness, leading to reduced slenderness and increased buckling resistance
- Possibility of plastic deformation and enhanced ductile behavior
- High resistance to compressive stresses
- Reduced risk of local buckling of the steel section
- Good fire resistance for the case of encased columns
- Erection of high rise building in an efficient manner.

2.2. Analysis of Composite Columns According to the Eurocode 4

The (Eurocode 4), (EN 1994-1-1, 2015) provision for design of composite columns is limited to:

- ✓ Composite columns that is part of steel frame or composite frame;
- ✓ Design of composite columns with cross-sections as shown in [Figure 2.1](#);
- ✓ Limited material strength class of steel grades S235 to S460 and normal weight concrete of strength class C20/25 to C50/60;
- ✓ Limited structural steel contribution ratio, δ :

$$0.2 \leq \delta \leq 0.9$$

$$\delta = \frac{A_a f_{yd}}{N_{pl,Rd}} \quad (2.1)$$

Where:-

A_a - is the cross-sectional area of the structural steel section

f_{yd} - is the design value for the yield strength of structural steel

$N_{pl,Rd}$ -is design value of the plastic resistance of the composite section to compressive normal force

If δ is less than 0.2, the column should be treated as reinforced concrete and

If δ is greater than 0.9 the column should be treated as steel column.

(EN 1994-1-1, 2015) provides two methods of design of composite columns. These are “a general method” and “a simplified method”. The general method can be applied for all types of composite columns including columns of non-symmetrical or non-uniform cross-sections over the column length. The simplified method is applicable for columns of doubly symmetric and uniform cross section over the member length.

Both methods of design assumed full interaction among the concrete, reinforcement steel and structural steel and hence plane sections remain plane while the column deforms up to failure.

2.3. The Simplified Method

2.3.1. Scope

To use the simplified procedure of (EN 1994-1-1, 2015), the composite member has to meet the following requirements:

- ✓ The member has to be doubly symmetrical and uniform cross section along the length.
- ✓ The relative slenderness $\bar{\lambda}$ of the column should be less than 2.0.
- ✓ If the longitudinal reinforcement is considered in design, then it should not exceed 6% of the concrete area.

A minimum reinforcement ratio of 0.3% is required to be considered in the contribution of resistance of concrete encased sections.

- ✓ For a fully encased steel section (Figure 2.1), limits to the maximum thickness of concrete cover that may be used in calculation are:

$$C_z \leq 0.3h \text{ and } C_y \leq 0.4b$$

Furthermore, to maintain the safe transmission of bond forces, for the protection of steel against corrosion and to prevent spalling of concrete, a minimum cover to the structural steel is required. According to (EN 1994-1-1, 2015), this cover should be the maximum of 40mm or one-sixth of the flange width of the structural steel section.

- ✓ The ratio of depth (h_c) to width (b_c) of the cross-section (Figure 2.1), should be within the limits $0.2 \leq h_c / b_c \leq 5.0$.

2.3.2. Resistance of Cross-sections and Members in Axial Compression

The plastic resistance of encased cross-sections subjected to axial load $N_{pl,Rd}$ is given by equation 2.4. This equation superposes the contribution of the structural steel, the concrete and the reinforcement.

$$N_{pl,Rd} = A_a f_{yd} + 0.85 A_c f_{cd} + A_s f_{sd} \quad (2.2)$$

Where:

A_c is the cross-sectional area of concrete in the compression zone

A_s is the cross-sectional area of reinforcement bars

f_{cd} is design value of the cylinder compressive strength of concrete

f_{sd} is design value of the yield strength of reinforcing steel

A short ideal compression member, which is perfectly straight and loaded centrally, can carry as much load as its section capacity. However, columns in reality have imperfections. In addition to the axial load, the column must resist the associated imperfection moment. Thus, the axial load capacity of the column is reduced than its full section capacity due to member imperfections

together with the slenderness effect. In (EN 1994-1-1, 2015), the design action effect should satisfy the following to meet the stability requirement:

$$\frac{N_{Ed}}{\chi N_{pl,Rd}} \leq 1.0 \quad (2.3)$$

Where:

N_{ED} is the design value of the applied axial force

χ is the reduction factor for flexural buckling

In (EN 1994-1-1, 2015), the verification of a composite column under axial compression is based on the European buckling curves that were initially developed for structural steel columns. The initial member imperfections are accounted in these buckling curves. Out of the five European buckling curves in (EN 1994-1-1, 2015),

Only curve a, b and c are adopted for composite columns (Figure 2.2). This is due to the fact that concrete reduces the effective buckling length of the steel section. The relevant buckling curves for different cross-sections of composite columns are given in Table 2.4. For concrete encased sections buckling curve b and c are adopted for bending about the major and minor axis respectively. The value of χ is based on the relevant buckling mode given in (EN 1994-1-1, 2015) in terms of the relevant relative slenderness $\bar{\lambda}$.

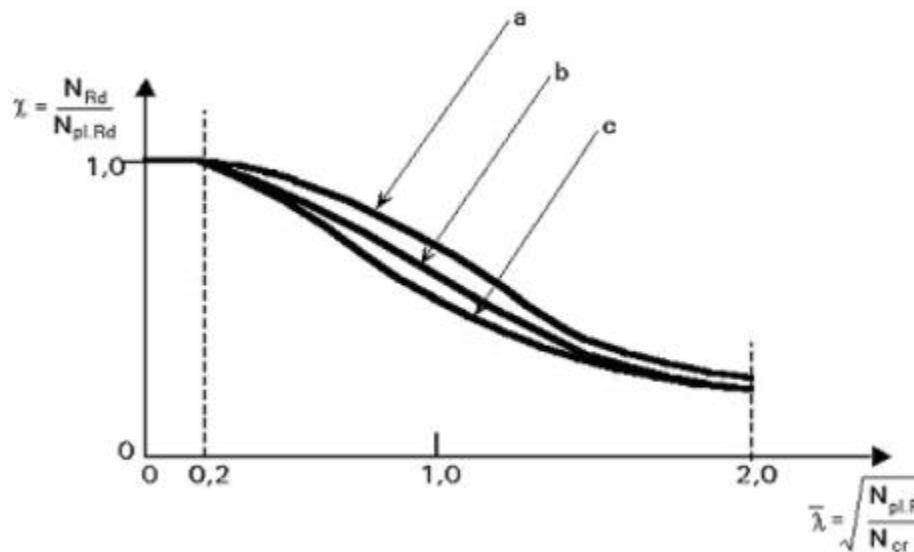


Figure 2. 2: European buckling curve for composite columns (EBCS-EN 1994-1-1: 2013)

$$\chi = \frac{1}{\phi + \sqrt{\phi^2 - \bar{\lambda}^2}} \leq 1.0 \quad (2.4)$$

$$\phi = 0.5 \left[1 + \alpha (\bar{\lambda} - 0.2) + \bar{\lambda}^2 \right] \quad (2.5)$$

The imperfection factor α is given in *Table 2.1* corresponding to the appropriate buckling curve.

Table 2. 1 Imperfection factor (EBCS-EN 1994-1-1: 2013)

European bulking curve	a	b	c
Imperfection factor α	0.21	0.34	0.49

The relative slenderness for the plane of bending is given by:

$$\lambda^- = \sqrt{\frac{N_{pl,Rk}}{N_{cr}}} \quad (2.6)$$

Where: $N_{pl,Rk}$ is the characteristic value of plastic resistance to compression.

N_{cr} is the elastic critical force for the relevant buckling mode The characteristic squash load

$N_{pl,Rk}$ is evaluated as in stated by (2.4) but instead of the design strength, the characteristic values of strength of materials are used.

$$N_{pL,Rd} = A_a f_y + 0.85 A_c f_{ck} + A_s f_{sk} \quad (2.7)$$

Where:

f_{ck} is characteristic value of the cylinder compressive strength of concrete at 28 days

f_{sk} is characteristic value of the yield strength of reinforcing steel

f_y is nominal value of the yield strength of structural steel

The critical buckling load N_{cr} is evaluated by Euler's formula, in which the flexural rigidity of the column is computed taking in account of the reduced stiffness of the concrete due to cracking.

$$N_{cr} = \frac{\pi^2 (EI)_{eff}}{L^2} \quad (2.8)$$

Where:

L is the buckling length of the column

$(EI)_{eff}$ is the effective flexural stiffness of the composite cross-section

By reducing the stiffness of the concrete, the characteristic effective flexural stiffness is calculated based on the gross cross-section of the concrete.

$$(EI)_{eff} = E_a I_a + E_s I_s + K_e E_{cm} I_c \quad (2.9)$$

Where:

I_a is second moment of area of the structural steel section

I_s is second moment of area of the steel reinforcement

I_c is second moment of area of the un-cracked concrete section

E_{cm} is secant modulus of elasticity of concrete

K_e is a correction factor to account for a reduced stiffness of concrete due to cracking and in (EN 1994-1-1, 2015) the recommended value is 0.60.

The long term effects of sustained loads should also be accounted on the effective flexural rigidity of the column. In (EN 1994-1-1, 2015) the modulus of the concrete is further reduced to $E_{c,eff}$ and the effective flexural rigidity is evaluated by (2.11).

$$E_{c,eff} = \frac{E_{cm}}{[1 + \left(\frac{N_{G,Ed}}{N_{Ed}}\right) * \Phi t]} \quad (2.10)$$

Where:

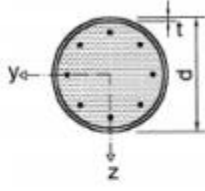
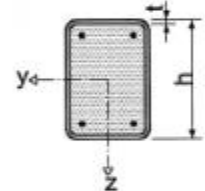
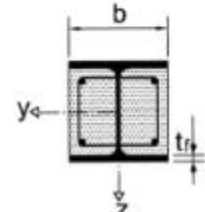
Φt is the creep coefficient according to (EN 1994-1-1, 2015),

$N_{G,Ed}$ is part of N_{Ed} that is permanent. If the increase in the first order bending moments as a result of creep deformations is not more than 10%, creep and shrinkage effects can be neglected.

2.3.3. Local Buckling of Steel Members, Second Order Effects and Member Imperfections

For compression members, local buckling of the structural steel has to be checked first. According to (EN 1994-1-1, 2015), the effects of local buckling may be ignored for composite sections fulfilling a specified depth to thickness ratios as stated in *Table 2.2*. Otherwise allowance should be made to account for the reduction of the ultimate capacity as a result of local buckling. For sections completely encased in concrete satisfying at least the minimum concrete cover code requirements, local buckling need not be checked.

Table 2. 2 Maximum values of $(d/t, h/t$ and $d/t)$ with f_y in N/mm^2 (EN 1994-1-1, 2015)

Cross-section	max (d/t) , max (h/t) and max (b/t)
Circular hollow steel sections 	$\max (d/t) = 90 \frac{235}{f_y}$
Rectangular hollow steel sections 	$\max (h/t) = 52 \sqrt{\frac{235}{f_y}}$
Partially encased I-sections 	$\max (b/t_f) = 44 \sqrt{\frac{235}{f_y}}$

For member verification, second order effects due to both the global ($P-\Delta$) and local ($P-\delta$) deformations have to be considered while determining the action effects. According to(EN 1994-1-1, 2015), the evaluation of internal forces should be based on the design effective flexural stiffness $(EI)_{eff,II}$.

$$(EI)_{eff,II} = K_a(E_a I_a + E_s I_s + K_{e,II} E_{cm} I_c) \tag{2.11}$$

Where:

$K_{e,II}$ is a correction factor which should be taken as 0.5

K_a is a calibration factor which should be taken as 0.9

The influence of second order effects may be neglected for braced and non-sway frames:

If the relevant action effects increase by less than 10% of the first-order analysis results due to deformations of a member. This condition is assumed to be fulfilled if the following criterion is satisfied:

$$\alpha_{cr} = \frac{N_{ed}}{N_{cr,eff}} \leq 10. \quad (2.12)$$

Where:

α_{cr} is the factor by which the design loading would have to be increased to cause elastic instability

$N_{cr,eff}$ is the critical normal force for the relevant axis and corresponding to the effective flexural stiffness with the effective length taken as the column length

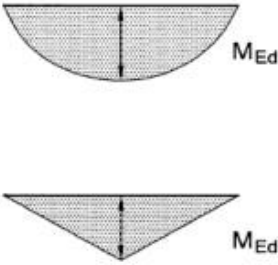
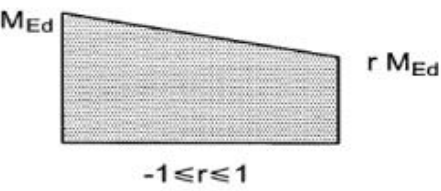
If the elastic critical load is determined with $(EI)_{eff,II}$. If the above conditions are not satisfied, second-order analysis shall be carried out. Second order effects may also be allowed approximately by amplifying the maximum first order design moment within the column length with factor k :

$$K = \frac{\beta}{1 - N_{Ed}/N_{cr,eff}} \geq 1.0 \quad (2.13)$$

Where:

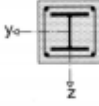
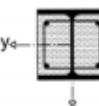
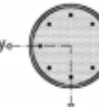

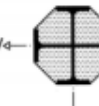
The equivalent moment factor, β , is given in [Table 2.3](#) for different types of moment distributions along the column length. In [Table 2.3](#), r is the ratio of smaller to the larger end moments.

Table 2. 3: Factors β for the determination of moments to second order theory (EN 1994-1-1, 2015)

Moment distribution	Moment factors β	Comment
	First-order bending moments from member imperfection or lateral load: $\beta = 1.0$	M_{Ed} is the maximum bending moment within the column length ignoring second-order effects
	End moments: $\beta = 0.66 + 0.44r$ but $\beta \geq 0.44$	M_{Ed} and $r M_{Ed}$ are the end moments from first-order or second-order global analysis

Imperfections in composite frame may arise due to lack of verticality of columns, lack of fit between members, effect of residual stresses in steel section and temperature gradient within the structure. (Johnson, 2012b) and (Johnson, 2012a) In (EN 1994-1-1, 2015) the geometrical and structural imperfections are considered by equivalent geometrical imperfections (initial bows) as given in Table 2.4, where L is the column length. This eccentricity is allowed locally in verification of members only. The initial bow is assumed to occur at the mid length of the member. Hence, multiplying the geometrical imperfection by the design axial force gives the imperfection moment. Furthermore, the imperfection moment is amplified to account for the second order effects if the frame is susceptible to secondary effects. Therefore, the column length must have sufficient capacity to resist the design moment plus the imperfection moment for a given design axial load.

Table 2. 4 :Buckling curves and member imperfections for composite columns (EN 1994-1-1, 2015)

Cross-section	Limits	Axis of buckling	Buckling curve	Member imperfection
concrete encased section 		y-y	b	$L/200$
		z-z	c	$L/150$
partially concrete encased section 		y-y	b	$L/200$
		z-z	c	$L/150$
circular and rectangular hollow steel section 	$\rho_s \leq 3\%$	any	a	$L/300$
	$3\% < \rho_s \leq 6\%$	any	b	$L/200$
circular hollow steel sections with additional I-section 		y-y	b	$L/200$
		z-z	b	$L/200$
partially concrete encased section with crossed I-sections 		any	b	$L/200$

2.3.4. Resistance of Cross-sections and Members under Axial Load and Uniaxial Bending

The ultimate capacity of a cross-section subjected to axial load and bending moment is determined from the moment-axial force interaction curve of a particular section. In a steel beam-column interaction curve, the moment resistance reduces with increasing axial load. However, in a composite beam-column, the moment resistance increases up to the balanced point for a lower value of axial compression. This is due to the pre-stressing effect of the compressive force which prevents excessive cracking of concrete. According to the simplified method of (EN

1994-1-1, 2015), the points of the interaction curve can be determined by assuming a full plastic stress distribution known as rigid-plastic approximation. The structural steel section and the reinforcing steel bars are assumed fully plasticized either in tension or compression with the stress ordinates equal to their design yield strengths. For the concrete, a rectangular compressive stress of $0.85f_{cd}$ that is distributed uniformly between the most compressed face and the plastic neutral axis is assumed. Initially several plastic neutral axis positions in the direction of bending are assumed. Then, the corresponding values of moment and axial load are evaluated from the resulting stress blocks. Finally, the equilibrium conditions are checked. In the simplified method, the interaction curve is further approximated by a polygon made by connecting four or five points of the interaction curve. For bending about the major axis, it is sufficient to know four of these points shown in Figure 2.3. For weaker axis bending however, additional point between A and C shall be determined as the polygon bulges from the curve significantly. Point A (Figure 2.3) represents the plastic axial load capacity of a composite section as given by equation (2.7).

$N_A = N_{pl,Rd}$ and $M_A = 0$ Point B is the plastic moment resistance of a section.

$N_A = 0$ and $M_A = M_{pl,Rd}$

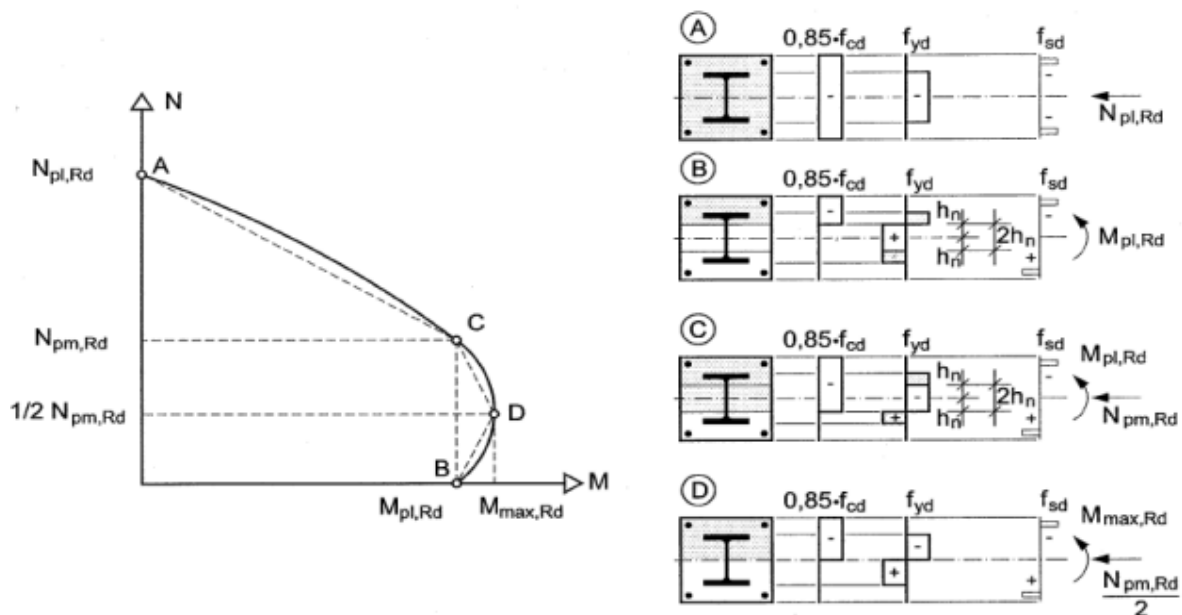


Figure 2. 3: Simplified interaction curve and corresponding stress distributions

Point C corresponds to the same plastic moment resistance as point B but with resultant axial compression force. For concrete encased sections:

$$N_C = N_{pm, Rd} = 0.85 \cdot A_C \cdot f_{Cd} \text{ and } M_C = M_{pl, Rd} \quad (2.14)$$

Point D is a balanced point representing the maximum moment carrying capacity of a composite section. For concrete encased sections:

$$N_D = 0.5 \cdot N_{pm, Rd} \text{ and } M_D = M_{max, Rd} \quad (2.15)$$

The depth h_n (Figure 2.3) is proportioned in a way that the stress distribution of type C provides the same value of moment as type B. It is assumed that the resulting resistance to axial force $N_{pm, Rd}$ is due to the concrete only. This can be seen by adding up the stress distributions in B and C, with regard to the equilibrium of forces, i.e. the resulting axial force.

Member resistance that is subjected to axial load and bending moments is determined from its cross-section capacity curve including the influence of Imperfections.

According to (EN 1994-1-1, 2015), a member must satisfy the following:

$$\frac{M_{Ed}}{M_{pl, N, Rd}} = \frac{M_{Ed}}{\mu_d M_{pl, Rd}} \leq \alpha_M \quad (2.16)$$

Where:

M_{Ed} is the greatest of the end moments and the maximum bending moment within the column length, calculated including imperfections and second order effects if necessary

$M_{pl, N, Rd}$ is the plastic bending resistance taking into account the normal force N_{Ed} , given by $\mu_d M_{pl, Rd}$;

$M_{pl, Rd}$ is the plastic bending resistance, given by point B in Figure 3

α_M is a correction factor for the un conservative assumption that the rectangular stress block for concrete extends to the plastic neutral axis. For steel grades up to S355, α_M is 0.9 and for steel grades S420 and S460 α_M is 0.8.

The value $\mu_d > 1.0$ is recommended only if the bending moment M_{Ed} depends directly on the action of the design normal force N_{Ed} , for example where the moment M_{Ed} results from an eccentricity of the normal force N_{Ed} . Otherwise an additional verification is necessary in

accordance with clause 6.7.1 (7) of (EBCS EN 1994-1-1, 2013) which states that, For composite compression members subjected to bending moments and normal forces resulting from independent actions, the partial factor γ_F for those internal forces that lead to an increase of resistance should be reduced by 20%.

2.3.5. Resistance of Members under Axial Load and Biaxial Bending

The verification of composite column subjected to biaxial bending is based on separate check in each of the principal axis as shown in Figure 2.4. Imperfections are accounted only in the plane on which failure is likely to occur. If this plane is not apparent, then separate checks is required in each of the planes (EN 1994-1-1, 2015).

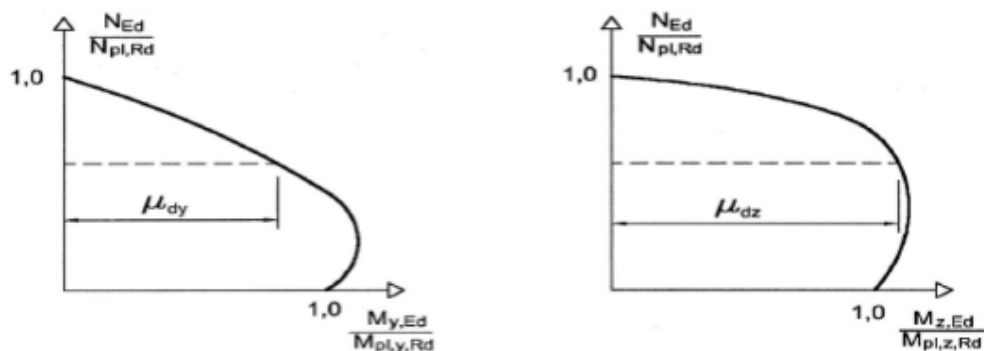


Figure 2. 4: Design of column length under axial load and biaxial bending (EN 1994-1-1, 2015)

The column must satisfy the following conditions for the stability within the column length and ends:

$$\frac{M_{y,Ed}}{\mu_{dy} M_{pl,y,Rd}} \leq \alpha_{M,y} \quad (2.17)$$

$$\frac{M_{z,Ed}}{\mu_{dz} M_{pl,z,Rd}} \leq \alpha_{M,z} \quad (2.18)$$

$$\frac{M_{y,Ed}}{\mu_{dy} M_{pl,y,Rd}} + \frac{M_{z,Ed}}{\mu_{dz} M_{pl,z,Rd}} \leq 1.0 \quad (2.19)$$

Where: $M_{pl,y,Rd}$ and $M_{pl,z,Rd}$ are the plastic bending resistances of the relevant plane of bending; about the y-y and z-z plane respectively.

$M_{y,Ed}$ and $M_{z,Ed}$ are the design bending moments including second-order effects and imperfections about the y-y and z-z plane respectively;

As mentioned above, it may not be obvious in which plane failure is anticipated. In this case, equations (2.17) and (2.18) are checked twice by taking the imperfections one at a time in both planes. First it is checked whether the moment capacity $\mu_{dy} M_{pl,y,Rd}$ is sufficient to resist the design moment $M_{y,Ed}$ about the y-axis plus the imperfection moment. But on the other axis $\mu_{dz} M_{pl,z,Rd}$ is checked if it is capable of resisting the design moment $M_{z,Ed}$ about the z-axis. Finally, the capacity of the column length is verified if it can resist the biaxial moment with equation (2.6). The reverse is repeated, taking the member imperfection about the z-direction only. The column length must satisfy all the conditions in both the cases.

2.3.6. The Influence of Transverse Shear Force

If the design shear force $V_{a,Ed}$ of the steel section exceeds 50% of the design shear resistance $V_{pl,a,Rd}$ of the steel section, then the influence of this shear force on the resistance to axial force and bending should be considered. According to (EN 1994-1-1, 2015), the influence of shear is accounted by using reduced steel strength for the web by $(1 - \rho) f_{yd}$ in the shear area A_v . For simplification the design shear force V_{Ed} may be assumed to act on the structural steel section alone. However, the design shear force on the steel section should not exceed the shear resistance of the steel section. If this is not the case and V_{Ed} is greater than $V_{pl,a,Rd}$, then the design shear force may be distributed between the structural steel $V_{a,Ed}$ and the reinforced concrete $V_{c,Ed}$. The design shear force on the reinforced concrete is verified with the same approach as for reinforced concrete members according to (1992-1-1, 2015). Unless there is a more accurate analysis to determine the shear distributed between the concrete and steel, in (EN 1994-1-1, 2015) the following is recommended:

$$V_{a,Ed} = V_{Ed} \frac{M_{pl,a,Rd}}{M_{pl,Rd}} \quad (2.20)$$

$$V_{c,Ed} = V_{Ed} - V_{a,Ed} \quad (2.21)$$

Where: $M_{pl,a,Rd}$ is the plastic moment resistance of the steel section The design plastic shear resistance $V_{pl,a,Rd}$ of the structural steel section is computed in the same way as for steel sections given in (1993-1-1, 2015).

$$V_{pl,a,Rd} = A_v \frac{f_{yd}}{\sqrt{3}} \quad (2.22)$$

The shear area, A_v , for rolled I or H sections is given by:

$$A_v = A_a - 2btf + (tw + 2r) tf \quad (2.23)$$

Where:

b is the overall breadth

h is the overall depth

h_w is the depth of web

t_f is flange thickness

For class 1 or 2 steel cross-sections, the reduction factor, ρ , is evaluated by:

$$\rho = \left(\frac{2V_{Ed}}{V_{pl,a,Rd}} - 1 \right)^2 \quad (2.24)$$

After reducing the yield strength of the web, the moment-axial load interaction curve can be evaluated in the same way using the simplified method.

2.4 Analytical and Experimental Investigation of Concrete Encased Composite Columns

Extensive experimental researches were carried out on FEC columns, by several research groups to investigate the behavior of columns under various loading conditions. A large number of tests were performed on short FEC columns constructed with normal strength concrete subjected to concentric, eccentric and biaxial load. A few long column tests were carried out using normal strength under static loading conditions. Findings of these experimental investigations are presented below:

([Ã et al., 2008](#)) conducted an experimental study on the behavior of reinforced and concrete encased composite columns subjected to biaxial bending and axial load. The primary objective of this investigation was to examine the ultimate strength capacity and load-deflection behavior of short and slender reinforced concrete columns. The experimental results were compared with the ultimate capacities obtained theoretically. Theoretical results were calculated using various stress

strain models for the materials done by previous authors. The experimental program included fifteen (15) reinforced concrete columns. Five specimens were Short Square (100 mm × 100 mm) tied columns with 870 mm length. Seven specimens were slender square tied columns with two different sizes. Other three specimens were L-shaped section slender tied columns. Ultimate capacity of these reinforced concrete columns were determined experimentally for eccentric axial load and compared with calculated theoretical results. A computer program was developed based on these theoretical calculations. The ultimate capacity was determined using this computer program for the tested FEC columns. The authors reported that the theoretical results could predict the experimental results for different cross section of reinforced and composite column members with good accuracy.

([Ã et al., 2008](#)) carried out experimental tests on bi axially loaded concrete encased composite columns. The main objective of this study was to observe the load deflection behavior and load carrying capacities of short and slender FEC columns. The researchers also, compared these experimental results with theoretical results. The theoretical results were calculated considering the flexural rigidity (EI) and slenderness ratio of these composite columns. The slenderness effect due to the additional eccentricity of the applied axial load was considered by the moment magnification method. The main variables in the tests were eccentricity of applied axial load, concrete compressive strength, cross section, and slenderness effect. This experimental study consisted of ten composite column specimens. The complete experimental load-deflection behaviors of the composite column specimens were determined. An interactive theoretical method including slenderness effect was suggested to perform the ultimate strength analysis and to determine the complete load-deflection behavior of composite columns. Good agreement was achieved between the complete experimental and the theoretical load-deflection diagrams in the study. In addition, the flexural rigidity was significant effect on the slenderness of composite columns.

([Kim et al., 2013](#)) carried out experimental study for eccentric axial load of concrete-encased steel column using high strength steel and concrete. Seven concrete-encased steel columns using high strength structural steel (nominal yield strength $f_{ys} = 913$ and 806 MPa) and high strength concrete (cylinder compressive strength $f_{cu} = 94$ MPa) were tested to investigate the seven

eccentric axial load-carrying capacity and the deformation capacity. Out of seven, four were fully encased square composite columns and designated as C1 to C4 with cross section 260mm*260mm. The test parameters of the fully encased composite columns were the eccentricity of the axial load. These columns were tested experimentally for two different eccentricities (120mm and 60mm). The test results showed that in the case of inadequate lateral confinement, the load-carrying capacity was limited by the early crushing of concrete. However, because of the high-strength steel section, all test specimens showed ductile flexural behavior after the delamination of the concrete. The test results were compared with the predictions by nonlinear numerical analysis and current design codes.

(Shih *et al.*, 2013) carried out study on axial strength and ductility of square composite columns with two interlocking spirals. The axial compressive capacity and load– displacement behavior of composite columns confined by two interlocking spirals were experimentally and analytically investigated. The innovative spiral cage used for a square column was fabricated by interlocking a circular spiral and a star-shaped spiral to enhance the confinement effect for the core concrete. Eight full-scale square composite columns were tested under monotonically increased axial compression. Experimental results demonstrated that, with significant savings of the transverse reinforcement, the composite columns confined by two interlocking spirals achieved excellent axial compressive strength and ductility. It revealed that the spirally reinforced concrete column achieved better load carrying capacity and behavior than the rectilinearly tied reinforced concrete column, although the amount of the spirals was less than that of the rectilinear hoops. Moreover, an analytical model was developed to take into account the concrete confinement due to the structural steel in addition to the transverse reinforcement and distributions of the longitudinal bars. The analytical results accurately predicted the axial compressive capacity and load– displacement behavior of the specimens.

Numerical and analytical investigations

Analytical methods were developed parallel to experimental study in early 1900 to determine the strength and behavior of FEC columns. Successively, computer analysis method was developed to determine the nonlinear behavior of FEC columns under different loading conditions. Numerical analyses for FEC columns using FE model started very recently as compared to other

methods. It has numbers of advantages over experimental research. However, it was found that very limited research on numerical simulation of FEC column has been conducted.

(Kim *et al.*, 2013, 2014) carried out numerical studies on FEC columns with high strength steel and concrete with varying eccentricity and structural steel shapes. Total eight (8) FEC columns were numerically investigated using fiber section analysis in these studies. The analysis results were compared with the test results, in terms of the axial load-strain relationship and the moment curvature relationship. In material models for the high-strength concrete the tensile stress of the concrete was ignored. The concrete area in the composite 18 section was divided into three regions according to confinement level: unconfined (concrete cover), partially confined (confined by lateral rebar's), and highly confined (confined by lateral rebar's and steel section) concrete zones. Authors reported that the nonlinear numerical analysis showed good agreement with the test results. But, it is observed from the study that the difference between experimental and numerical results of mentioned columns were 5% to 12%.

(Rahman, 2016) investigated the behavior of pin-ended axially loaded concrete encased steel composite columns. A non-linear 3-D finite model was developed to analyses the inelastic behavior of steel, concrete, longitudinal and transverse reinforcing bars as well as the effect of concrete confinement of the concrete encased steel composite columns. The experimental investigation on concrete encased steel composite columns was conducted with different slenderness ratio, different steel sections and different concrete and steel strength.

(Ellobody and Young, 2010) studied the responses of concrete encased steel composite columns to eccentrically load acting along the major axis. Many variables that influence this response such as the concrete strength, the steel section yield stress, eccentricities, column dimensions, and structural steel sizes were investigated. A three-dimensional finite element analysis using ABAQUS© has been developed and it has been validated against experimental result. Eccentric Load–concrete strength curves, axial load-moment curves, and ultimate capacity were obtained. The results showed that the increase in steel section yield stress has significant effect on the strength of eccentrically load composite column with small eccentricity with concrete lower than 70 MPa compressive strength.

(Ellobody, Young and Lam, 2011) investigated the behavior of pin-ended axially loaded concrete encased steel composite columns. The main objective of the study was to understand the structural response and modes of failure of the columns and to assess the composite column strengths against current design codes. A nonlinear 3-D finite element model was developed to analyse the inelastic behavior of steel, concrete, longitudinal and transverse reinforcing bars as well as the effect of concrete confinement on concrete encased steel composite columns. The finite element model was validated against published experimental results. Furthermore, the variables that influence the composite column behavior and strength comprising different slenderness ratios, concrete strength and steel yield stress were investigated in a parametric study. The authors reported that the increase in structural steel strength had a small effect on the composite column strength for the columns having higher relative slenderness ratios due to the flexural buckling failure mode.

The dominant point that was noticed during the review in literature was the cyclic behavior of the composite beam-columns has not received the same level of attention as monotonic behavior, especially for concrete-encased steel composite columns. A limited number of studies have been made on this behavior because it is expensive regarding the cost of research; preparing a full-scale testing is expensive and time consuming. However, a remarkable number of researchers tried to capture and monitor the composite columns seismic behavior by means of strength, stiffness, ductility, and energy dissipation. For instance, Varma, et al., (2004) investigated the seismic behavior of square concrete-filled steel tube beam-columns. Cyclic load tests conducted on eight beam-column specimens having different width-to-thickness ratio, different yield stress of the steel tube, and different level of axial load. The results indicate that in the plastic hinge zone, where the stress concentrations highly increase, most of the flexural energy was dissipated. Moreover, it was shown that the increase in axial load level has inverse effect on the cyclic curvature ductility. Also at lower axial load levels, the ductility is reduced for beam-columns having higher width-to thickness ratio or yield stress of the steel tube.

(Qian et al., 2016) studied an investigation on the analytical behavior of concrete-encased CFST columns under cyclic lateral loading. The main objectives of this research are firstly, to develop a nonlinear 3-D finite element analysis (FEA) model on composite columns under cyclic loading

with consideration of the cumulative damage of concrete as well as the interaction between concrete and steel. Secondly, to present analytical results of concrete-encased CFST columns under cyclic lateral loading, including the load–displacement relationships, the contact stress between steel tube and concrete and the axial load distribution among inner CFST and outer RC components. Meanwhile, comparisons on the behavior of concrete-encased CFST, conventional CFST and RC columns are also conducted. Thirdly, to provide a moment versus curvature hysteretic model using the verified FEA model, which can reasonably predict the behavior of composite columns under cyclic lateral loading. The analytical results show that components of the composite column work together well under cyclic loading. The axial load level effects on the axial load distribution among components. The proportion of the axial load resisted by the outer reinforced concrete increases at first, and then decreases with the increase of the displacement level when under a low axial load level.

In order to give a further understanding of steel-reinforced concrete-filled steel tubular (SRCFST) columns under cyclic loading conducted (Chang, Wei and Yun, 2012). In this contribution, the ABAQUS®/standard solver is employed to investigate and predict the resistances of SRCFST columns under cyclic loading. Validation of this numerical method is carried out by comparing the computed results with the experimental observation of five tested specimens. A parametric study, including the thickness of steel tube, steel ratio of section steel, yield strength of section steel and strength of concrete, is also carried out. The presence of the section steel can carry the lateral load and reduce the tensile zone of the concrete section. As a result, the SRCFST columns have higher stiffness and peak lateral load than the common CFST columns even with the same geometrical and material parameters. The section steel can also enhance the deformation ability of a SRCFST column.

Review of Effect of Confinement and stirrup

The strain in the materials during the early loading is different there is often little initial confinement of the concrete in a CFST. However, as the concrete begins to crack, it expands faster than the steel tube and becomes well confined at higher load value. This confinement results in a higher load carrying capacity. (EN 1994-1-1, 2015) allows an increase of concrete

compressive capacity factor from $0.85f_{ck}$ to f_{ck} for all CFSTs due to effect of confinement. Confinement has a significant effect of increasing load capacity for circular sections.

For the purpose of further increase of bearing capacity and survivability of encased composite column, it is offered to supply their concrete with additional tie reinforcement. Such reinforcement also has a positive effect on the fire resistance of the columns, as tie reinforcement, mounted with some distance from the inner surface of the steel pipe, is able to provide significantly longer resistance of the volumetrically compressed reinforced concrete core in fire conditions. The main variation was the spacing of the stirrup shear reinforcement. Due to the confinement effect of the stirrup shear reinforcement, the concrete core in the SRCFT specimens showed different behavior in shear failure compared to the CFST specimens (Hamidian, et al., 2016) and (Krishan, et al., 2017) and (Nguyen and Hong, 2021).

Review of Design code

For satisfaction of the main aim of this study; investigate the cumulative damage of composite columns subjected to axial and cyclic loading by comparing the effects of different parameter on the cyclic capacity of encased composite columns, it is first necessary to review the design procedures that will be used for composite, steel, and reinforce concrete columns to be able to use them in this investigation. In fact, Eurocode presents the most recent rules and comprehensive review among other design codes and specifications. As a result, Eurocode 2, 3, and 4 were chosen for design of reinforce concrete, steel, and composite columns, respectively. For the composite columns design, Eurocode has mentioned some limitations which shall satisfy; the longitudinal reinforcement which can be used should be no more than 6% and not less than 0.3% of the concrete area, concrete grade used was normal concrete from C20/25 to C60/75, the steel contribution ratio must between 0.2 and 0.9 and 0.2 and 5 are given as limits for the depth to width ratio of the composite cross-section.

In order to calculate the plastic resistance of composite columns, the plastic resistance of its components; the structural steel, the concrete and the reinforcement, should be adding. The plastic resistance equation for encased-composite column is:

$$N_{Pl,rd} = A_a f_{yd} + 0.85 A_c f_{cd} + A_s f_{sd} \quad (2.25)$$

Where,

A_a the cross-sectional area of the structural steel

A_c the cross-sectional area of the concrete

A_s the cross-sectional area of the reinforcement

f_{cd} Design value of the cylinder compressive strength of concrete

f_{sd} Design value of the yield strength of reinforcing steel

f_{yd} Design value of the yield strength of structural steel

As reviewed, (EN 1994-1-1, 2015) is suitable only for the analysis and design of composite columns fulfilling certain requirements. The simplified method is thus based on certain assumptions. Aside from aforementioned simplifications, different properties of the composite columns are not sufficiently considered. (Lai, Liew and Xiong, 2019) carried out analytical study on eccentrically loaded concrete encased steel composite columns along their major plane. They developed a nonlinear 3-D finite element model (FEM) that considered the inelastic behavior of constituent materials of the composite column. The effect of confinement to the concrete by the steel flanges and the transverse reinforcement was also accounted. To reveal the bond behavior, the interface between the structural steel and concrete, the concrete and transverse reinforcement, the concrete and longitudinal reinforcement and the longitudinal reinforcement and the transverse reinforcements were modeled. The initial geometrical imperfection was also comprised in the model. (Lai, Liew and Xiong, 2019) adopted the work of (Sheikh and Uzumeri and Mander et al. 1982) for reinforced concrete column to model the confined concrete. The composite columns were divided into highly confined concrete, partially confined concrete and the unconfined concrete zones (Figure 2.5). (Chen and Lin 2006) evaluated the confinement factors for the highly and partially confined concrete zones. (Mander, 1989) expressed the confined concrete compressive strength and the corresponding confined strain in terms of the lateral confining pressure. This pressure was determined approximately having known the

confinement factors for the highly and partially confined concrete as given by (Nguyen and Hong, 2021). Depending on the steel section shape and the spacing between the transverse reinforcements, the confinement factor varied from 1.10 to 1.97 for highly confined concrete and 1.09 to 1.50 for the partially confined concrete.

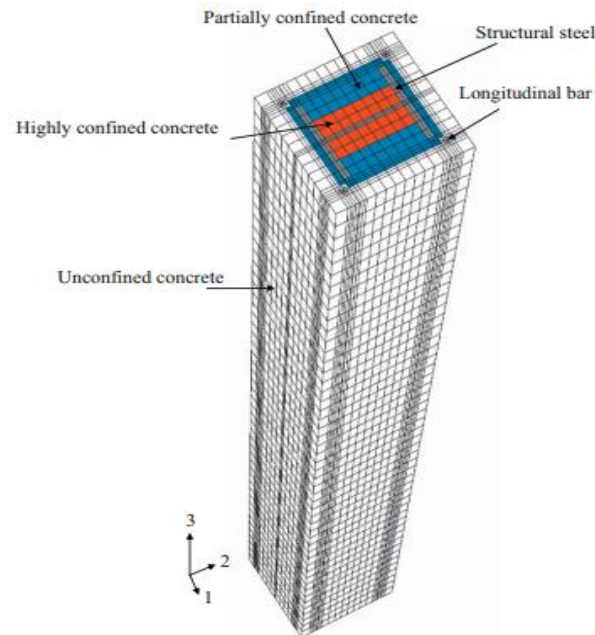


Figure 2. 5: Finite element model of concrete encased steel composite column (Ellobody, Young and Lam, 2011)

(E. Ellobody et al. 2011) verified the developed FEM against the test results by (Al-Shahari et al. 2006), SSRC Task Group, and (Morino et al. 1984). Good agreement was obtained with the test results with mean value of axial capacity from the finite element analysis (FEA) to the axial capacity from test ratio was 0.95. (Ellobody, Young and Lam, 2011) extended their work to parametric study of columns having different eccentricities, overall cross-section dimensions, structural steel sections, concrete strength and structural steel yield strength. Square and rectangular columns were considered in the parametric studies and the details of the studied columns can be found in the journal. From this study, it was observed that increase in the structural steel strength was significant for the columns with small eccentricities. For the columns with higher eccentricity, the increase of the yield strength of the steel was significant when the columns were encased in normal strength concrete. The axial load and moment obtained from the finite element analyses (FEA) in the parametric study were compared with the

unfactored design axial force and moment according to the Eurocode 4 simplified design method. The axial loads obtained from FEA and Eurocode 4 were almost the identical with mean values of axial load of FEA to axial load of Eurocode 4 ratio were 1.02 and 0.99 for the square and rectangular columns respectively. On the other hand, the calculated design moments were considerably higher than the FEA with the mean values of ratio were 0.73 and 0.75 for the square and rectangular columns respectively. However, unlike the FEA, it was not clearly realized that the effects of yield strength of the structural steel in relation to the concrete grade using the Eurocode 4. Mirza S.A. and (Lacroix E.A. 2004) compared the strength determined from 150 physical tests of rectangular concrete encased steel composite columns available in the published literature with the strength calculated from selected computational procedures, the ACI 318-02, AISC-LRFD and Eurocode 4 (CEN 1994). The tested columns were encased in normal density- normal strength concrete reinforced with longitudinal bars and transverse ties. The columns were pin ended and subjected to short term loads that produced pure axial force, axial force combined with equal and opposite end moments either in the major or minor axis, or pure bending moments. The computed strengths according to the codes were un factored. The Eurocode 4 simplified method was used to compute the axial load-bending moment interaction of the cross-sections and the columns capacity. The tested strengths were divided by the computed un factored capacities to obtain normalized strength ratio. The strength ratios were taken as bending moment ratios for columns that were subjected to pure flexure and for all others were axial load strength ratios. With the Eurocode 4 simplified method, the column strengths were computed more accurately with an average strength ratio of 1.04 and a coefficient of variation 0.15.

The different end eccentricities, slenderness ratio (the column length to depth ratio), structural steel contribution ratio, longitudinal steel contribution ratio and characteristic compressive cylindrical strength of the concrete that were used in the tests didn't affect the strength ratios pronouncedly. However, the various hoop volumetric ratio of the tested columns resulted in increased strength ratio. This was because the Eurocode 4 do not account for the increase in strength of the concrete due to the confinement by the transverse reinforcement.

FEC columns using finite element methods are therefore required to expand existing knowledge of the behavior of those columns. Finite element analysis can be used to improve the understanding of the effects of the variable parameters on the strength and behavior of such columns. The first goal of this part of the work was to create an entire finite element (FE) model to be used for the distribution of FEC column geometries, subject to varying loading conditions, and to provide accurate simulations of the behavior of the composite columns. ABAQUS is used to construct numerical model of FEC columns by using finite element code. Geometric and non-linearity materials were included in the FE model. A concrete damage plasticity model capable of predicting both compressive and tensile failures was used to model the behavior of the concrete material. The steel-concrete interface in the composite column was modeled using the built-in option in ABAQUS/Standard(Kartheek and Das, 2020).

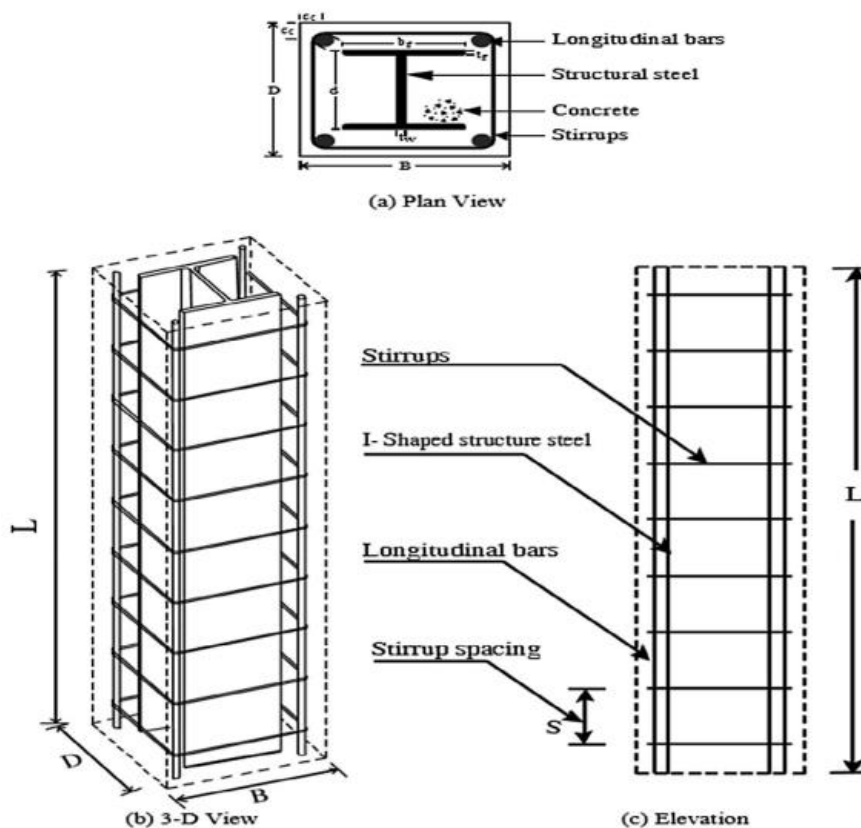


Figure 2. 6 :REC Column ;(a) plan view ;(b) 3D view and (c) Elevation(Kartheek and Das, 2020)

CHAPTER THREE

3. RESEARCH METHODOLOGY

3.1.General

This chapter presents and describes the approaches and techniques that I was used to collect data and investigate the research problem. This include the research design, study population, sample size and selection, sampling techniques and procedure, data collection methods, data quality control (validity and reliability), procedure of data collection, data analysis, Ethical consideration.

3.2 Research Methodology

The research design was theoretical researches which were essential for the comparative study of encased composite column with different concrete strengths and lengths on the action of axial load using finite element analysis of ABAQUS©CAE. This research was a systematic investigation to fill the gap of knowledge on the performance of encased composite column. On the other hand, it was a process for collecting, analyzing and interpreting information to provide a recommendation to the research findings. After comprehensively, organizing literature review of different previous published researches, designate the comparative study of encased Composite column with different concrete strengths, lengths and diameter of rebar. Validation for the finite element modeling is conducted on pre-qualified and practical tested for encased composite column under axial loading. After that specific study parameters were introduced in this study for encased composite column to investigate the influence of these parameters on performance of composite column in cooperative technique.

The study programs divided into four main parts of research design are:-

- ✓ Identify the property of materials (Concrete, Reinforcement bars and steel sections) used as in put of finite element Analysis as discussed under section 3.12.
- ✓ Modeling of fully encased steel composite Column by using ABAQUS©CAE. See (section 3.10.)
- ✓ The validation of the finite element (FE) analysis result with the results from experimental test. In order to verify the simulation process is correct discussed in sec 4.2,
- ✓ Parametric study.(discussed in section 3.13)

3.3 Study Variables

- **Dependent Variables**

The dependent variables, which were to be observed and measured to determine the effect of the independent variables is;-

- ✓ Axial Performance (load capacity and axial deformation) of steel concrete composite columns of concrete encased steel sections.

- **Independent Variables**

The independent variables, which were to be measured and manipulated to determine its relationship to observed phenomena, are selected and listed below.

- ✓ Compressive strength of concrete.
- ✓ Length of columns
- ✓ Diameter of longitudinal reinforcement bars
- ✓ Diameter and spacing of transverse reinforcement bars

3.4 Population and Sampling Method

The main purpose of this study was to investigate the cumulative damage of encased composite column subjected to concentric axial loading by comparing the effect of profile of encasement and effect of length to width ratio of the column to evaluate the stiffness, strength and ductility of the column. To achieve this, a finite element analysis was conducted with all appropriate parameters considered. The finite element method is a numerical analysis technique for obtaining approximate solutions to a wide variety of engineering problems. For this study there were a total of nineteen (19) columns which was selected as a sample with different independent variable. Of nineteen, eighteen (18) are for parametric study and one (1) column is from experimental literature for validation of the model. Axial loads of (4475.4 KN) (Lai, Liew and Xiong, 2019) of column capacity were applied concentrically on top of the columns. The failure modes, peak load, load-deflection behavior of the specimens were examined for this type of load in this study.

Table 3. 1 Sample of independent variables data

Table of Specifications					
S.NO	Specimen Samples	Concrete grade(MPa)	Length of column(mm)	Diameter of Longitudinal bar(mm)	Column cross section(mm)
01	A	C50	600	13	240*240
1	A1	C25	600	12	240*240
2	B1	C30	600	12	240*240
3	C1	C35	600	12	240*240
4	A2	C25	600	14	240*240
5	B2	C30	600	14	240*240
6	C2	C35	600	14	240*240
7	A3	C25	800	12	240*240
8	B3	C30	800	12	240*240
9	C3	C35	800	12	240*240
10	A4	C25	800	14	240*240
11	B4	C30	800	14	240*240
12	C4	C35	800	14	240*240
13	A5	C25	1000	12	240*240
14	B5	C30	1000	12	240*240
15	C5	C35	1000	12	240*240
16	A6	C25	1000	14	240*240
17	B6	C30	1000	14	240*240
18	C6	C35	1000	14	240*240

CONSTANTS

Table 3. 2 Samples of constant parameters

thickness of steel sections	diameter of reinforcement bars and numbers	load (KN)	displacement (mm)	concrete cover (mm)	stirrup cross section (mm)
$t_f=9.4\text{mm}$ & $t_w=6.5\text{mm}$	Longitudinal(mm)= 8 Φ 13 Ties(mm)=10	4475.40	5	30	180*180
Structural steel size Encasement type is I-section of $d \times w \times t_f / t_w$ (mm) =157.6*152.9*9.4/6.5(mm)					

The material data and their properties such as concrete, reinforcing steel and structural steel were used as discussed in ES EN 2015 code. The Square fully concrete encased steel composite Column cross section, thickness of steel sections, diameter of reinforcement bars and numbers, load, displacement, cross sections of stirrups and concrete covers were used as per journals and code as tables of specifications above.

3.5 Sources of Data

The primary data from *ABAQUS* results and secondary data's were from ES EN 2015 code and different journals including published research papers.

3.6 Data Collection Procedure

The data collection for this research used the related topic literatures from high rated journals, ongoing researches, books, and seismic resistance structural design journals, construction engineering journals and construction management journals, relevant practices related to comparative study of encased composite column with previous experimental results using finite elements analysis *ABAQUS*©CAE software and which was related to performance of encased composite column was accessed. An approach was going to conduct number of Finite Element Analysis to observe the behavior of encased composite column with different Compressive strength of concrete, Length of column and Diameter of Reinforcement bars under axial loading.

3.7 Model samples and cross sections used in this study Program

The study program consisted of eighteen (18) fully encased composite columns (FEC) columns of all different encasement with square rectangular columns with I section steel section of composite columns. These FEC columns were square in size and constructed with normal strength concrete. The columns were tested for concentric loads, to observe the failure behavior

and the lateral load carrying capacity of FEC columns. The loads versus deformation behavior of these FEC are analyzed by finite element method.

Description of model specimens

In total, 18 FEC columns were analyzed for the parametric study. Details of these columns are given in [Table 3.1](#) and [Table 3.2](#). The first letter in the column designation refers (A= groups of concrete strength with grade of 25), second letter to refers (B= groups of concrete strength with grade of 30), the third letters (C = groups of concrete strength with grade of 35) and L=Length of column), (D= diameter of longitudinal bars). The number used in the column designation was simply the serial number as they appeared in the table. Depending on the parametric study of this model the whole columns were categorized into three groups. Group 1, 2 and 3 are for investigation of effect of concrete strengths on composite columns. All columns of these groups have modeled with identical material properties except length of columns and diameter of longitudinal reinforcement bars.

3.8 Finite element method

Finite element analysis is a powerful computer method of analysis that can be used to obtain solutions to a wide range of structural problems involving the use of ordinary or partial differential equations. FE solvers can either use linear or non-linear analysis. Initially, the use of FE required the designer to define the location of every node for each element by hand and then the data were entered as code that could be understood by a computer program written to solve the stiffness matrix. Nowadays this is often known as the ‘solver’. The output was produced as text data only. The use of FEA has been the preferred method to study the behavior of encased composite column (for economic reasons). Now a day FEA is applied almost in all engineering areas of study such as flexural performance of concrete-encased column ([An and Roeder, 2014](#)). Nonlinear analysis of concrete-filled steel ([Ellobody, Young and Lam, 2011](#)), cyclic performance of concrete-filled composite columns under flexural loading ([Han and Yang, 2005](#)) behavior of concrete-encased concrete filled steel tube (CFST) members under axial tension ([Han et al., 2009](#)).

3.9 Data Presentation and Analysis

An analysis of encased composite column was used finite elements analysis. Finite Element Analysis (FEA) of encased composite column specimens is performed in a nonlinear static analysis format and the analysis procedure considers both material and geometric nonlinearities. In a nonlinear analysis, the total specified loads acting on a finite element body will be divided into a number of load increments. At the end of each increment the structure is in approximate equilibrium and the stiffness matrixes of structure were modified in order to reflect nonlinear changes in structure's stiffness.

The general-purpose finite element program ABAQUS®CAE used in this study is to investigate the effect of using different Concrete strength, different length of column and varying diameter of longitudinal reinforcement bars under axial load. A three-dimensional 3D finite element model will be developed to account for geometric and material nonlinear behavior of encased composite column. Every complete finite-element analysis consists of three separate stages:

- ✓ **Pre-processing or modeling:** This stage involves creating an input file, which contains an engineer's design for a finite-element analyzer. Pre-processing involves creating a geometric representation of the structure, then assigning properties, then outputting the information as a formatted data file (.dat) suitable for processing by ABAQUS®.
- ✓ **Processing or finite element analysis (solver):** This is sets of linear or nonlinear algebra equations are solved simultaneously to obtain nodal results, such as displacement values at different nodes or temperature values at different nodes in heat transfer problems.
- ✓ **Post-processing or generating:** In this process, the results can be processed to show the contour of displacements, stresses, strains, reactions and other important information. Graphs as well as the deformed shapes of a model can be plotted and report, image, animation are also prepared from this output.

ABAQUS/Standard uses the Newton-Raphson method to obtain solutions for nonlinear problems. Newton–Raphson equilibrium iterations provide convergence at the end of each load increment within tolerance limits for all degrees of freedom in the model. In addition to this commercial computer software package ABAQUS® program, the following programs will be applying: Microsoft Word and Microsoft excel were used for preparation of the report.

3.10 Finite Element Modeling of encased composite column

The modeling and analysis procedures were described one by one as shown below.

Note: All the specimens were modeled and analyzed after the FEA software is validated for the specific case of this research. The validation process was described in detail in the next chapter.

Parts (Geometry)

I. Concrete Column

Concrete Column parts were modeled on a 3D modeling space as deformable type with solid shape and extrusion type base feature. The column cross section (240*240) mm extruded with column lengths.

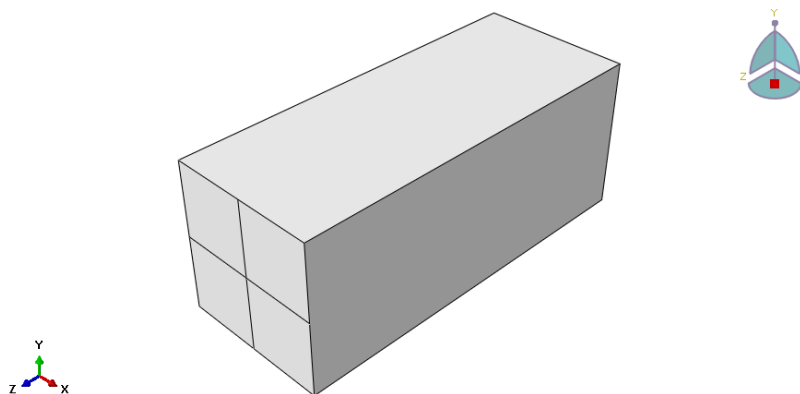


Figure 3. 1 Concrete Column part

II. Longitudinal Reinforcement Bars

Longitudinal reinforcement bars were modeled on a 3D modeling space as deformable type with wire shape and planar type base feature.

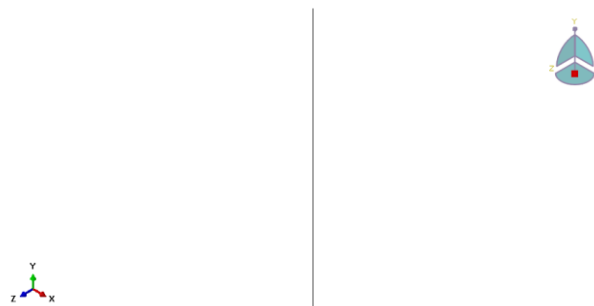


Figure 3. 2 Longitudinal Reinforcement Bar

III. *Transverse Reinforcement (Stirrups)*

Transverse Reinforcement (Stirrups) was also modeled on a 3D modeling space as deformable type with wire and planar type base feature of cross section (180*180) mm.

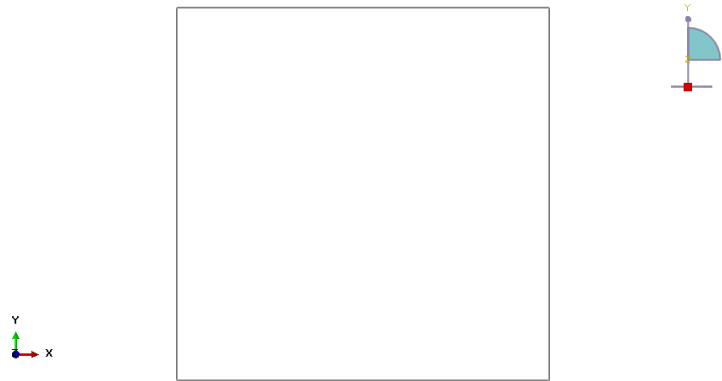


Figure 3.3. *Transverse Reinforcement Bar (Stirrup)*

IV. *Support and Loading Steel Plates*

Steel Plates were used at the bottom end as support and on top of the column as loading plate. They were modeled on a 3D modeling space as discrete rigid type with shell shape and planar shape base feature. The cross section of plate is 300mm*300mm. The part is face partitioned and has reference point at the center for the purpose of support, loading and boundary conditions.

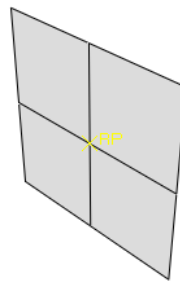


Figure 3.4. *Support and Loading Steel Plate*

V. *Structural steel section*

Structural steel section parts were modeled on a 3D modeling space as deformable type with solid shape and extrusion type base feature. The thickness of flange is 9.4mm with 152.9mm width, for web thickness is about 6.5mm with the height of 138.80mm.

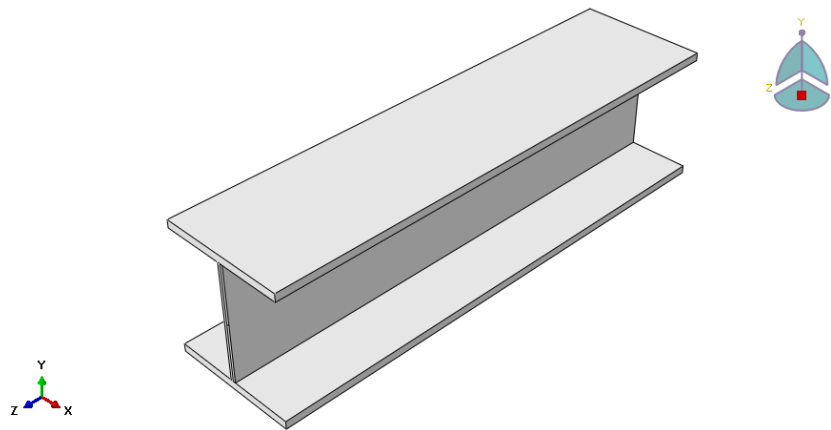


Figure 3.5: Structural Steel Section

This section provides a description of the finite element model developed in this study. It begins with an overview of the process that led to development of the model followed by a more in-depth look at individual aspects of the model; examining first the simplification of the physical specimens geometry, followed by a description of the mesh elements used to discretize the geometry, an overview of boundary conditions imposed on the mesh, and a description of the various material models that define the behavior of the model.

A complete 3D finite element model was developed in this study to investigate the behavior and strength of FEC columns encompassing a wide variety of geometry and material properties. Both material and geometric nonlinearities were incorporated in the FE model. ABAQUS®/Standard (ABAQUS element Analysis User's Manual) finite code was used to develop the nonlinear FE model for FEC columns in this study. Descriptions of the mesh and elements used in the finite element models of the test specimens, along with the boundary conditions including steel concrete interaction are presented in the subsequent sections.

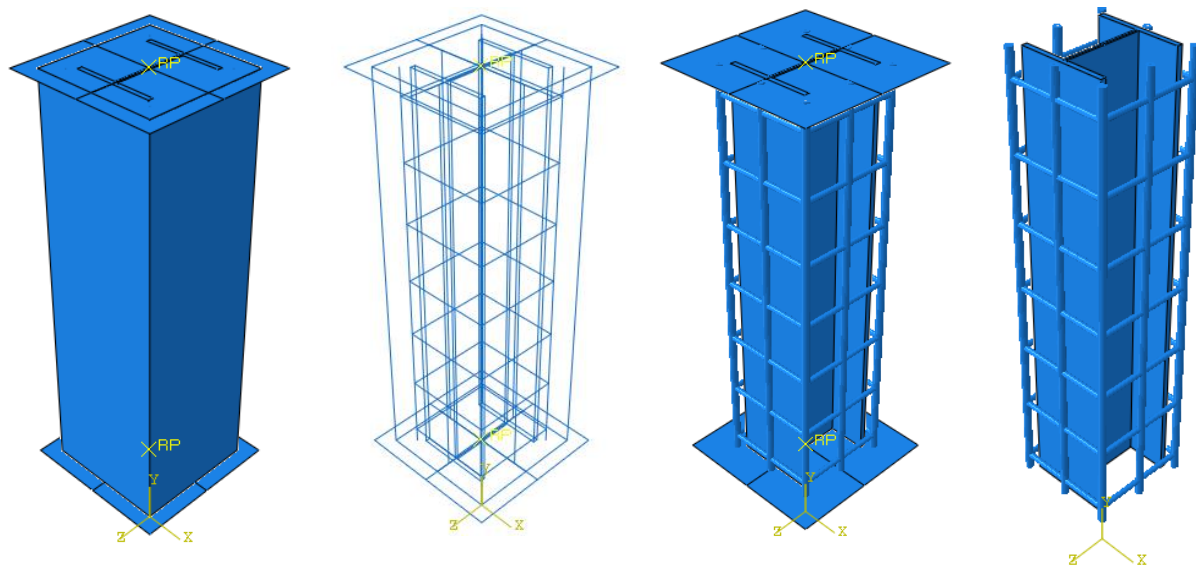


Figure 3. 6: Modeling of Encased Composite Column components In ABAQUS/CAE.

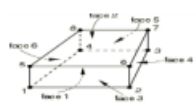
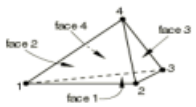
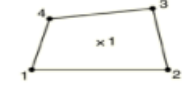
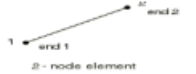

A total of 5 parts were used to represent Rectangular Encased composite column in finite element model. The FEM of the concrete-encased steel composite columns was carried out by modeling the longitudinal reinforcement bars, stirrups, I-section structural steel, plate part and concrete column part which consists the concrete cover their properties.

Element type and selection

The FEC columns investigated in this study comprised of four components, such as structural steel section, longitudinal reinforcement, transverse reinforcement and concrete. The key in finite element analysis is the appropriate selection of element type. The ABAQUS/CAE standard modules consist of a comprehensive element library that provides different types of elements catering to different situations. When carrying out FEA analysis, the selection of a particular type of element is no longer necessary, as most commercially available software packages for composite column design do not offer an option. For reference, it is usual to use a ‘beam’ element; this will provide results for flexure, shear and displacement directly. Beam and truss elements are generally triangular or quadrilateral with a node at each corner. However, elements have been developed that include an additional node on each side, this gives triangle elements with six nodes and quadrilateral elements with eight nodes. Since the only places where the forces are accurately calculated are at the nodes (they are interpolated at other positions), the accuracy of the model is directly related to the number of nodes. By introducing more nodes into

an element, the accuracy of the results is increased; alternatively, the number of elements can be reduced for the same number of nodes, so reducing computational time. For this reason 3D 8-noded hexahedral (brick) elements having 3 degrees of freedom in each node (translations in X, Y and Z directions) are utilized for modeling concrete elements and structural steel with reduced integration (C3D8R) to prevent the shear locking effect. In order to model reinforcements, 2-noded truss elements (T3D2) having 3 degrees of freedom in each node (translations in X, Y and Z directions of global coordinates system) are used. The embedded method with perfect bond between reinforcement and surrounding concrete is adopted to properly simulate the reinforcement-concrete bonding interaction. It is notable that the effects usually associated with reinforcement-concrete interface, such as bond slip and dowel action are modeled indirectly by defining "tension stiffening" into the reinforced concrete model to approximately simulate load transfer across cracks through the rebar (ABAQUS© user’s manual (2014)). ABAQUS© has an extensive library of elements that can be used to model concrete, including both continuum and structural elements. Elements are classified first by the “family” to which they belong.

Table 3. 3: Various Elements Used in ABAQUS© (ABAQUS, 2014)

Element	Description	D.O.F	Element shape
C3D8	Hexagonal Element	24	
C3D4	Tetrahedral Element	12	
S4R	shell elements	8	
T3D2	3-dimensional 2-node truss elements	6	
T2D3	2-dimensional 3-node truss elements	6	

3.11 Meshing

There were two of bodies needed to be discretized through meshing in this study. These are line bodies and solid bodies. Line bodies can be represented by beam and/or truss elements, solid bodies can be meshed with a variety of solid elements ranging from four node tetrahedral elements to polyhedral shapes, shell bodies can be meshed using a variety of shell elements. In ABAQUS© meshing can be done individually on parts and then assembled or vice-versa. In this analysis parts will individually meshed and then assembled for further process. Meshes are composed by tridimensional continuum solid elements with 8 nodes called C3D8R, 8 node linear brick elements with reduced integration and hourglass control are used for both materials, concrete and steel. The engineer has to assess how fine the mesh should be; a coarse mesh may not give an accurate representation of the forces, especially in locations where the stresses change quickly in a short space e.g. at supports, near openings or under point loads. This is because there are insufficient nodes and the results are based on interpolations between the nodes. However, a very fine mesh took an excessive time to compute.

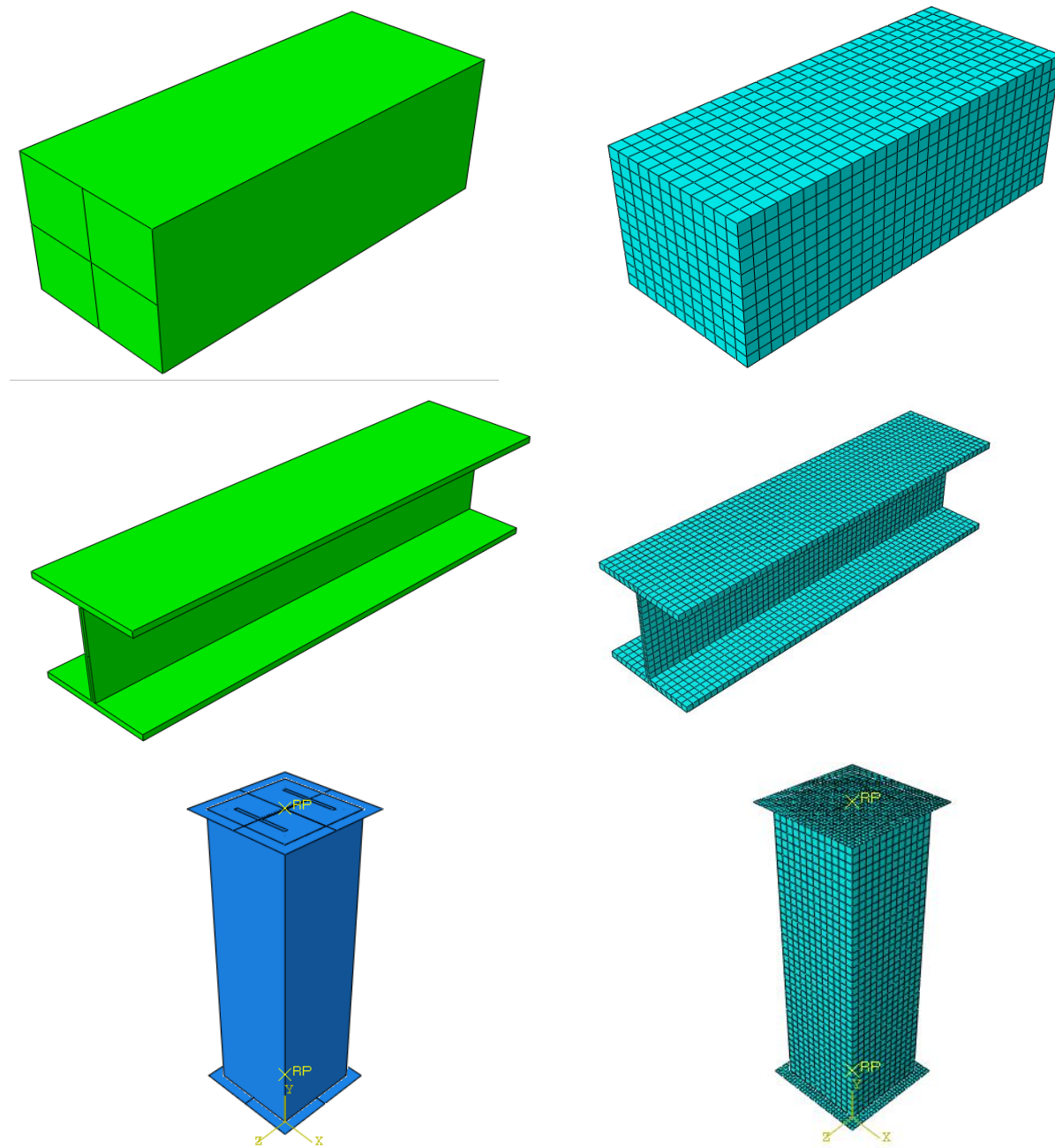


Figure 3. 7: Unmeshed and Meshed solid parts and meshed composite Column

3.12 Interactions and Kinematic Constraints between Components

Kinematic relationships between the various components are required to be defined within the finite element model in order to ensure strain compatibility between the various components. In other words, interactions had to be defined such that the equal and opposite loading applied between the bodies results in the one or more bodies deforming together. The interaction that was utilized

in the construction of this model was embedded constraints that were used to define the interaction between the concrete and the steel reinforcement. The second one is surface to surface interaction between structural steel and concrete.

A.Embedded Region Constraint type

The elements used for rebar's and the structural steel shape of the FEC columns were defined using embedded element option in ABAQUS®/Standard (ABAQUS® user's manual (2014)). This option ensures bonding between concrete and steel part of the column. The embedded element technique is used to specify an element or groups of elements embedded in host elements. In FEC columns, the concrete was defined as the host element whereas the structural steel section and reinforcement were defined as the embedded elements.

B.Tie Constraint type

The second interactions defined in this model take the form of a tie constraint in which a constraint is formed between two parts on the geometry, a master and a slave geometry. First the surfaces of different components that will be in contact must be created. After that pairs of surfaces which are going to be in contact must be identified. There are two components which define the interaction of contacting surfaces, one normal to the surfaces and one tangential. In ABAQUS® the default normal interaction between the surfaces is called the 'hard contact', meaning that the surfaces can contact each other when the clearance between them becomes zero and they can transmit between each other the unlimited magnitude of pressure but cannot penetrate each other. For interaction, surface to surface contact was created between structural steel profile and concrete with tangential behavior. Penalty method (also known as stiffness method) is used for imposing frictional constraints. This stiffness method allows the relative motion between the surfaces of two materials even when they are sticking.

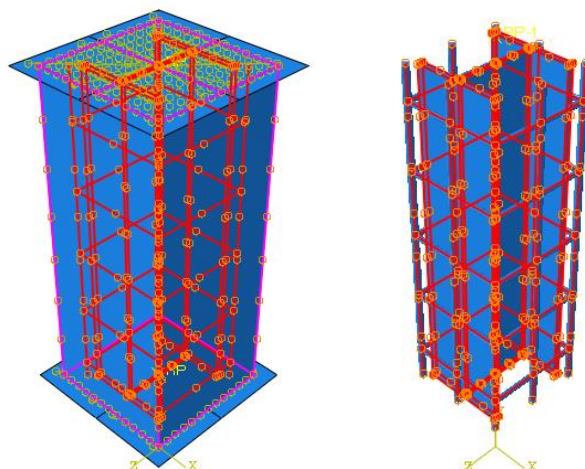


Figure 3. 8: Tie Constraints between column and both loading and support plate

3.13 Boundary Conditions and Loading

The way in which the bodies within the finite element model interact with each other and with the imposed boundary conditions can impact both the results and stability of the analysis. The first were reactionary boundary conditions that are constant conditions externally imposed on the model. Another type of external boundary condition is those intended to load the structure and change during the course of an analysis.

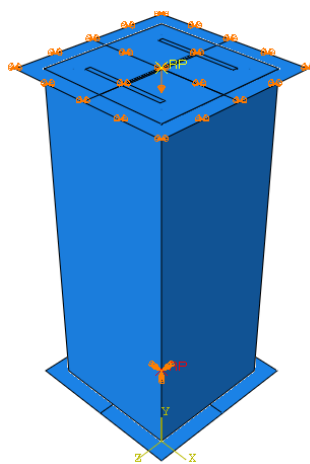


Figure 3. 9: End boundary conditions (fixed support) and loading.

The boundary conditions applied in the FEA model to simulate the conditions for concentrically loaded specimens are shown in Figure 3.9. In concentrically loaded column tests, the bottom end of the column was fixed and the axial load was applied through rigid body reference node at the center of the top end of the column. The rotations and horizontal translations at the top surface

were fixed. Since the load is applied at the top the vertical restraint was released. The axial load was applied using a displacement control technique. In the finite element model for concentrically loaded test specimens, cantilever conditions were applied at the end eccentric points located on the end rigid planes. A rigid body reference node is defined on the top of the column to apply displacement.

3.14 Material Modeling

The material definition is an important part of finite element analysis, and each component should be defined carefully and all parts should be defined with appropriate material parameters. Steel, concrete and rebars are the main materials used in construction of FEC columns for this study. The nonlinear behavior of these three materials were incorporated in the FE model using the appropriate material models for steel, concrete and rebars that available in the ABAQUS® (HKS 2013) finite element code. The description of the material models for steel and concrete along with their mechanical properties (stress versus strain relationship) used in the FE model is described in the following sections.

3.15 Compression properties of concrete

Concrete is one of our most common building materials and is used both for buildings, bridges and other heavy structures. Typically, concrete structures are very durable, but sometimes they need to be strengthened. Concrete is a material that can withstand compressive loads very well but is sensitive to tensile forces. Therefore, concrete structures are typically reinforced by casting in steel bars in areas where tension can arise. This study involve two major variation in concrete application in encased composite column, concrete is in state of confinement and in concrete cover only it is in state of un confined. Concrete experiences different characteristics in both conditions. But for this study, since the concrete in the concrete section is very small it is modeled as confined concrete as whole in the column.

a. Unconfined properties of concrete in concrete cover section

(EBCS EN1992, 2015) will be used in this study for the unconfined concrete, the relation between σ_C and ε_C under uniaxial loading was described in (EBCS EN1992, 2015), and it proposed single equation to describe unconfined concrete stress strain behavior as follow by expression (3.1). On the basis of uniaxial compression test results one can accurately determine the way in which the material behaved. However, a problem arises when the person running such

a numerical simulation has no such test results or when the analysis is performed for a new structure. Then often the only available quantity is the average compressive strength (f_{cm}) of the concrete. Another quantity which must be known in order to begin an analysis of the stress-strain curve is the longitudinal modulus of elasticity (E_{cm}) of the concrete. Its value can be calculated using the relations available in the literature (EBCS EN1992, 2015).

$$\frac{\sigma_c}{f_{cm}} = \frac{k\eta - \eta^2}{1 + (k - 2)\eta} \quad (3.1)$$

$$\text{where, } k = 1.05E_{cm} \frac{\varepsilon_{c1}}{f_{cm}} \quad (3.2)$$

$$\eta = \frac{\varepsilon_c}{\varepsilon_{c1}} \quad (3.3)$$

$$\varepsilon_{c1} = 0.7(f_{cm})^{0.31} \quad (3.4)$$

$$\varepsilon_{cm} = 22(0.1f_{cm})^{0.3} \quad (3.5)$$

$$\varepsilon_{cu} = 3.5\% \quad (3.6)$$

$$f_{cm} = f_{ck} + 8 \quad (3.7)$$

Where,

ε_{c1} is strain at average compressive strength,

f_{cm} is mean value of concrete cylindrical comparative strength (Mpa)

E_{cm} is the longitudinal modulus of elasticity (Mpa)

f_{ck} is characteristic cylindrical strength of concrete(Mpa) all of the equation are from (EBCS EN 1992-1-1:2013).

The above equation is valid for $0 < \varepsilon_c < \varepsilon_{cu1}$ where ε_{cu1} nominal ultimate strain. Figure 3.10 describe the developed stress strain relationship as provided in (EBCS EN1992, 2015), the specific development for this study was provided in appendix A.

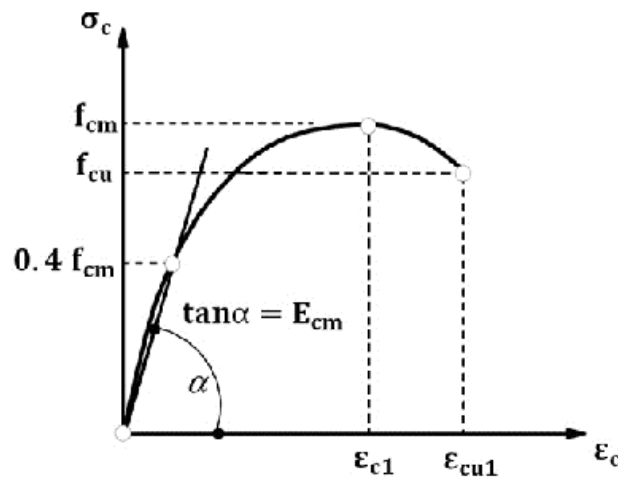


Figure 3. 10: Stress-Strain relations for non-linear structural analysis (EBCS EN 1992, 2015).

b. Confined properties of concrete in column

The confinement of the concrete by stirrups has been recognized in early research. This confinement can provide a confining pressure which leads in an enhancement in the strength and ductility of concrete (Yu *et al.*, 2010). Confinement of concrete results in a modification of the effective stress relationship: higher strength and higher critical strains are achieved. The other basic material characteristics may be considered as unaffected for design. For encased composite columns, the amount of the confining pressure depends on the steel section shape and its yield strength in addition to the factors that mentioned earlier. As a result, a highly confined zone occurs resulting from arching action formed by steel section. In the absence of more precise data, the stress-strain relation shown in Figure 3.10 (compressive strain shown positive) may be used, with increased characteristic strength and strains according to:

$$f_{ck,c} = f_{ck} \left(1.00 + 5.0 \frac{\sigma_2}{f_{ck}} \right) \quad \text{for } \sigma_2 \leq 0.05 f_{ck} \quad (3.8)$$

$$f_{ck,c} = f_{ck} \left(1.25 + 2.5 \frac{\sigma_2}{f_{ck}} \right) \quad \text{for } \sigma_2 \geq 0.05 f_{ck} \quad (3.9)$$

$$\epsilon_{c2,c} = \epsilon_{c2} \left(\frac{f_{ck,c}}{f_{ck}} \right)^2 \quad (3.10)$$

$$\epsilon_{cu2,c} = \epsilon_{cu2} \frac{\sigma_2}{f_{ck}} \quad (3.11)$$

Where: $\sigma_2 = \sigma_3$ is the effective lateral compressive stress at the ULS due to confinement and $\epsilon_{c2,c}$ and $\epsilon_{cu2,c}$ follow from code provision;

$$\varepsilon_{c2} = 2\% \tag{3.12}$$

$$\varepsilon_{cu2} = 3.5\% \tag{3.13}$$

Confinement can be generated by adequately closed links or cross-ties, which can reach the plastic condition due to lateral extension of the concrete

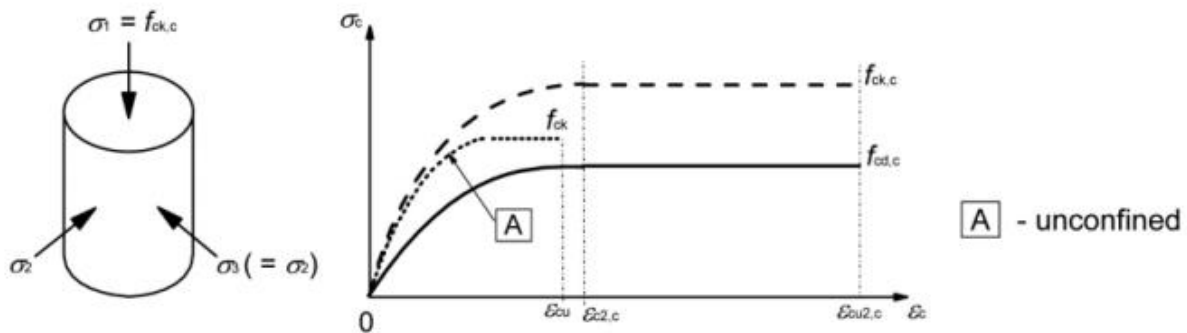


Figure 3. 11: Stress-Strain relationships for confined concrete (EBCS EN 1992, 2015)

c. Tension properties of concrete

ABAQUS© provides a number of option for defining tensile behavior of concrete. The stress can be related to the strain in the direction of the cracking or displacement which refers to crack width, and fracture energy, G_f . Alternatively, the fracture energy, G_f can be specified directly as a material property; in this case, define the failure stress, as a tabular function of the associated fracture energy. This model assumes a linear loss of strength after cracking (ABAQUS© software (SIMULIA, 2014). The cracking displacement at which complete loss of strength takes place is, therefore, $\varepsilon_{to} = 2G_f/\sigma_{to}$ Typical values of G_f range from 40 N/m for a typical construction concrete (with a compressive strength of approximately 20 MPa, to 120 N/m for a high-strength concrete (with a compressive strength of approximately 40 MPa. If tensile damage, d_t is specified, ABAQUS© automatically converts the cracking displacement values to “plastic” displacement values using the relationship:

$$\varepsilon_t^{pl} = \varepsilon_t^{ck} - \frac{d_t}{(1-d_t)} * \left(\frac{\sigma_t}{E_o}\right) \tag{3.14}$$

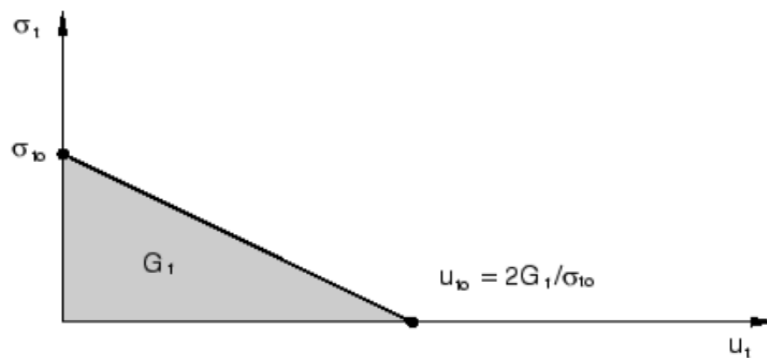


Figure 3. 12: Post failure stress-fracture energy curve. (ABAQUS user Manual, 2014)

d. Damage plasticity modeling of concrete

Damage is defined both for uniaxial tension and compression on during softening procedure in concrete damage plasticity model. Damage in compression occurs just after reaching to the maximum uniaxial compressive strength corresponding to strain level ϵ_0 . The degradation of elastic stiffness in softening regime is characterized by two damage variables, d_t and d_c corresponding to tensile and compressive damage, respectively, which are assumed to be functions of the plastic strains. Tensile and compressive damage in concrete damage plasticity model in the presented numerical model is assumed to be according to equations above and diagrams of Figure 3.11 and Figure 3.12.

ABAQUS© software (SIMULIA, 2014) provides the capability of simulating the damage using either of the three crack models for concrete elements: (1) Smeared crack concrete model, (2) Brittle crack concrete model, and (3) Concrete damaged plasticity model. Out of the three concrete crack models, the concrete damaged plasticity model is selected in the present study as this technique has the potential to represent complete inelastic behavior of concrete both in tension And compression including damage characteristics (Najafgholipour *et al.*, 2017). Further, this is the only model which can be used both in ABAQUS©/Standard and ABAQUS©/Explicit and thus enable the transfer of results between the two. Therefore, development of a proper damage simulation model using the concrete damaged plasticity model will be useful for the analysis of reinforced concrete structures under any loading combinations including both static and dynamic loading (“ABAQUS© Analysis User Manual-ABAQUS© Version 6.14” [ABAQUS© Manual],2014).

The concrete damaged plasticity model assumes that the two main failure mechanisms in concrete are the tensile cracking and the compressive crushing. In this model, the uniaxial tensile and compressive behavior is characterized by damaged plasticity (Wahalathantri et al, 2012) Concrete damaged plasticity model “takes into consideration the degradation of the elastic stiffness Induced by plastic straining both in tension and compression. It also accounts for stiffness recovery Effects under cyclic loading.” The compressive behavior is elastic until initial yield and then is characterized by stress hardening followed by strain softening after the ultimate point. ABAQUS© manual proposes an exponential function which can calculate the tensile damage variable (d_t) and the compressive damage variable (d_c)

$$\sigma_t = (1 - d_t)E_0(\varepsilon_t - \varepsilon_{tpl}) \quad (3.15)$$

$$\sigma_c = (1 - d_c)E_0(\varepsilon_c - \varepsilon_{cpl}) \quad (3.16)$$

e. Tension Stiffening Relationship

In order to simulate the complete tensile behavior of reinforced concrete in ABAQUS©, a post failure stress-strain relationship for concrete subjected to tension (similar to Figure 3.12) is used which accounts for tension stiffening, strain-softening, and steel concrete interaction with concrete. To develop this model, user should input young’s modulus (E_0), stress (σ_t), cracking strain (ε_{tck}) values and the damage parameter values (d_t) for the relevant grade of concrete. (Allam et al., 2013) The cracking strain (ε_{tck}) should be calculated from the total strain using (equation 3.15) below:

$$\varepsilon_t^{ck} = \varepsilon_t - \varepsilon_{ot}^{el} \quad (3.17)$$

$$\text{Where, } \varepsilon_{ot}^{el} \quad (3.18)$$

$$= \frac{\sigma_t}{E_0}, \text{ the Elastic Strain corresponding to the undamaged material,}$$

$$\varepsilon_t = \text{total strain}$$

Having defined the yield stress-inelastic strain pair of variables, one needs to define now degradation variable d_c . It ranges from zero for an undamaged material to one for the total loss of load-bearing capacity (Kmieciak and Kamiński, 2011). These values can also be obtained from uniaxial compression tests, by calculating the ratio of the stress for the declining part of the curve to the compressive strength of the concrete. Thanks to the above definition the CDP model allows one to calculate plastic strain from the formula:

$$\varepsilon_t^{pl} = \varepsilon_t^{ck} - \frac{d_c}{(1-d_c)} * \left(\frac{\sigma_t}{E_0}\right) \quad (3.19)$$

Where; E_0 stands for the initial modulus of elasticity for the undamaged material. Knowing the plastic strain and having determined the flow and failure surface area one can calculate stress σ_t for uniaxial compression and its effective stress σ_t^- .

$$\sigma_t = (1 - d_c)E_0(\varepsilon_t - \varepsilon_t^{pl}) \quad (3.20)$$

The damage plasticity constitutive model was based on the following stress–strain relationship:

$$\sigma_t^- = \frac{\sigma_t}{(1-d_c)} = E_0(\varepsilon_t - \varepsilon_t^{pl}) \quad (3.21)$$

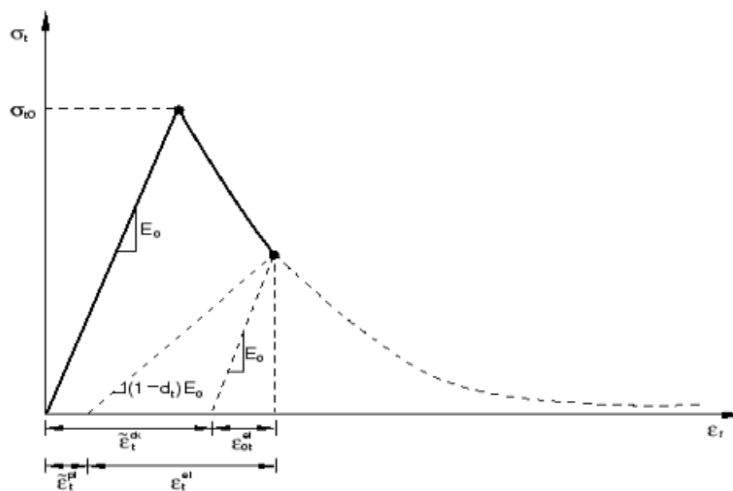


Figure 3. 13: Terms for Tension Stiffening Model (ABAQUS user Manual, 2014)

Where d_t and d_c were two scalar damage variables, ranging from 0 (undamaged) to 1 (fully damaged) (Hafezolghorani *et al.*, 2017). The damage model used for concrete was based on plasticity and considered the failure process of tensile cracking and compressive crushing. The uniaxial compressive and tensile responses of concrete with respect to the concrete damage plasticity model subjected to compression and tension load were given by:

$$\varepsilon_c^{pl} = \varepsilon_c^{ck} - \frac{d_c}{(1-d_c)} \frac{\sigma_c}{E_0} \quad (3.22)$$

$$\sigma_c = (1 - d_c)E_0(\varepsilon_c - \varepsilon_c^{pl}) \quad (3.23)$$

$$\sigma_c^- = \frac{\sigma_c}{(1-d_c)} = E_0(\varepsilon_c - \varepsilon_c^{pl}) \quad (3.24)$$

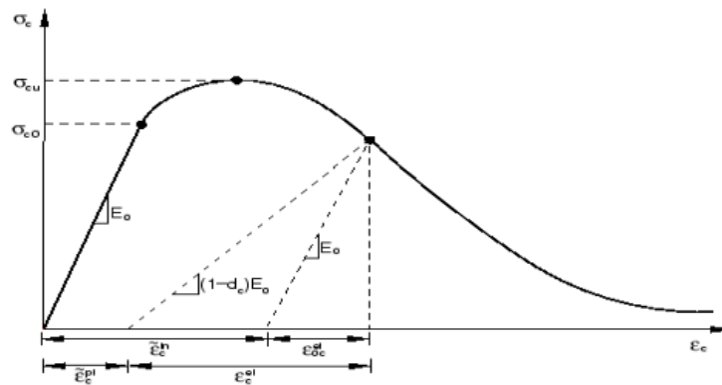


Figure 3. 14: Response of concrete to a uniaxial loading condition in compression (ABAQUS Manual, 2014)

Another parameter describing the state of the material is the point in which the concrete undergoes failure under biaxial compression. (f_{b0} / f_{c0}) is a ratio of the strength in the biaxial state to the strength in the uniaxial state. The ABAQUS user’s manual specifies default $(f_{b0} / f_{c0}) = 1.16$. The last parameter characterizing the performance of concrete under compound stress is dilation angle, i.e. the angle of inclination of the failure surface towards the hydrostatic axis, measured in the failure plane. Physically, dilation angle ψ is interpreted as a concrete internal friction angle. In simulations usually $\psi = 32^\circ$, 34° , 36° and $\psi = 38^\circ$ were used for the corresponding concrete grades C25, C30, C35 and C50 respectively.

Table 3. 4: Default parameters of CDP model under compound stress

Parameters	Dilation angle	Eccentricity γ	f_{b0} / f_{c0}	k	viscosity
Value	32/34/36/38	0.1	1.16	0.6667	0.0001

3.16 Structural Steel and Reinforcement material modeling

The structural steel section and the reinforcement bars are modeled as an elastic– plastic material in both tension and compression as given in (Euro code 3, 2005), (Abaqus Manual, 2014) and (Euro code 2, 2005). Steel is a ductile material which experiences large inelastic strain beyond the yield point. So the true stress and logarithmic strain graph which is also called hardening curve, as shown in Figure 3.15, is considered for modeling the material behavior of steel. The stress-strain responses in compression and tension are assumed to be the same. This response exhibits a linear elastic portion followed strain hardening stage until reach the ultimate stress. The metal plasticity model in ABAQUS© was used to define the non-linear behavior of

materials. The “ELASTIC” option was used to assign the value of 2.0×10^5 N/mm² for the Young’s modulus and 0.3 for the Poisson’s ratio. The “PLASTIC” option also used to define the plastic part of the stress-strain curve. According to ABAQUS© manual (ABAQUS, 2014), true stress and true Strain should be used to define the non-linear behavior of material properties. So, the true stresses were assigned in ABAQUS© as a function of the true plastic strain. To investigate numerically the Post buckling behavior of the columns it is necessary to represent correctly the inelastic material properties in the FE models. The Mises yield surface is defined by giving the value of the uniaxial yield stress as a function of uniaxial equivalent plastic strain. The curve in Figure 3.15 Named “ABAQUS input” depicts the relation between true stresses σ_{true} And true plastic strain ϵ_{true} : The stress and strain data obtained from the uniaxial tension tests are converted to true stress, σ_{true} And logarithmic plastic strain, ϵ_{true} , for FE analysis using the following relationships:

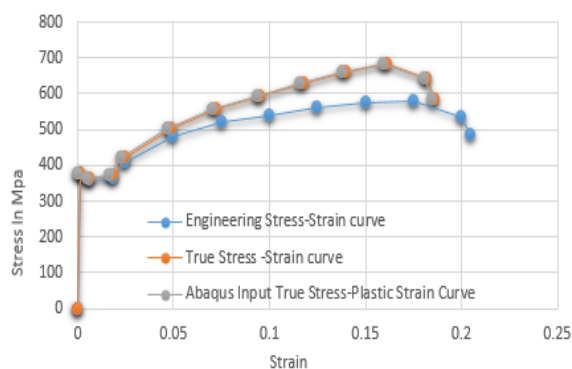
$$\sigma_{true} = \sigma_{nom}(1 + \epsilon_{nom}) \tag{3.24}$$

$$\epsilon_{true} = \ln(1 + \epsilon_{nom}) \tag{3.25}$$

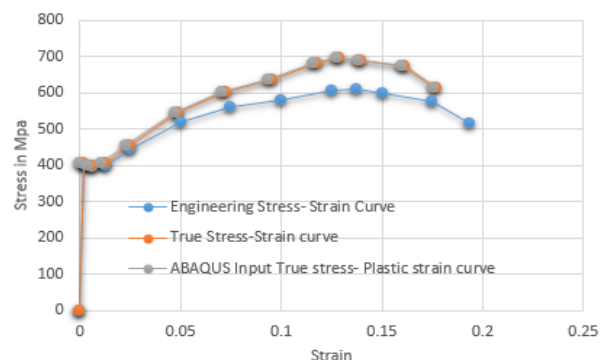
Where;

ϵ_{nom} is the nominal or engineering strain

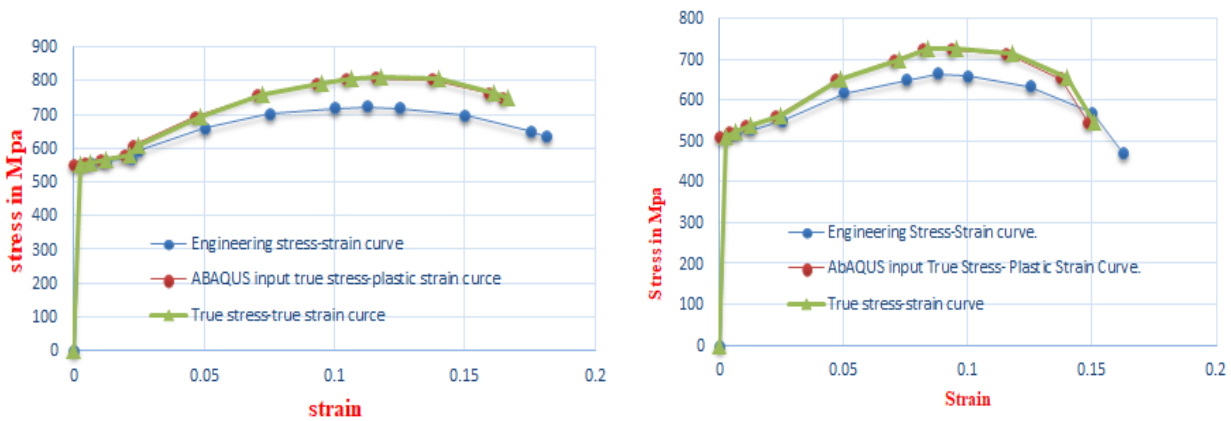
σ_{nom} is the nominal or engineering stress



a. Steel Flange and Plate



b. Steel web



c. Longitudinal Reinforcement bar

b. Transverse Reinforcement

Figure 3. 15: ABAQUS input stress-strain curves for reinforcements and steels(Lai, Liew and Xiong, 2019)

Mechanical properties for the steel section and reinforcement bars that are used in these simulations are given in Table 3.5.

Table 3. 5: Mechanical properties of the steel sections and Reinforcement Bars used for this study(Lai, Liew and Xiong, 2019).

Materials		Yield stress (N/mm ²)	Ultimate stress (N/mm ²)	Density (Kg/m ³)	Young's modulus (N/mm ²)	Poisson ratio
Steel section	flange	375	580	7850	226600	0.3
	web	404	611	7850	223900	0.3
Reinforcement bars	Rebar	550	725	7850	228200	0.3
	Stirrup	510	667	7850	197700	0.3

The mechanical properties of structural steel material coefficients to be adopted in calculations for the structural steels covered by this Eurocode Part should be taken as follows:

Modulus of elasticity $E = 210\,000\text{ N/mm}^2$

Shear modulus $G = E/2(1+\nu) = 81000\text{ N/mm}^2$

Poisson's ratio $\nu = 0.3$

Hot rolled or cold rolled steel was used for composite structure construction. But hot rolled was recommended for their rough surface finish which was used in bondage of concrete to steel.

3.17 PARAMATRIC STUDY

For this parametric study a square column with outer dimensions of 240 mm × 240 mm was selected as per journal. Typical cross section and elevation of FEC column used in the parametric study are shown in Figure 3.6 and Figure 3.7. This column was designed and analyzed during the parametric study to incorporate the effects of several geometric parameters that can significantly affect the FEC column behavior. The geometric variables are compressive strength of concrete, overall length of column and Diameter of longitudinal reinforcement.

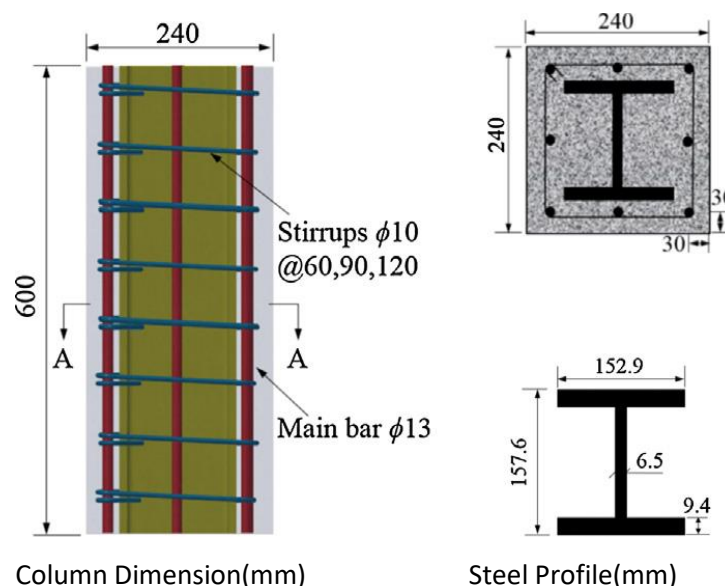


Figure :3.16 a Dimension details of specimen(Lai, Liew and Xiong, 2019)

- a) **Concrete strength:-**The compressive strength concrete used from the journal for validation is C₅₀ and for analysis in this paper are three different concrete strengths like C25, C30 and C35 by five intervals and C50 for control as discussed in the following tables.
- b) **Length of Column (L):-**The different lengths used are 600mm from the journal for control and three different lengths which are 600mm,800mm and 1000mm used for analysis of composite column to know the effect of lengths of column for the same other parameters as explained in the following tables.
- c) **Diameter of longitudinal reinforcement bars:-**The diameter of reinforcement bars used in this study are 13mm for longitudinal reinforcement bars and 10mm for the Transverse reinforcement bars (stirrups).For the analysis two different diameter of reinforcement bars used are 12mm,14mm and 16mm of the same other parameters as the following.

Table 3.6 Independent parameters sample data for column analysis

Group No.	Concrete Grade(MPa)	Length of column(mm)	Diameter longitudinal bar (mm)	Variable Remark
Group-1	C25	600	12	Concrete strength
	C30	600	12	Concrete strength
	C35	600	12	Concrete strength
Group-2	C25	600	12	Length of column
	C25	800	12	Length of column
	C25	1000	12	Length of column
Group-3	C25	600	12	Rebar Diameter
	C25	600	14	Rebar Diameter
	C25	600	16	Rebar Diameter

Table 3. 7: Constant parameters from journal(Lai, Liew and Xiong, 2019)

Thickness of steel sections	Diameter of Reinforcement bars and numbers	Load (KN)	Displacement(mm)	Concrete Cover (mm)	X-Sec Stirrup
$t_f=9.4\text{mm}$ & $t_w=6.5\text{mm}$	Longitudinal(mm)= $8\Phi 13$ Ties(mm)=10	4475.4	5	30	180*180
Structural steel size Encasement type is I-section of $d \times w \times t_f / t_w(\text{mm}) = 157.6*152.9*9.4/6.5(\text{mm})$ Column cross section=240mm*240mm					

CHAPTER FOUR

RESULTS AND DISCUSSIONS

4.1.General

The main purpose of this study was to determine the effects of different compressive strength of concrete and length of column on the axial loading capacity of square rectangular encased, composite columns. To achieve this, a finite element analysis was conducted with all appropriate parameters considered and data was collected. This data was then analyzed to provide understandings into encased composite columns behavior under axial loading. Factors explored included lateral load capacity and axial deformation, Lateral Load versus lateral displacement response (Hysteretic behavior) and failure mode. Observations are made through the aid of plots of output data and photographs in developing relationships between parameters and behavior. Next sections provide a summary of key specimen results.

4.2.VALIDATION OF FINITE ELEMENT MODELLING

An experimental research done by (Lai, Liew and Xiong, 2019). With a title, Experimental study on high strength concrete encased steel composite short columns was used as benchmark experiment. Specimen of column cross section 240mm*240mm with height of 600mm was selected for validation of the models in this thesis.

- **Geometrical property**

Test specimens of the column specimens have the cross section with 240*240 mm dimension and 600 mm height. All specimens are reinforced longitudinally with 8 D13 rebars distributed at the perimeters of section with the distance from rebar centroid to concrete surface equaling to 30 mm, giving a constant reinforcement ratio of 1.84%. 10 mm transverse bars laterally support the main bar with clear spacing of 120 mm, 90 mm or 60 mm, thus giving the volumetric ratio of 1.29%, 1.72% and 2.57%, respectively. It shall be noted that only the core area bounded by the center line of lateral reinforcement is considered in calculating volumetric ratio as adopted by Eid et al. The structural steel encased in concrete adopts the standard British steel section UC152 * 152 * 30, of which the area accounts for 6.56% of the entire section, and this steel section is classified as class 1 according to EN1993-1-1,2015. The compressive strength of concrete cylinders is C50-S120.

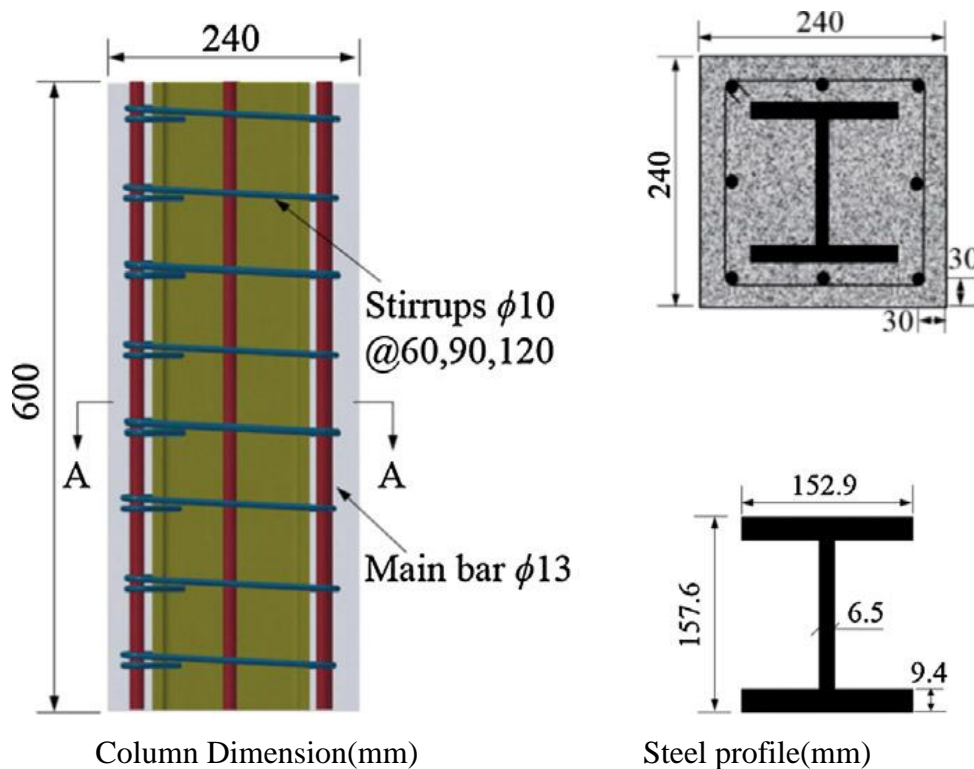


Figure 4. 1: Dimensions Details of test specimens(Lai, Liew and Xiong, 2019)

- **Materials property**

- a) **Concrete**

Standard concrete 240 * 240 mm were cast during casting the column and cured under the same conditions as the test columns. The average compressive strengths at the time of beam testing were 52.3MPa, young's modulus of 32.9Gpa and poisons ratio 0.2.

- b) **Steel property**

Deformed steel bars with diameter of 13mm were used as longitudinal reinforcement and 10mm transverse reinforcement used. The corresponding yield strengths of the Longitudinal and transverse reinforcement bars were a high yield steel with yield strength $f_y = 550\text{Mpa}$ and $f_y = 510\text{Mpa}$ respectively. The ultimate tensile strength (f_u) of reinforcing steel bars are $f_u = 725\text{Mpa}$ for longitudinal bar and $f_u = 667\text{Mpa}$ for transverse reinforcement bars. Similarly for structural steel section the yield steel with yield strength $f_y = 375\text{Mpa}$ for flange and plate and $f_y = 404\text{Mpa}$ for web are given. Also the ultimate tensile strength (f_u) for steel flange and plate are $f_u = 580\text{Mpa}$ and for steel web is $f_u = 611\text{Mpa}$.

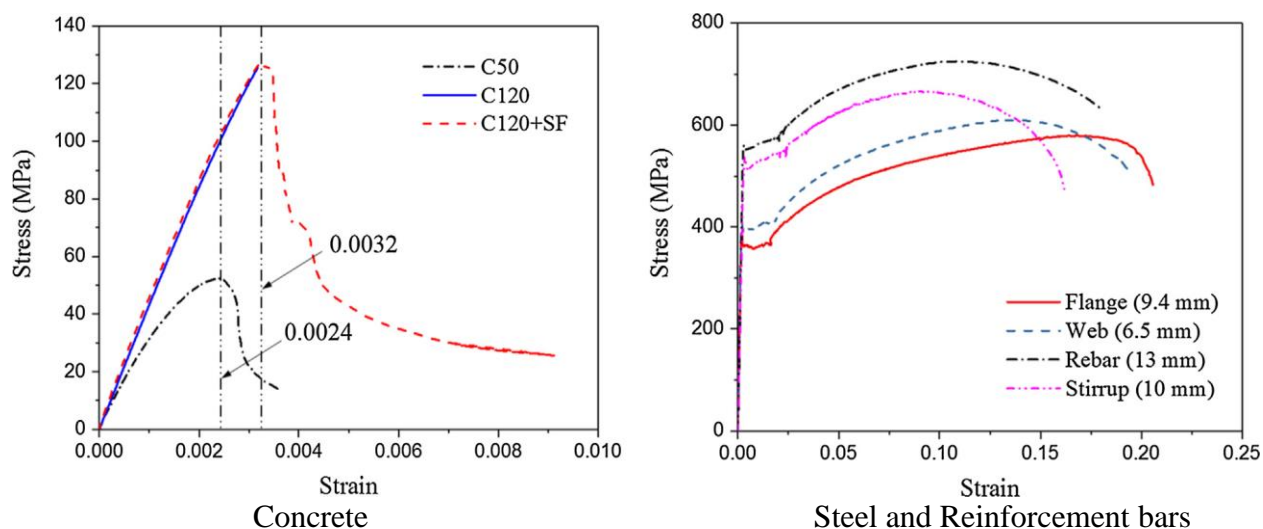


Figure 4. 2: Stress-strain curve of concrete, steel section and reinforcement bars (Lai, Liew and Xiong, 2019)

- **Experimental result**

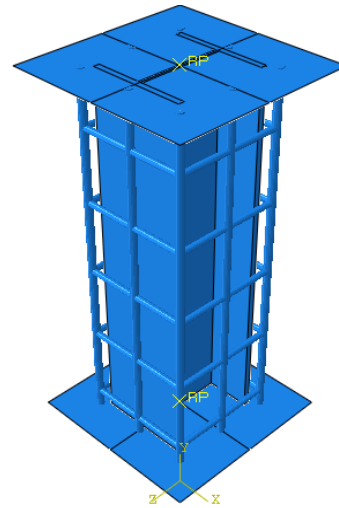
The maximum load is 4475.4 KN and its corresponding deflection is 5mm. Load displacement curve is plotted together with finite element results in Figure 4.5.

4.3 FEA result for validation

Before starting modeling of the research specimen, the validation work was done in order to decide on different parameters. Therefore, using the method, which is described in chapter three, the above described specimen was modeled. Bulk viscosity and mesh size different analysis was done and load-displacement curve was recorded. These of them are selected and presented here together with the experimental curve. Bulk viscosity of zero and mesh size of 20mm had given the load that was closest to the experimental result (4475.4KN)(Lai, Liew and Xiong, 2019). The ultimate load capacity of the modeled Composite column was found to be 4701.012KN. Therefore, the experimental result is about 95.20079% of the FEA result. The difference Between FEA and Experimental test is about 4.80% which is less than 10% is the best result and this proves that ABAQUS program is an appropriate method to predict the Performance of fully encased steel composite columns. Moreover, the load-displacement curve of the FEA result matched with the load-displacement curve of the experimental result. This indicates that FEA result well conformed to the experimental result. Therefore, it has been modeled and analyzed the specimens using this FEA software.

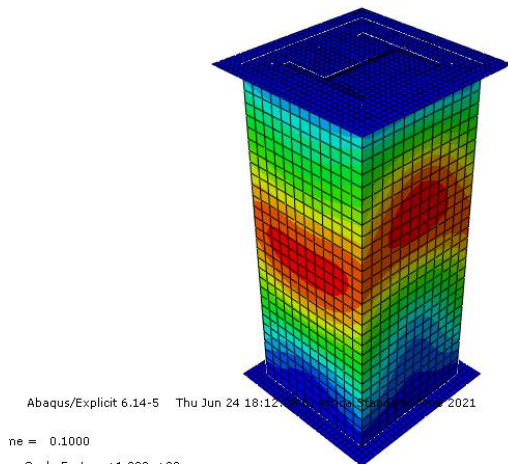


Experiment set up of reinforcements and steel sections

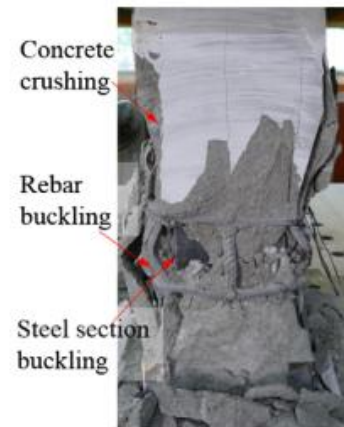


Model of reinforcements and steel sections in ABAQUS

Figure 4. 3: Experiment and FEA Model set up



FEA failure mode



Experiment failure mode

Figure 4. 4: FEA of Experimental for FEC Composite column for validation

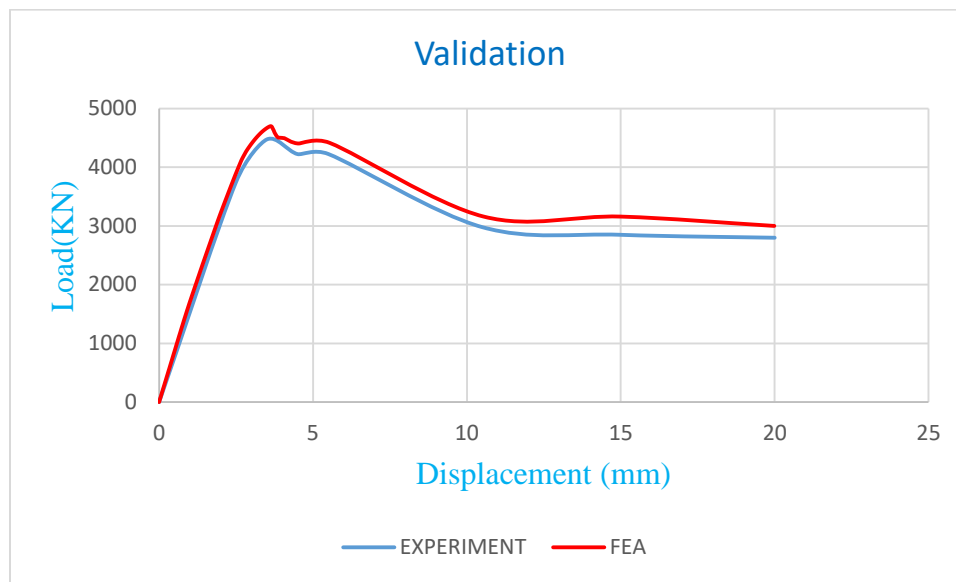


Figure 4. 5: FEA Load-displacement curve Vs. Experimental load-displacement curve

4.4. Results from Analysis

Load and displacement data were taken from the software and the load vs. displacement curves are drawn. From these curves, the ultimate loads and displacements were taken for all of the specimens for each of the Specimens and presented in a tabular form as shown in Figure 4.6.a Show the compressive Concrete Strength as below. The load and displacement data for Length of column effects were shown in Figure 4.6.b and the load and displacement data for diameter of longitudinal bars shown in figure 4.6.c below. The load -displacement curves for all the other specimens are plotted and presented in appendix C of this report.

A. Manual Load Calculation According to Eurocode 4 of Composite Column

According to Eurocode 4, the simplified steps to design encased steel columns subjected to axial are as follows;

1. Determine the ultimate axial load on the column N_{Ed}
2. Select a trial section and determine its properties
3. Obtain the buckling length of the column L
4. Obtain the effective flexural stiffness $(EI)_{eff}$ of the composite section
5. Calculate the plastic resistance to compression of the composite section $N_{pl,Rk}$
6. Calculate the relative slenderness of the section (λ) using Euler's critical load
7. Choose the appropriate buckling curve and calculate the corresponding reduction factor χ

8. Multiply the plastic resistance to compression with the reduction factor to obtain the buckling resistance of the section $N_{b,Rd}$

9. Check if $N_{Ed} < N_{b,Rd}$ else return to step 2.

Given,

At ultimate limit state;

✓ $N_{ED} = 1.35G_k + 1.5Q_k = 4475.4 \text{ kN}$.

✓ The structural steel encased in concrete adopts the standard British steel section UC152 * 152 * 30.

✓ Effective Length of the column = $L_e = 0.7 * L = 0.7 * 600 = 420 \text{ mm}$

✓ Area of UC section (A_a) = 3830 mm^2

✓ Radius of Gyration (i_y) = 67.6 mm

✓ Radius of Gyration (i_z) = 38.30 mm

✓ Design strength (f_y) = 375 N/mm^2 (since the thickness of flange = 9.4 mm)

✓ $I_y = 1748 \text{ cm}^4$

✓ $I_z = 560 \text{ cm}^4$

✓ $E = 226600 \text{ N/mm}^2$

The plastic resistance to compression

$$N_{pl,Rk} = A_a f_y + 0.85 A_c f_{ck} + A_s f_{yk}$$

$$A_a = 3830 \text{ mm}^2$$

$$f_y = 375 \text{ N/mm}^2$$

$$A_c = 240 * 240 = 57,600 \text{ mm}^2$$

$$f_{ck} = 50 \text{ N/mm}^2$$

$$A_s = 1061.86 \text{ mm}^2$$

$$f_{yk} = 550 \text{ N/mm}^2$$

$$N_{pl,Rk} = (3830 * 375) + (0.85 * 57600 * 50) + (1061.86 * 550) * 10^{-3}$$

$$= 4468.27 \text{ kN}$$

The relative Slenderness $\lambda_i = \sqrt{\frac{N_{pl,Rk}}{N_{cr}}}$

$$N_{cr} = \frac{\pi^2 (EI)_{eff}}{L^2}$$

$$(EI)_{eff} = E_a I_a + E_s I_s + 0.6 E_{cm} I_c$$

$$E_a = \text{Elastic Modulus of structural steel} = 226600 \text{ N/mm}^2$$

E_s = Elastic Modulus of reinforcement = 228200 N/mm²

I_a = Moment of inertia of structural steel in relevant axis.

E_{cm} = Modulus of elasticity of concrete = $22(f_{ck}/10)^{0.3}$ (GPa) = 35650 N/mm² (see table 3.1 Eurocode 2)

I_c = Moment of inertia of uncracked concrete section = $bd^3/12 = (240 \times 240^3)/12 = 2764.8 \times 10^5 \text{ mm}^4$

I_s = Moment of inertia of the reinforcement = $\pi D^4/64 = (\pi \times 13^4)/64 = 1401.98 \text{ mm}^4$ (for eight bars = $8 \times 1401.98 = 11215.88 \text{ mm}^4$

Hence;

$$(EI)_{eff,y} = (226600 \times 1748 \times 10^4) + (228200 \times 11215.88) + (0.6 \times 35650 \times 2764.8 \times 10^5) \\ = 9.87743 \times 10^{12} \text{ N.mm}^2$$

$$(EI)_{eff,z} = (226600 \times 560 \times 10^4) + (228200 \times 11215.88) + (0.6 \times 35650 \times 2764.8 \times 10^5) \\ = 7.18543 \times 10^{12} \text{ N.mm}^2$$

$$N_{cr,y} = \left[\frac{\pi^2 \times (9.87743 \times 10^{12})}{420^2} \right] \times 10^{-3} = 552643.57483 \text{ KN.}$$

$$N_{cr,z} = \left[\frac{\pi^2 \times (7.18543 \times 10^{12})}{420^2} \right] \times 10^{-3} = 402025.80245 \text{ KN.}$$

$$\lambda_y = \sqrt{\frac{4468.27}{552643.57483}} = 0.09$$

$$\lambda_z = \sqrt{\frac{4468.27}{402025.80245}} = 0.11$$

Check h/b ratio = $157.6/152.9 = 1.03 < 1.2$, and $t_f < 100 \text{ mm}$ (table 6.2 EN 1993-1-1:2005)

Therefore buckling curve b is appropriate for y-y axis, and buckling curve c for z-z axis. The imperfection factor for buckling b = 0.34 and curve c = 0.49 (Table 6.1)

$$\phi = 0.5 \left[1 + \alpha (\bar{\lambda} - 0.2) + \bar{\lambda}^2 \right]$$

$$\phi_y = 0.5 [1 + 0.34(0.09 - 0.2) + 0.09^2] = 0.49$$

$$\phi_z = 0.5 [1 + 0.49(0.11 - 0.2) + 0.11^2] = 0.48$$

$$X = \frac{1}{\phi + \sqrt{\phi^2 - \lambda^2}}$$

$$X_y = 1 / [0.49 + (0.49^2 - 0.09^2)^{0.5}] = 1.03$$

$$X_z = 1 / [0.48 + (0.48^2 - 0.11^2)^{0.5}] = 1.05$$

Therefore $N_{b,Rd}=(X_y N_{PL,Rk})=(1.03*4468.27)= 4,602.3181\text{KN}$

$N_{Ed}/ N_{b,Rd}=4475.4/4,602.3181=0.972423<1.00 \dots\dots\dots\text{OK.}$

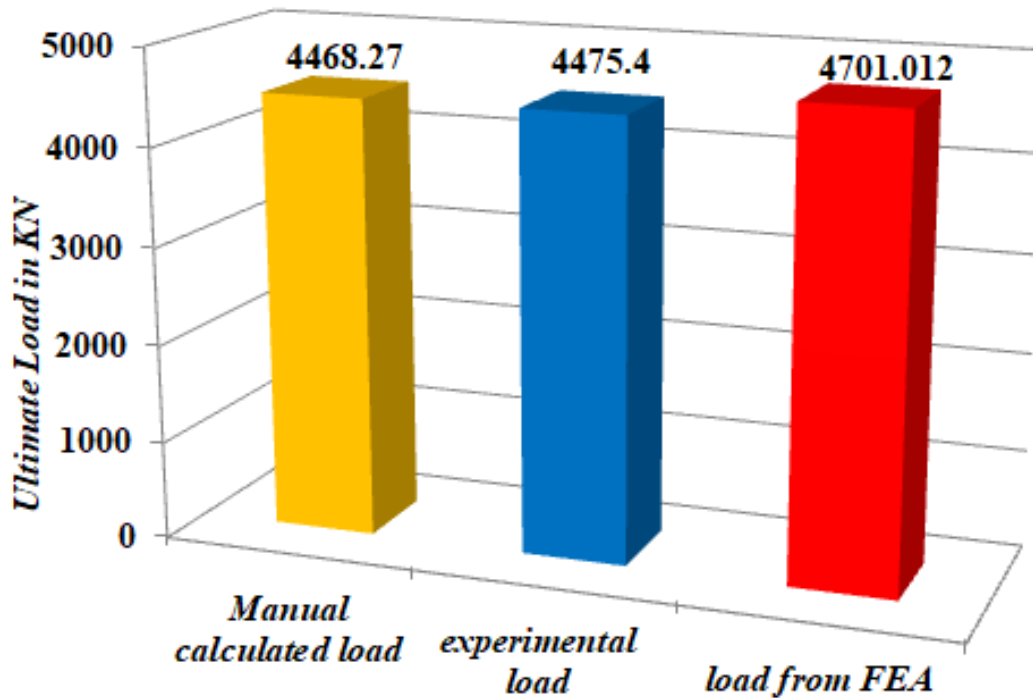


Figure 4.6. Loads from manual calculation, Experimental load and Load from FEA

B.Effects of Concrete strength

The performance or the load capacity of the composite columns increased with increasing concrete strengths, from concrete grade C25 to C30 the load capacity increased by 6.38% from 3901.606KN to 4167.429KN and between C30 to C35 there is 5.93% capacity interval from 4167.429KN to 4430.213KN and the average difference capacity between C25 and C35 is about 11.93% as shown in Table 4.1 and Figure 4.6a. In general from this finite element analysis of composite columns by varying compressive concrete strength we can conclude as the higher compressive concrete strength have high load bearing capacity in fully encased steel composite columns.

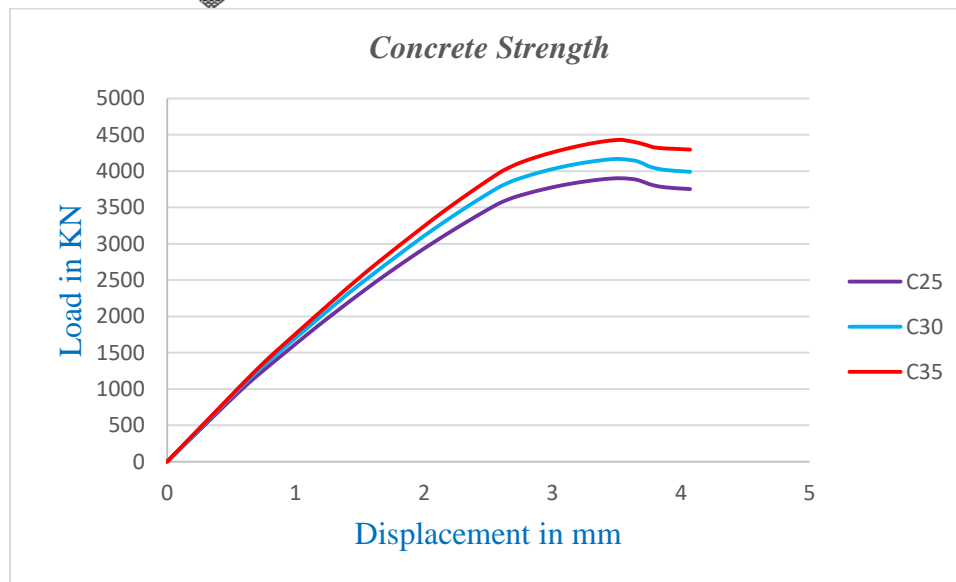
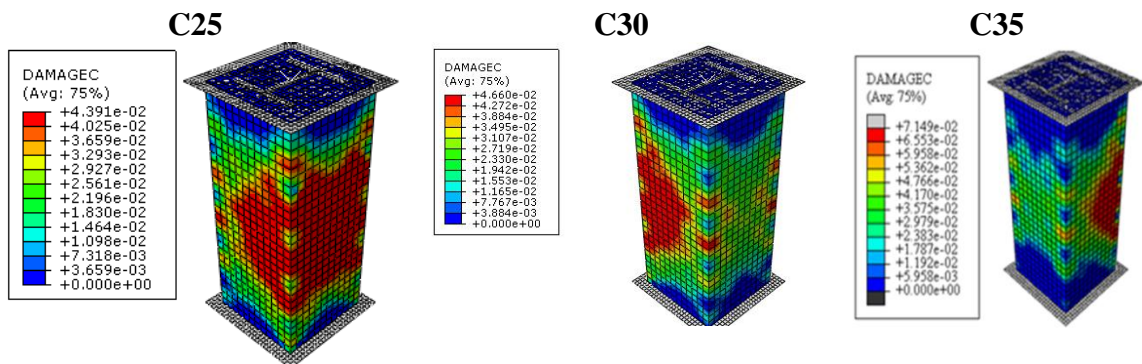


Figure: 4.7 Effects of Concrete Strength

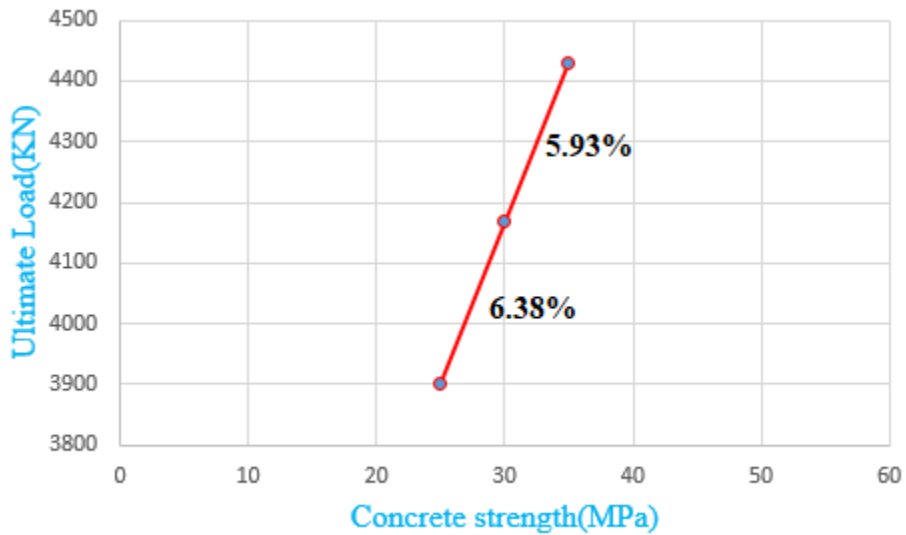


Figure 4.8 Result comparisons between concrete strengths Vs Ultimate loads

Table 4. 1:-Load -Displacement of concrete strength (C25, C30, C35)

<i>Concrete strengths</i>					
C25		C30		C35	
U2(mm)	RF2(KN)	U2(mm)	RF2(KN)	U2(mm)	RF2(KN)
0	3.1E-20	0	3.1E-20	0	3.1E-20
0.18908	325.609	0.18908	338.77	0.18908	345.575
0.2102	362.252	0.2102	376.328	0.2102	384.034
0.42096	724.811	0.42096	754.23	0.42096	768.743
0.44196	761.208	0.44196	791.909	0.44196	807.354
0.65196	1108.93	0.65196	1159.94	0.65196	1187.83
0.67296	1141.51	0.67296	1195.16	0.67296	1224.89
0.88296	1450.48	0.88296	1524.72	0.88296	1574.95
0.90396	1481.04	0.90396	1556.68	0.90396	1608.23
1.11396	1784.24	1.11396	1875.4	1.11396	1939.16
1.13496	1814.18	1.13496	1907.12	1.13496	1972.22
1.36596	2133.19	1.36596	2250.41	1.36596	2333.72
1.57989	2417.39	1.57989	2550.58	1.57989	2655.07
1.60136	2445.32	1.60136	2579.71	1.60136	2686.06
1.81602	2713.91	1.81602	2867.41	1.81602	2988.24
1.83749	2740.1	1.83749	2895.89	1.83749	3018.06
2.05216	2993.25	2.05216	3172.98	2.05216	3312.88
2.07362	3017.61	2.07362	3199.4	2.07362	3341.85
2.25743	3221.24	2.25743	3419.52	2.25743	3580.31
2.27756	3242.83	2.27756	3443	2.27756	3605.61
2.45868	3432.42	2.45868	3647.36	2.45868	3827.64
2.47881	3452.87	2.47881	3669.16	2.47881	3851.62
2.68006	3626.41	2.68006	3858.18	2.68006	4063.75
2.85739	3718.06	2.85738	3961.15	2.85737	4183.34
2.87664	3726.71	2.87663	3970.98	2.87662	4194.1
3.04989	3795.98	3.04988	4048.95	3.04987	4281.42
3.26164	3859.23	3.26163	4120.23	3.26162	4367.11
3.43489	3894.62	3.43488	4159.55	3.43487	4417.31
3.45414	3897.03	3.45413	4162.55	3.45412	4420.98
3.62739	3889.07	3.62738	4147.05	3.62737	4403.47
3.81989	3791.32	3.81988	4031.58	3.81987	4319.91
3.83914	3785.42	3.83913	4025.86	3.83912	4316.68
4.01239	3758.89	4.01238	3997.31	4.01237	4301.27
4.07014	3752.4	4.07013	3989.91	4.07012	4295.63

C. Effects of Length of column

The performance or the load capacity of the composite columns decreased with increasing Length of column, from 600mm to 800mm the load capacity reduced by 3.50% from 3900KN to 3765.156KN and between 800mm to 1000mm load capacity reduced by 10.20% capacity interval from 3765.156KN to 3380KN and the average difference capacity between 600mm column length to and 1000mm there is a reduction about 13.30% as shown in Table 4.2 and Figure 4.6b. In general from this finite element analysis of composite columns by varying Length of column we can conclude as the Longer columns have less load capacity in fully encased steel composite columns.

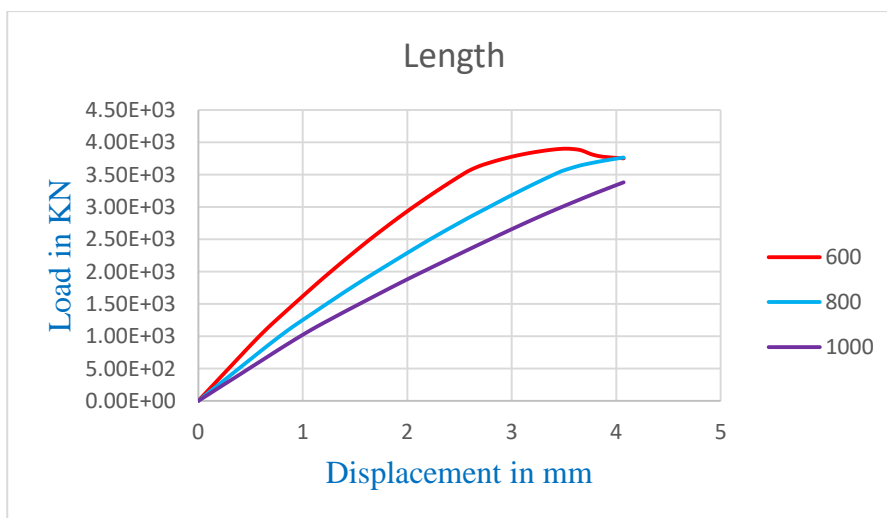
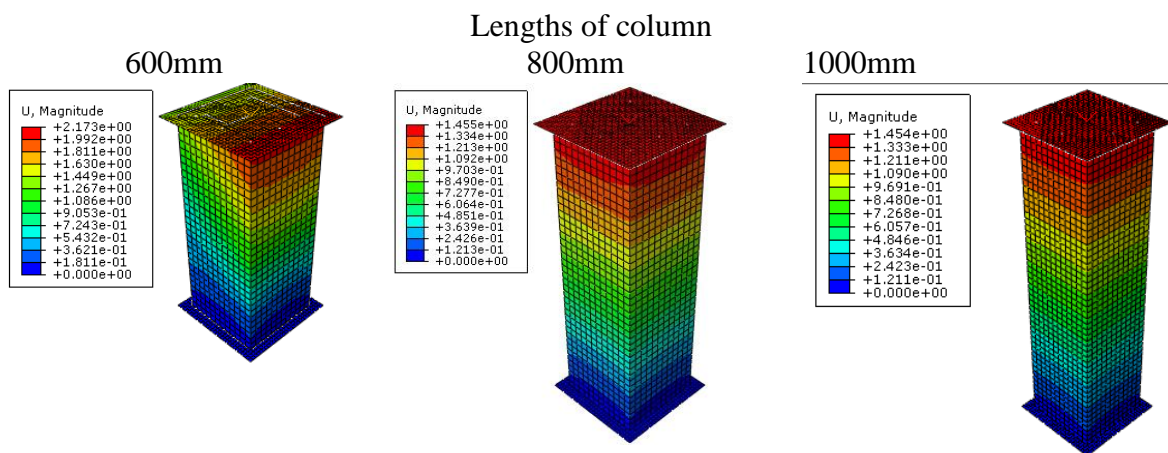


Figure: 4.9. Effects of Column Length

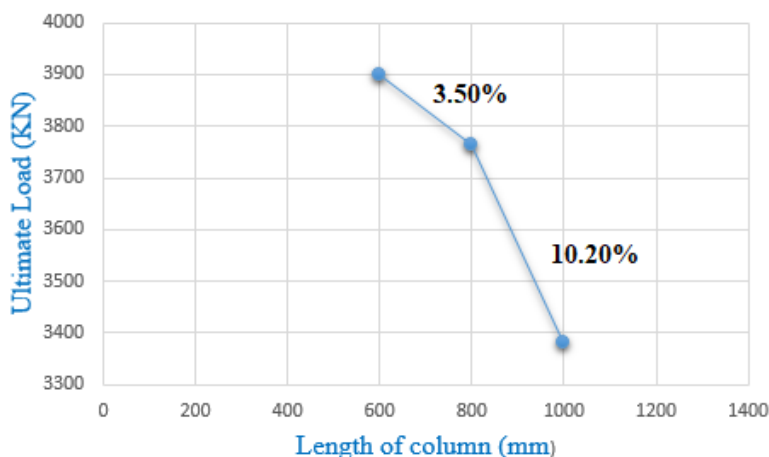


Figure 4.10. Result comparison between column lengths Vs ultimate loads

Table 4. 2: Load Vs. Displacements of Lengths of column.

Length of columns					
600mm		800mm		1000mm	
U2(mm)	RF2(KN)	U2(mm)	RF2(KN)	U2(mm)	RF2(KN)
0	3.1E-20	0	0	0	0
0.18908	325.609	0.18908	243.187	0.18908	194.405
0.2102	362.252	0.21019	271.121	0.21019	216.37
0.42096	724.811	0.42096	542.164	0.42096	432.663
0.44196	761.208	0.44196	569.299	0.44196	454.526
0.65196	1108.93	0.65196	839.715	0.65196	671.136
0.67296	1141.51	0.67296	866.172	0.67296	692.904
0.88296	1450.48	0.88296	1121.79	0.88296	906.902
0.90396	1481.04	0.90396	1145.89	0.90396	927.956
1.11396	1784.24	1.11396	1375.73	1.11396	1129.63
1.13496	1814.18	1.13496	1398.5	1.13496	1148.73
1.34496	2104.6	1.34496	1625.38	1.34496	1331.71
1.36596	2133.19	1.36596	1647.98	1.36596	1349.87
1.57989	2417.39	1.57983	1871.34	1.5798	1531.07
1.60136	2445.32	1.6013	1893.16	1.60127	1549.09
1.81602	2713.91	1.81597	2106.74	1.81593	1728.93
1.83749	2740.11	1.83744	2127.89	1.8374	1746.8
2.05216	2993.25	2.0521	2339.05	2.05207	1922.03
2.07362	3017.61	2.07357	2360.12	2.07353	1939.05
2.25743	3221.24	2.25738	2535.62	2.25734	2084.04
2.27756	3242.83	2.2775	2554.29	2.27747	2099.83

2.45868	3432.42	2.45862	2719.04	2.45859	2241.71
2.47881	3452.87	2.47875	2737.14	2.47872	2257.21
2.65993	3612.77	2.65988	2896.25	2.65984	2398.19
2.68006	3626.41	2.68	2913.41	2.67997	2413.41
2.85739	3718.06	2.85751	3064	2.8576	2548.98
2.87664	3726.71	2.87676	3080.34	2.87685	2563.42
3.04989	3795.98	3.05001	3225.05	3.0501	2693.98
3.06914	3802.71	3.06926	3240.7	3.06935	2708.06
3.24239	3854.41	3.24251	3378.6	3.2426	2834.87
3.26164	3859.23	3.26176	3393.59	3.26185	2848.64
3.43489	3894.62	3.43501	3524.9	3.4351	2970.17
3.45414	3897.03	3.45426	3538.79	3.45435	2982.86
3.62739	3889.07	3.62751	3630.17	3.6276	3100.08
3.64664	3883.88	3.64676	3638.88	3.64685	3112.08
3.81989	3791.32	3.82001	3697.66	3.8201	3225.71
3.83914	3785.42	3.83926	3703.46	3.83935	3237.21
4.01239	3758.89	4.01251	3751.01	4.0126	3346.02
4.07014	3752.4	4.07026	3765.16	4.07035	3380.8

D.Effects of Diameter of Longitudinal Reinforcement Bars

The performance or the load capacity of the composite columns increased with increasing diameter of longitudinal reinforcement bars, from concrete grade 12mm to 14mm the load capacity increased by 4.14% from 3900KN to 4070KN and between 14mm to 16mm there is 4.77% capacity interval from 4070KN to 4274.086KN and the average difference capacity between 12mm and 16mm is about 8.71% as shown in [Table 4.3](#) and [Figure 4.6c](#). In general from this finite element analysis of composite columns by varying diameter of longitudinal reinforcement Bars we can conclude as the higher diameter of longitudinal reinforcement bars have high load bearing capacity in fully encased steel composite columns.

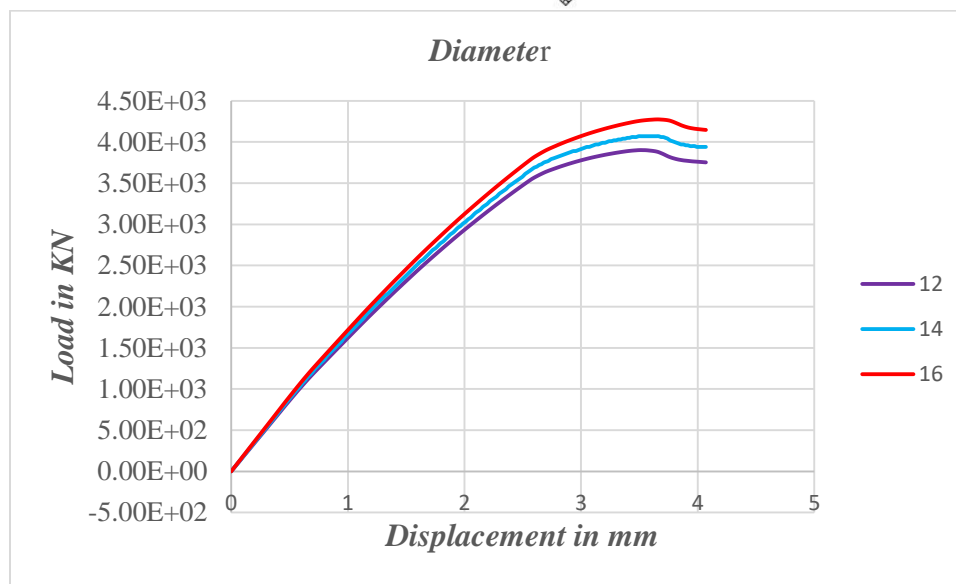
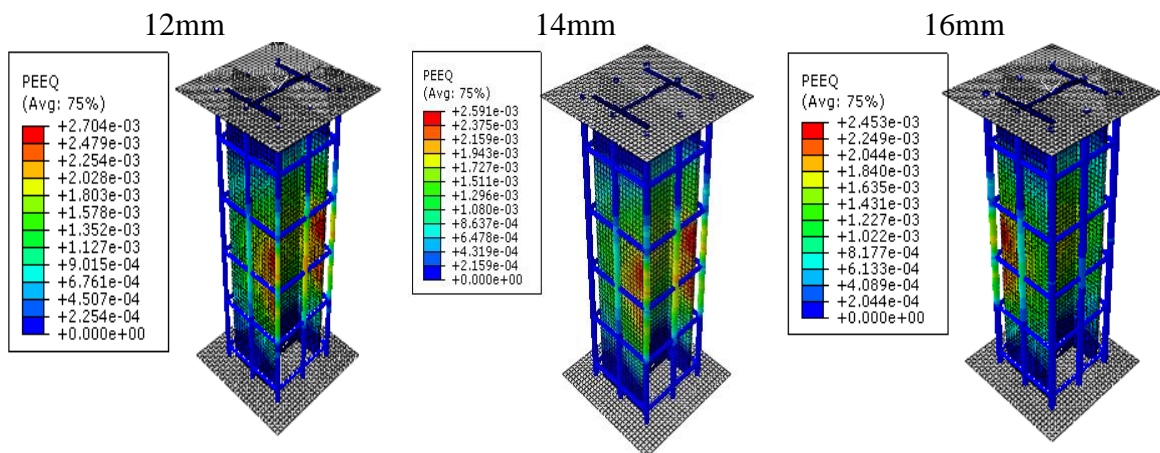


Figure: 4.11.Effects of diameter of longitudinal bars

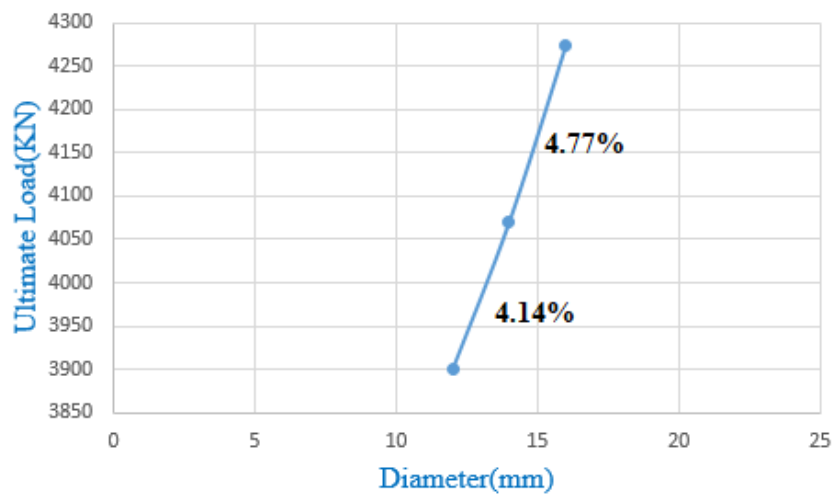


Figure 4.12 Comparison between longitudinal reinforcement bar Vs. Ultimate load

Table 4. 3: Load verses Displacements of Diameters of longitudinal reinforcement bars

<i>Diameter of Longitudinal bar</i>					
12mm		14mm		16mm	
U2(mm)	RF2(KN)	U2(mm)	RF2(KN)	U2(mm)	RF2(KN)
0	3.1E-20	0	0	0	-1.6E-20
0.18908	325.609	0.18908	334	0.18908	344.1221
0.2102	362.252	0.21019	372	0.21019	382.3014
0.42096	724.811	0.42096	744	0.42096	765.1818
0.44196	761.208	0.44196	781	0.44196	803.4915
0.65196	1108.93	0.65196	1140	0.65196	1171.407
0.67296	1141.51	0.67296	1170	0.67296	1206.026
0.88296	1450.48	0.88296	1490	0.88296	1535.228
0.90396	1481.04	0.90396	1520	0.90396	1567.792
1.11396	1784.24	1.11396	1830	1.11396	1891.21
1.13496	1814.18	1.13496	1860	1.13496	1923.169
1.34496	2104.6	1.34496	2160	1.34496	2233.895
1.36596	2133.19	1.36596	2190	1.36596	2264.548
1.57989	2417.39	1.57989	2490	1.57989	2568.954
1.60136	2445.32	1.60136	2520	1.60136	2598.96
1.81602	2713.91	1.81602	2790	1.81602	2887.953
1.83749	2740.11	1.83749	2820	1.83749	2916.265
2.05216	2993.25	2.05216	3080	2.05216	3189.876
2.07362	3017.61	2.07362	3110	2.07362	3216.345
2.25743	3221.24	2.25743	3320	2.25743	3437.573
2.27756	3242.83	2.27756	3340	2.27756	3461.112
2.45868	3432.42	2.45868	3540	2.45868	3667.647
2.47881	3452.87	2.47881	3560	2.47881	3690.087
2.65993	3612.77	2.65993	3730	2.65993	3869.376
2.68006	3626.41	2.68006	3750	2.68006	3885.074
2.85739	3718.06	2.85739	3850	2.8574	3996.637
2.87664	3726.71	2.87664	3860	2.87665	4007.357
3.04989	3795.98	3.04989	3940	3.0499	4095.591
3.06914	3802.71	3.06914	3940	3.06915	4104.447
3.24239	3854.41	3.24239	4010	3.2424	4175.854
3.26164	3859.23	3.26164	4010	3.26165	4182.901
3.43489	3894.62	3.43489	4060	3.4349	4239.52
3.45414	3897.03	3.45414	4060	3.45415	4245.006
3.62739	3889.07	3.62739	4070	3.6274	4272.869

3.64664	3883.88	3.64664	4070	3.64665	4274.086
3.81989	3791.32	3.81989	3990	3.8199	4226.981
3.83914	3785.42	3.83914	3980	3.83915	4215.249
4.01239	3758.89	4.01239	3940	4.0124	4154.791
4.07014	3752.4	4.07014	3940	4.07016	4146.366

E. The effect of equivalent area and different diameter/numbers of longitudinal reinforcement bars

Under this concept the diameters of longitudinal reinforcement bars are 12mm, 13mm and 14mm with 8 numbers of longitudinal reinforcement bars with the corresponding equivalent area of longitudinal reinforcement bars are 24mm, 26mm and 28mm with 4 numbers of longitudinal reinforcement bars respectively. The following are graphs from the ABACUS results which used to compare the effect of equivalent area and different diameter/numbers of longitudinal reinforcement bars.

i. #8Φ12mm and #4Φ24mm

As introduced in the following graph and table the #4Φ24mm is with ultimate load 5710KN has the greater load carrying capacity than #8Φ12mm is with ultimate load 3900KN about 31.60%.

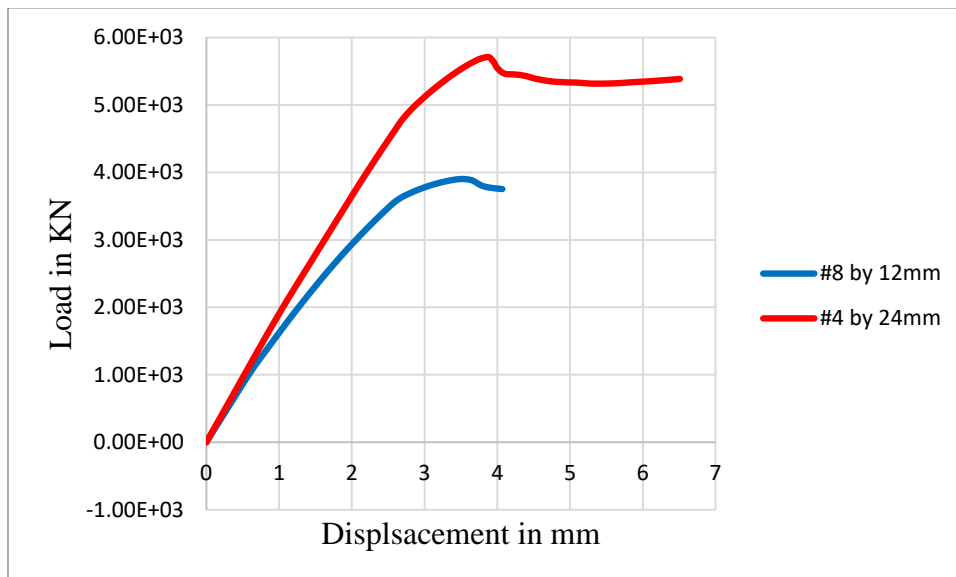


Figure 4.13 the effects between #8Φ12mm and #4Φ24mm.

ii. #8Φ13mm and #4Φ26mm

As introduced in the following graph and table the #4Φ26mm is with ultimate load 5200KN has the greater load carrying capacity than #8Φ13mm is with ultimate load 4700KN about 9.63%.The ultimate load from experimental is 4475.4KN which is 4.80% from #8Φ13mm.

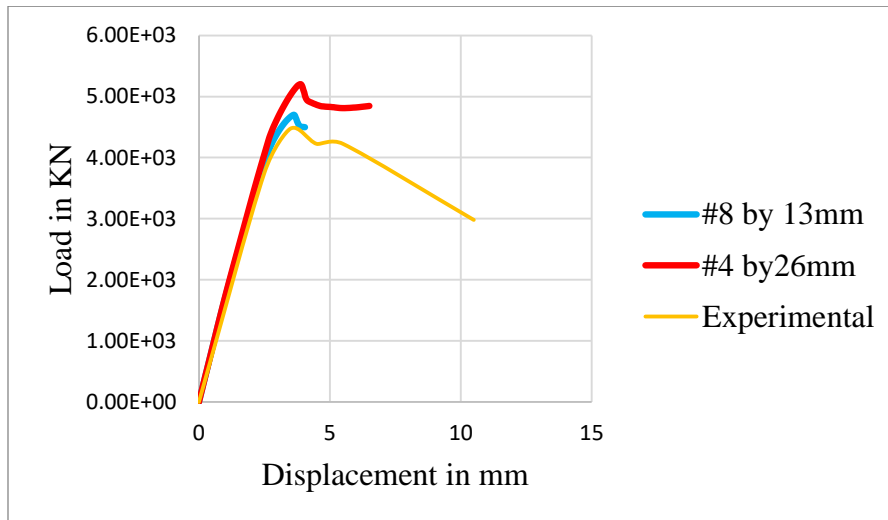


Figure 4.14. The effects between #8Φ13mm and #4Φ26mm

iii. #8Φ14mm and #4Φ28mm

As introduced in the following graph and table the #4Φ28mm is with ultimate load 6060KN has the greater load carrying capacity than #8Φ14mm is with ultimate load 4070KN about 32.90%.

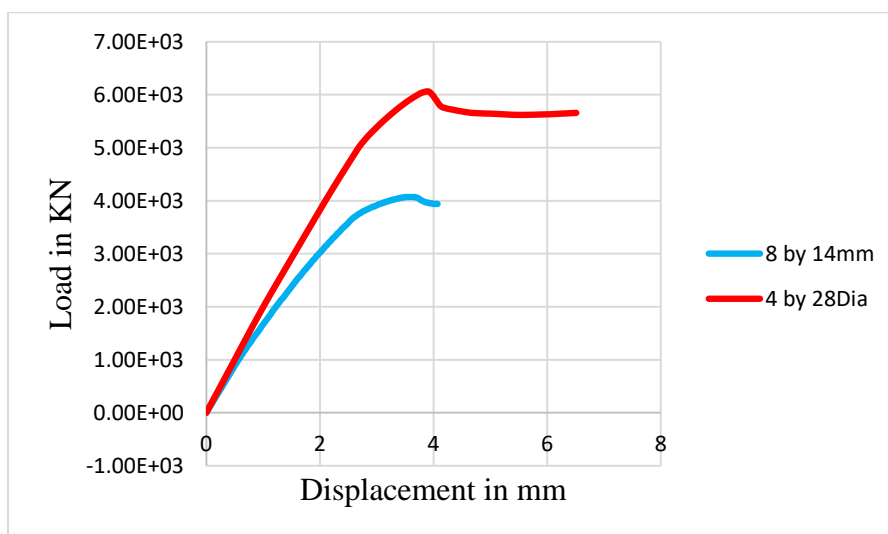


Figure 4.15. The effects between #8Φ14mm and #4Φ28mm

Table 4.4. Euivalent area effects of longitudinal bars

#8 by 12mm		#4 by 24mm	
U2	RF2	U2	RF2
0	3.08E-20	0	-9.3E-20
0.189078	325.6087	0.302625	578.824
0.210195	362.252	0.336342	642.2859
0.420959	724.8105	0.672384	1287.506
0.441959	761.2081	0.705985	1351.761
0.651959	1108.927	1.041985	1979.183
0.672958	1141.51	1.075582	2039.712
0.882959	1450.482	1.411585	2626.842
0.903958	1481.038	1.445182	2685.117
1.113958	1784.239	1.781182	3268.062
1.134958	1814.182	1.814783	3326.254
1.344958	2104.597	2.150782	3903.856
1.365958	2133.185	2.184383	3960.099
1.579889	2417.393	2.520383	4507.659
1.601356	2445.318	2.553983	4561.379
1.816023	2713.909	2.889983	5007.97
1.83749	2740.105	2.923584	5041.501
2.052156	2993.247	3.259583	5346.166
2.073623	3017.608	3.293184	5373.538
2.257432	3221.239	3.580884	5581.919
2.277557	3242.832	3.612385	5601.498
2.45868	3432.418	3.895882	5700.757
2.478806	3452.868	3.927383	5665.883
2.680057	3626.408	4.242384	5449.044
2.857387	3718.062	4.525885	5387.931
2.876635	3726.712	4.557382	5380.409
3.049886	3795.978	4.840883	5339.513
3.069136	3802.712	4.872384	5338.232
3.242387	3854.407	5.155884	5325.271
3.261637	3859.226	5.187385	5322.685
3.454136	3897.032	5.502383	5315.464
3.627386	3889.074	5.785882	5329.797
3.646637	3883.876	5.817383	5332.091
3.839135	3785.417	6.132381	5351.983
4.012386	3758.885	6.415881	5375.242
4.070138	3752.396	6.510385	5383.191

#8 by 13mm		#4 by 26mm	
U2	RF2	U2	RF2
0	3.88E-20	0	4.57E-20
0.189078	326.3719	0.302625	522.9076
0.210193	362.9522	0.336342	581.9415
0.420958	727.2502	0.672384	1164.663
0.44196	763.6191	0.705985	1223.139
0.65196	1127.568	1.041985	1791.092
0.672958	1163.587	1.075582	1845.937
0.88296	1517.738	1.411585	2378.396
0.903958	1552.21	1.445183	2431.261
1.113958	1884.157	1.781182	2960.041
1.134958	1916.619	1.814783	3012.828
1.365958	2272.942	2.184383	3588.047
1.579889	2596.701	2.520383	4085.631
1.601356	2628.95	2.553983	4134.475
1.816021	2951.311	2.889983	4542.872
1.837489	2983.482	2.923584	4573.855
2.052156	3293.308	3.259583	4856.649
2.073624	3323.143	3.293184	4882.173
2.257433	3575.488	3.580884	5078.037
2.277556	3602.874	3.612385	5096.592
2.45868	3846.865	3.895882	5200.915
2.478806	3873.422	3.927383	5183.62
2.680056	4126.793	4.242384	4910.509
2.857366	4294.922	4.525885	4860.203
2.876616	4310.22	4.557382	4855.894
3.049866	4435.865	4.840883	4834.08
3.069116	4448.756	4.872384	4833.374
3.242366	4552.912	5.155884	4824.347
3.454116	4652.151	5.502383	4810.785
3.627366	4701.012	5.785884	4814.876
3.646616	4697.635	5.817385	4815.96
3.839116	4520.924	6.132383	4826.914
4.012366	4500.091	6.415884	4840.808
4.070119	4495.895	6.510387	4845.802

#8 by 14mm		#4 by 28Dia	
U2	RF2	U2	RF2
0	-3E-20	0	-2.6E-21
0.189078	334	0.302625	604.9877
0.210193	372	0.336342	672.7734
0.420958	744	0.672384	1347.289
0.44196	781	0.705985	1414.624
0.65196	1140	1.041985	2072.084
0.672958	1170	1.075582	2135.614
0.88296	1490	1.411585	2752.828
0.903958	1520	1.445183	2814.117
1.113958	1830	1.781182	3427.188
1.134958	1860	1.814783	3488.394
1.344958	2160	2.150783	4096.239
1.365958	2190	2.184383	4155.512
1.579892	2490	2.520383	4733.326
1.601356	2520	2.553983	4790.076
1.816024	2790	2.889983	5267.302
1.837492	2820	2.923584	5303.835
2.052156	3080	3.259583	5639.258
2.073624	3110	3.293184	5669.69
2.257433	3320	3.580884	5904.556
2.277559	3340	3.612385	5927.07
2.458683	3540	3.895882	6062.768
2.478806	3560	3.927383	6053.198
2.659933	3730	4.210883	5746.366
2.680059	3750	4.242384	5736.458
2.857389	3850	4.525885	5679.031
2.876636	3860	4.557382	5673.489
3.049886	3940	4.840883	5647.348
3.069136	3940	4.872384	5646.38
3.261639	4010	5.187385	5633.49
3.434886	4060	5.470882	5619.51
3.454136	4060	5.502383	5619.275
3.819889	3990	6.100885	5634.489
3.839136	3980	6.132383	5636.276
4.012386	3940	6.415883	5651.496
4.070139	3940	6.510387	5657.195

F. Confinement of effects by transverse reinforcement bars with different diameters and spacing.

The 6mm diameters of transverse reinforcement bars with 6c/c60mm spacing, the 8mm diameters of transverse reinforcement bars with 8c/c 90mm spacing and the 10mm diameters of transverse reinforcement bars with 10c/c120mm spacing are considered. The following are graphs from the ABACUS results which used to compare the Confinement of effects of transverse reinforcement bars by different diameters and spacing.

As introduced in the following graph and table the 10c/c120mm is with ultimate load 3765.156KN has the greater load carrying capacity than 8c/c90mm is with ultimate load 3695.671KN and 6c/c60mm is with ultimate load 3695.661KN by 1.845475% and by 1.84574% respectively. The 8c/c90mm has the greater load carrying capacity than 6c/c60mm by 0.000271%. Since the diameters and the spacing's of transverse reinforcement bars used for analysis are according to how to design concrete structures using Eurocode 2 standards their confinement effects by transverse reinforcement bars on load carrying capacity of composite columns haven't more difference as it shown on the following [Figure 4.16](#) below.

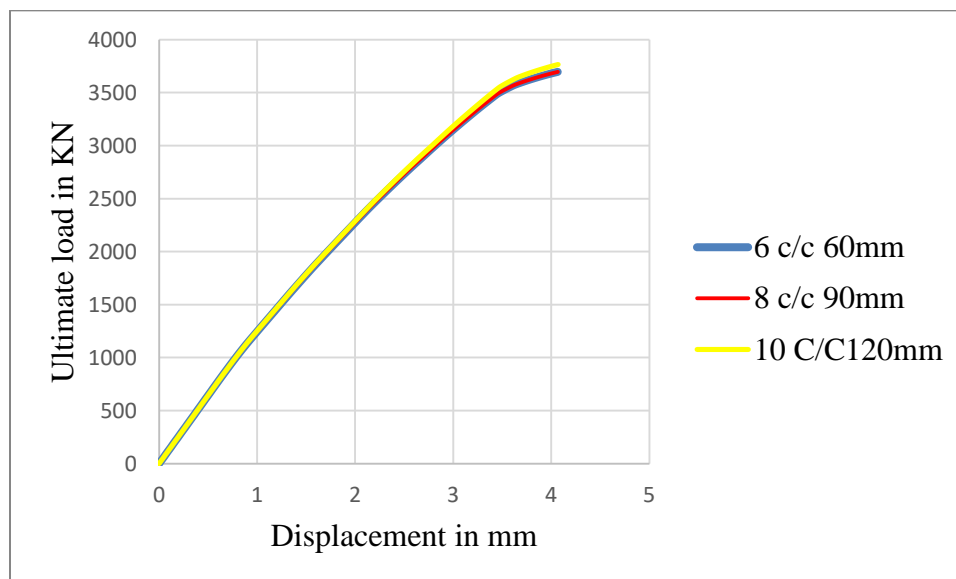


Figure 4.16. Confinement effects of transverse reinforcement bars

Table 4.5. Confinement effects of transverse reinforcement bars

6c/c60mm		8c/c90mm		10C/C120mm	
U2	RF2	U2	RF2	U2	RF2
0	0	0	0	0	0
0.189098	242.8077	0.189092	242.8163	0.189078	243.1869
0.210215	270.1691	0.210207	270.1795	0.210193	271.1211
0.420894	541.1651	0.420915	541.1778	0.420963	542.1635
0.441893	568.2152	0.441913	568.2243	0.44196	569.2993
0.651895	838.3925	0.651913	838.4043	0.65196	839.7151
0.672893	864.8306	0.672913	864.8468	0.67296	866.1717
0.882893	1117.946	0.882913	1117.972	0.88296	1121.791
0.903893	1141.465	0.903913	1141.49	0.90396	1145.888
1.113893	1369.146	1.113913	1369.183	1.11396	1375.73
1.134893	1391.791	1.134913	1391.838	1.13496	1398.503
1.345068	1618.107	1.344913	1618.155	1.34496	1625.376
1.366534	1640.659	1.366136	1640.711	1.36596	1647.978
1.5812	1863.23	1.580803	1863.288	1.579833	1871.339
1.602668	1884.712	1.60227	1884.779	1.6013	1893.161
1.817334	2096.203	1.816936	2096.282	1.815968	2106.735
1.838801	2117.179	1.838403	2117.258	1.837436	2127.894
2.053468	2326.238	2.05307	2326.316	2.0521	2339.045
2.074935	2346.942	2.074537	2347.018	2.073568	2360.12
2.258743	2517.918	2.258345	2517.995	2.257377	2535.617
2.278867	2536.146	2.278469	2536.215	2.2775	2554.285
2.459992	2697.508	2.459594	2697.591	2.458624	2719.035
2.480117	2715.099	2.479719	2715.182	2.47875	2737.136
2.66081	2868.82	2.660845	2868.933	2.659877	2896.25
2.68006	2885.295	2.68097	2885.391	2.68	2913.412
2.853312	3030.944	2.854526	3031.002	2.857509	3063.999
2.87256	3046.817	2.873776	3046.864	2.876759	3080.342
3.045811	3186.03	3.047026	3186.158	3.050009	3225.045
3.065061	3201.104	3.066276	3201.22	3.069259	3240.703
3.238311	3334.404	3.239527	3334.547	3.242509	3378.597
3.25756	3348.855	3.258776	3349.002	3.261759	3393.587
3.43081	3475.348	3.432026	3475.494	3.435009	3524.904
3.450061	3488.397	3.451276	3488.546	3.454259	3538.787
3.623311	3571.762	3.624526	3571.836	3.627509	3630.169
3.642561	3578.774	3.643777	3578.84	3.646759	3638.881
3.815812	3632.822	3.817025	3632.859	3.820009	3697.655
3.83506	3638.245	3.836276	3638.294	3.839259	3703.457

CHAPTER FIVE

CONCLUSIONS AND RECOMMENDATIONS

5.1 Conclusions

The aim of this study was to assess the Performance of fully encased composite columns under axial loading using non-linear analysis by ABAQUS/CAE .The result shows that from normal strength of concrete the higher strength is better for load carrying capacity of composite Steel-concrete column construction where high load of structure happen. The performance of composite columns specified in this study was investigated using nonlinear finite element method. The effect of strength of concrete, Length of column and Diameters of longitudinal reinforcements on composite columns was assessed. A nonlinear 3-D finite element models were developed to model different composite columns and Based on the Findings of this study, and within the present scope of work and performances carryout, After the careful check of the analysis results, the following conclusions are drawn. The load capacity of the composite columns increased by 6.38% and 5.93% with increasing concrete strengths from C25 to C30 and C35 decreased from 3.50% to10.20% with increasing column lengths from 600mm to 800mm and 1000mm respectively. As the diameter of longitudinal reinforcement of Composite Column increased from 12mm to 14mm and 16mm the load carrying capacity of composite column is increased from 4.14% to 4.77% respectively.

According to the results discussed above, the performance or the load capacity of the composite columns increased with increasing concrete strengths and decreased with increasing column lengths and increases as diameter of longitudinal reinforcement bars increases.

- The Compressive strength of concrete in fully encased composite columns which resulted in a noticeable as increased from C25 to C35, increase load capacity of the columns by 11.93%.
- The load capacity and stiffness of FEC columns were decreased with the increase in the length of columns. As the Length is increased from 600mm to 800mm and 1000mm the lateral load capacity of FEC columns were reduced by 3.50% to10.20% respectively.
- The axial capacity of the FEC column was affected by the less diameter of the longitudinal reinforcement bar. As the diameter of longitudinal reinforcement bar increased from 12mm to

14mm and 16mm the load carrying capacity of composite columns increased about 4.14% and 4.77% respectively.

5.2. Recommendations

The following recommendation is made from this study;

- It was concluded as the analysis results of this study verify that, in the construct of composite column it is better to select higher concrete strength, less height of column and with higher diameter of longitudinal reinforcement bars depending upon the function of the structures related to the load carrying capacity of Composite column.
- In the same area effects of longitudinal bars the higher diameters have the higher load carrying capacity in Composite column.
- The higher diameters of transverse reinforcement bar resist the confinement effects than the lower diameters of transverse reinforcement bars.

The following recommendations are made for future researches, which are not covered in the present study:-

- The effects of thickness of structural steel and Steel grade on the behavior of encased composite columns should be investigated in the future study.
- Experimental investigation of the Composite columns of the same title.
- The influence of different shapes of the encased steel sections on performance of composite columns.

REFERENCES

- 1992-1-1, E. (2015) ‘Compulsory Ethiopian Standard Design of Concrete Structures-Part 1-1 : General rules and rules for buildings’, *CES EN 1994-1-1*, PART 1-1.
- 1993-1-1, E. (2015) ‘Compulsory Ethiopian Standard Design of Steel Structures – Part 1-1 : General rules and rules for buildings’.
- Ã, C. D. *et al.* (2008) ‘Behaviour of reinforced and concrete-encased composite columns subjected to biaxial bending and axial load’, 43, pp. 1109–1120. doi: 10.1016/j.buildenv.2007.02.010.
- Allam, S. M. *et al.* (2013) ‘Evaluation of tension stiffening effect on the crack width calculation of flexural RC members’, *Alexandria Engineering Journal*, 52(2), pp. 163–173. doi: 10.1016/j.aej.2012.12.005.
- An, Y. and Roeder, C. (2014) ‘Flexural performance of filled steel tubes’, 66(5), pp. 249–267.
- Chang, X., Wei, Y. and Yun, Y. (2012) ‘Analysis of steel-reinforced concrete-filled steel tubular (SRCFST) columns under cyclic loading Symmetry plane’, *Construction and Building Materials*, 28(1), pp. 88–95. doi: 10.1016/j.conbuildmat.2011.08.033.
- EBCS EN 1994-1-1, C. (2013) ‘EBCS-EN 1994 : 2013 : Design of composite steel and concrete structures Part 1-1 : General rules and rules for buildings’, (August).
- Ellobody, E. and Young, B. (2010) ‘Thin-Walled Structures Investigation of concrete encased steel composite columns at elevated temperatures’, *Thin Walled Structures*, 48(8), pp. 597–608. doi: 10.1016/j.tws.2010.03.004.
- Ellobody, E., Young, B. and Lam, D. (2011) ‘Thin-Walled Structures Eccentrically loaded concrete encased steel composite columns’, *Thin Walled Structures*, 49(1), pp. 53–65. doi: 10.1016/j.tws.2010.08.006.
- EN 1994-1-1, C. (2015) ‘Compulsory Ethiopian Standard Design of Composite Steel and Concrete Structures - Part 1-1 : General rules and rules for buildings’.

Hafezolghorani, M. *et al.* (2017) ‘Simplified Damage Plasticity Model for Concrete’, (1). doi: 10.2749/101686616X1081.

Han, L. H. *et al.* (2009) ‘Performance of concrete filled steel tube reinforced concrete columns subjected to cyclic bending’, *Journal of Constructional Steel Research*, 65(8–9), pp. 1607–1616. doi: 10.1016/j.jcsr.2009.03.013.

Hanswille, P. D.-I. G. (2008) ‘Eurocode 4’.

Johnson, R. P. (2012a) *Composite Structures of Steel and Concrete*.

Johnson, R. P. (2012b) *COMPOSITE STRUCTURES OF STEEL AND CONCRETE SECOND EDITION*.

Kartheek, T. and Das, T. V. (2020) ‘3D modelling and analysis of encased steel-concrete composite column using Materials Today : Proceedings 3D modelling and analysis of encased steel-concrete composite column using ABAQUS’, *Materials Today: Proceedings*, (August). doi: 10.1016/j.matpr.2020.03.200.

Kim, C. *et al.* (2013) ‘Eccentric Axial Load Testing for Concrete-Encased Steel Columns Using 800 MPa Steel and 100 MPa Concrete’, 138(8), pp. 1019–1031. doi: 10.1061/(ASCE)ST.1943-541X.0000533.

Kim, C. *et al.* (2014) ‘Eccentric Axial Load Capacity of High-Strength Steel-Concrete Composite Columns of Various Sectional Shapes’, (2001). doi: 10.1061/(ASCE)ST.1943-541X.0000879.

Kim, D. K. (2005) ‘A database for composite columns’, (August).

Kmiecik, P. and Kamiński, M. (2011) ‘Modelling of reinforced concrete structures and composite structures with concrete strength degradation taken into consideration’, XI(3). doi: 10.1016/S1644-9665(12)60105-8.

Lai, B., Liew, J. Y. R. and Xiong, M. (2019) ‘Experimental study on high strength concrete encased steel composite short columns’, *Construction and Building Materials*, 228, p. 116640. doi: 10.1016/j.conbuildmat.2019.08.021.

Mander (1989) 'conducted providing the stress-strain relation for the concrete and steel are-known . The moments and curvatures associated with increasing flexural deformations of the column may be computed for various column axial loads by incrementing the curvature α ', 114(8), pp. 1804–1826.

Najafgholipour *et al.* (2017) 'Finite Element Analysis of Reinforced Concrete Beam-Column Connections with Governing Joint Shear Failure Mode', pp. 1200–1225.

Nguyen, D. H. and Hong, W. (2021) 'Part I : failure criteria of the steel-concrete columns (SRC columns) confined by cross-shaped flange sections', *Journal of Asian Architecture and Building Engineering*, 20(2), pp. 179–192. doi: 10.1080/13467581.2020.1782211.

Qian, W. *et al.* (2016) 'Analytical behavior of concrete-encased CFST columns under cyclic lateral loading', *JCSR*, 120, pp. 206–220. doi: 10.1016/j.jcsr.2015.12.018.

Rahman, M. S. (2016) 'Behaviour and Strength of Fully Encased Composite Columns', (December, 2016), pp. 1–198.

Rahman, S., Begum, M. and Ahsan, R. (2016) 'Comparison between Experimental and Numerical Studies of Fully Encased Composite Columns', 10(6), pp. 762–769.

Shih, T. *et al.* (2013) 'Axial strength and ductility of square composite columns with two interlocking spirals', *JCSR*, 90, pp. 184–192. doi: 10.1016/j.jcsr.2013.07.021.

Wahalathantri *et al* (2012) 'A MATERIAL MODEL FOR FLEXURAL CRACK SIMULATION IN REINFORCED CONCRETE ELEMENTS USING ABAQUS', pp. 260–264.

Yu, Q. *et al.* (2010) 'Analysis and calculations of steel tube confined concrete (STCC) stub columns', *Journal of Constructional Steel Research*, 66(1), pp. 53–64. doi: 10.1016/j.jcsr.2009.08.003.

APPENDICES

A. MATERIAL INPUT DATA SHEET FOR ANALYSIS OF CONTROL AS A SAMPLE.

I. Unconfined concrete input for CDP Model in Abaqus CAE.

Concrete compression,

Density	2.4E-09	
Elasticity & poison Ratio	E_c	ν
	32900	0.2

Plasticity parameters	Dilation angle	eccentricity	f_b/f_c		viscosity
	38	0.1	1.16	0.6667	0.0001

f_{cm} (Mpa)	58
E_{cm} (Gpa)	37.27786909
ϵ_{c1}	2.464681005
ϵ_{cu}	3.5
η	$\epsilon_c/\epsilon_{c1}=0.2600968$
k	1.663309632

Tabular Amplitude	
Time	Amplitude 0.3mm/ in
0	0
1	0.3
2	0.6
3	0.9
4	1.2
5	1.5
6	1.8
7	2.1
8	2.4
9	2.7
10	3

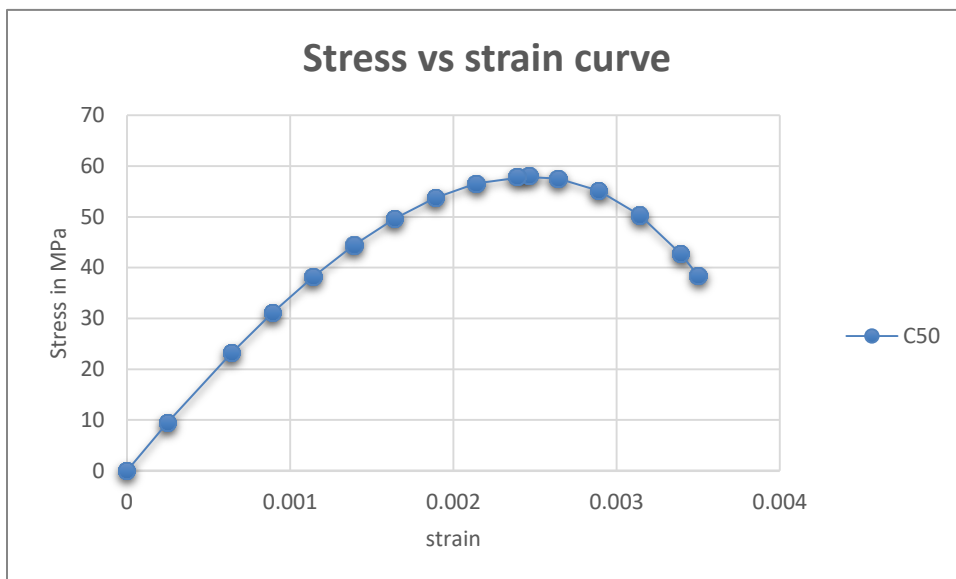


Figure A. 1: Unconfined concrete input stress-strain curve

Table A 1: Compressive behaviors

ϵ_c	η	σ_c	ϵ_{el}	ϵ_{in}	d_c	yield stress	inelastic strain
0	0	0	0	0	0	0	0
0.000641056	0.260097	23.2	0.000622	1.87E-05	0	23.2	1.87E-05
0.000891056	0.36153	31.07982	0.000834	5.73E-05	0	31.07982	5.73E-05
0.001141056	0.462963	38.18336	0.001024	0.000117	0	38.18336	0.000117
0.001391056	0.564396	44.4144	0.001191	0.0002	0	44.41244	0.0002
0.001641056	0.665829	49.65159	0.001332	0.000309	0	49.65159	0.000309
0.001891056	0.767262	53.76404	0.001442	0.000449	0	53.76404	0.000449
0.002141056	0.868695	56.58664	0.001518	0.000623	0	56.58664	0.000623
0.002464681	1	58	0.001556	0.000909	0.016828	58	0.000909
0.002391056	0.970128	57.92314	0.001554	0.000837	0.0153	57.92314	0.000837
0.002641056	1.071561	57.53534	0.001543	0.001098	0.021013	57.53534	0.001098
0.002891056	1.172994	55.13128	0.001479	0.001412	0.028444	55.13128	0.001412
0.003141056	1.274427	50.34912	0.001351	0.00179	0.038091	50.34912	0.00179
0.003391056	1.37586	42.73493	0.001146	0.002245	0.050593	42.73493	0.002245
0.0035	1.420062	38.38965	0.00103	0.00247	0.057135	38.38965	0.00247

yield stress	displacement	Damage parameter(d_t)	Crack strain
4.093341766	0	0	0
2.84965272	0.01	0.004183542	7.7376E-06
2.026639941	0.02	0.278291196	0.000539867
1.50091438	0.03	0.650594638	0.001561129
1.169862962	0.04	0.892133046	0.00307471

Table A 2: Tensile behaviors

f_{c_k} (Mpa)	50
f_{ctm} (Mpa)	4.093341766
G_F (N/m)	151.614207
w_c (mm)	0.190381617
$0.2f_{ctm}$	0.814325285

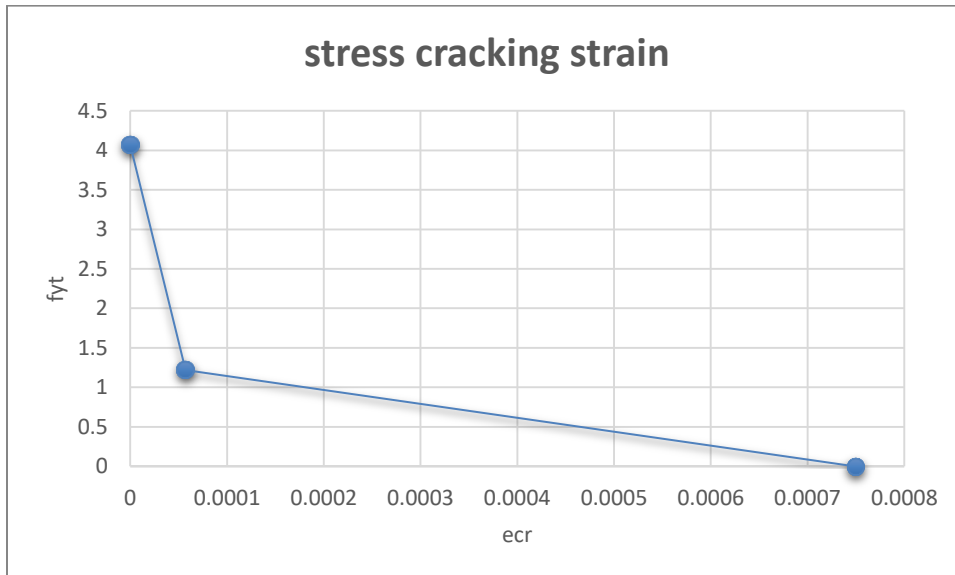


Figure A. 2: Stress-crack opening relation for uniaxial tension.

ii. Confined concrete CDP model

Plasticity parameters	Dilation angle	eccentricity	f_b/f_c	k	viscosity
	38	0.1	1.16	0.6667	0

Table A 3: ABAQUS Compression input

σ_c (MPa)	ϵ_{in}	d_c
0	0	0
23.2	1.87E-05	0
31.07982	5.73E-05	0
38.18336	0.000117	0
44.41244	0.0002	0
49.65159	0.000309	0
53.76404	0.000449	0
56.58664	0.000623	0
58	0.000909	0.016828
57.92314	0.000837	0.0153
57.53534	0.001098	0.021013
55.13128	0.001412	0.028444
50.34912	0.00179	0.038091
42.73493	0.002245	0.050593
38.38965	0.00247	0.057135

Table A 4: ABAQUS Tension input

σ_t (MPa)	d_t	ϵ_{tin}
4.093341766	0	0
2.84965272	0.004183542	0.000113485
2.026639941	0.278291196	0.000613485
1.50091438	0.650594638	0.001613485
1.169862962	0.892133046	0.003113485

Table A 5: Input values for plastic behavior of longitudinal/transverse reinforcement and structural steel

Longitudinal reinforcement bar			diameter=13mm	
Density	7.85E-09		f_{ys}	550Mpa
Elastic property	E_s	ν	ϵ_{ys}	0.0023
	228200	0.3	f_{us}	725Mpa

f_y	e_t	σ_{true}	ϵ_{pl}
0	0	0	0
550	0.0023	551.265	0
555	0.00625	558.469	0.00378
560	0.0125	567	0.00994
570	0.022	582.54	0.01 21
595	0.025	609.875	0.02202
660	0.05	693	0.04575
705	0.075	757.875	0.069
720	0.1	792	0.09184
725	0.1125	806.563	0.10308
720	0.125	810	0.11423
700	0.15	805	0.13623
650	0.175	763.75	0.15792
635	0.18125	750.094	0.16329

Transverse reinforcement bar			diameter=10mm	
Density	7.85E-09		f_{ys}	510Mpa
Elastic property	E_s	ν	ϵ_{ys}	0.0024
	197700	0.3	f_{us}	667Mpa

f_y	e_t	σ_{true}	ϵ_{pl}
0	0	0	0
510	0.0024	511.224	0
520	0.00625	523.25	0.00358
530	0.0125	536.625	0.00971
550	0.025	563.75	0.02184
620	0.05	651	0.0455
650	0.075	698.75	0.06879

667	0.0875	7 5.3 3	0.08021
660	0.1	726	0.09164
635	0.125	714.375	0.11417
570	0.15	655.5	0.13645
470	0.1625	546.375	0.14781

Steel flange($t_f=9.4\text{mm}$) and		plate, $t_{plate}=20\text{mm}$	
Density	7.85E-09		f_{ys} 375Mpa
Elastic property	E_s	ν	ϵ_{ys} 0.0017
	226600	0.3	F_{us} 5 0Mpa

f_y	e_t	σ_{true}	ϵ_{pl}
0	0	0	0
375	0.0017	375.638	0
360	0.00625	362.25	0.00463
365	0.01875	371.844	0.01694
410	0.025	420.25	0.02284
480	0.05	504	0.04657
520	0.075	559	0.06985
540	0.1	594	0.09269
560	0.125	630	0. 15
575	0.15	661.25	0.13684
580	0.175	681.5	0.15826
535	0.2	642	0.17949
485	0.205	584.425	0.1839

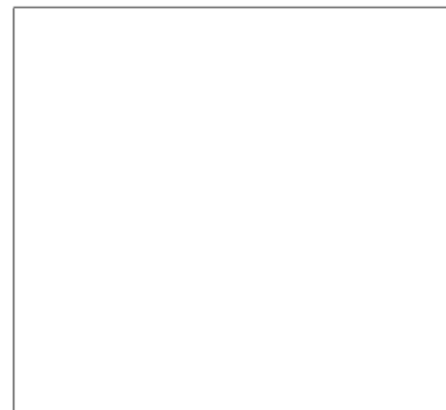
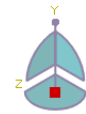
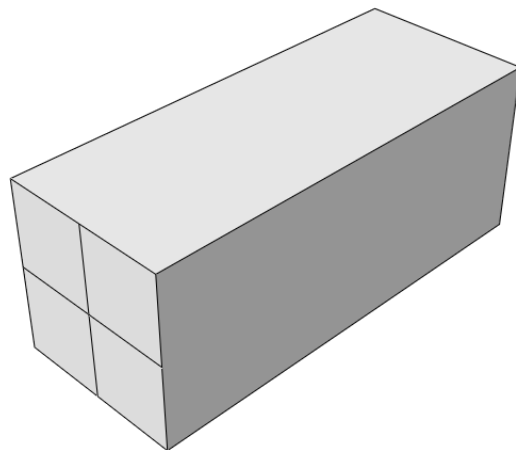
Web		$t_w=6.5\text{mm}$	
Density	7.85E-09		F_{ys} 404Mpa
Elastic property	E_s	ν	ϵ_{ys} 0.0018
	223900	0.3	F_{us} 611Mpa

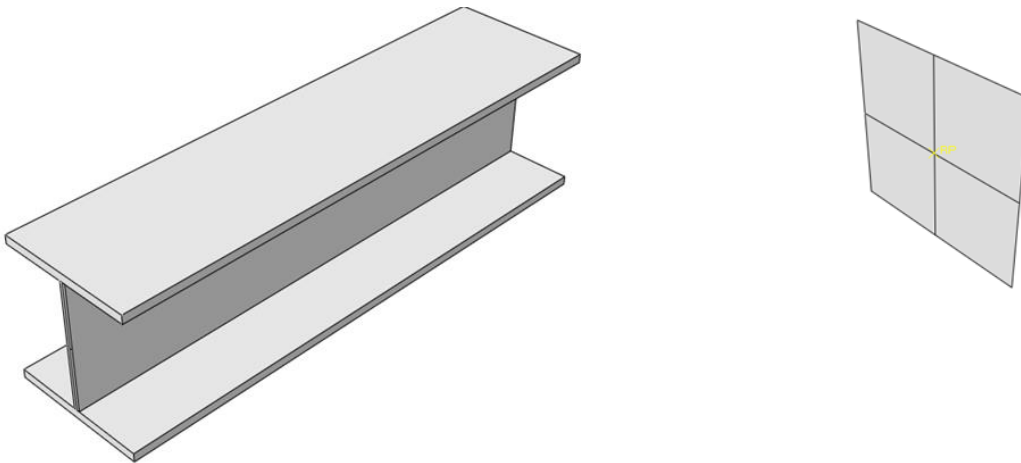
f_y	e_t	σ_{true}	ϵ_{pl}
0	0	0	0
404	0.0018	404.727	0
395	0.00625	397.469	0.00446
400	0.0125	405	0.01061

445	0.025	456.125	0.02266
520	0.05	546	0.04635
560	0.075	602	0.06963
580	0.1	638	0.09246
605	0.1 5	680.625	0.11474
611	0.1375	695.013	0.12573
600.5	0.15	690.575	0.13668
575	0.175	675.625	0.15825
515	0.19375	614.781	0.17435

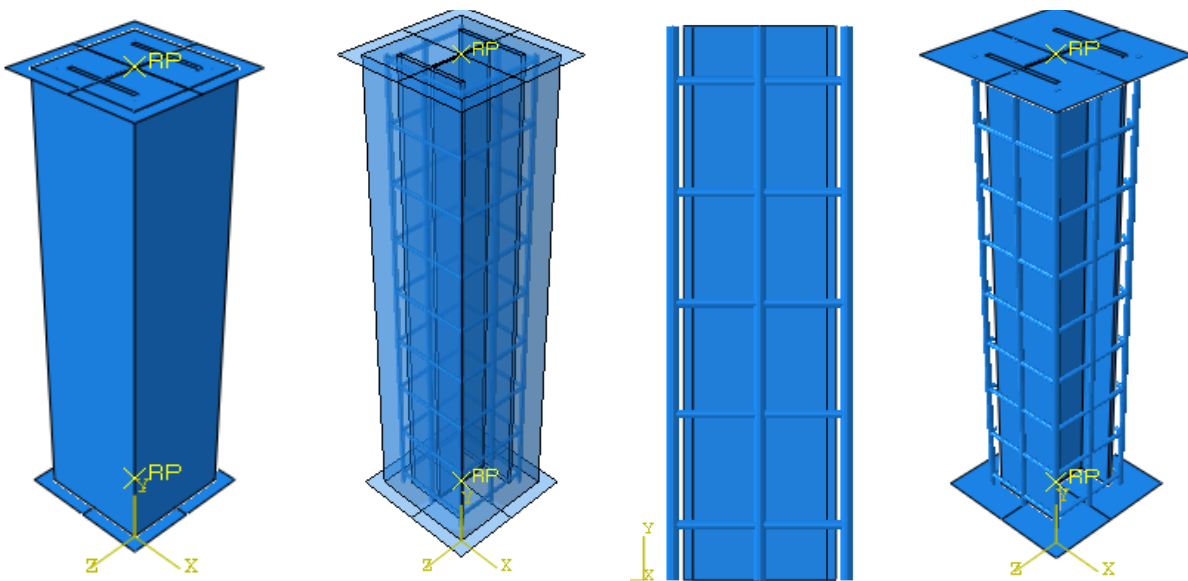
B. MODEL OF COLUMN UNDER STUDY

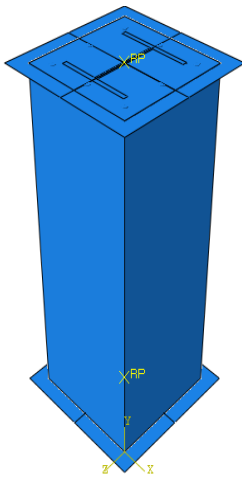
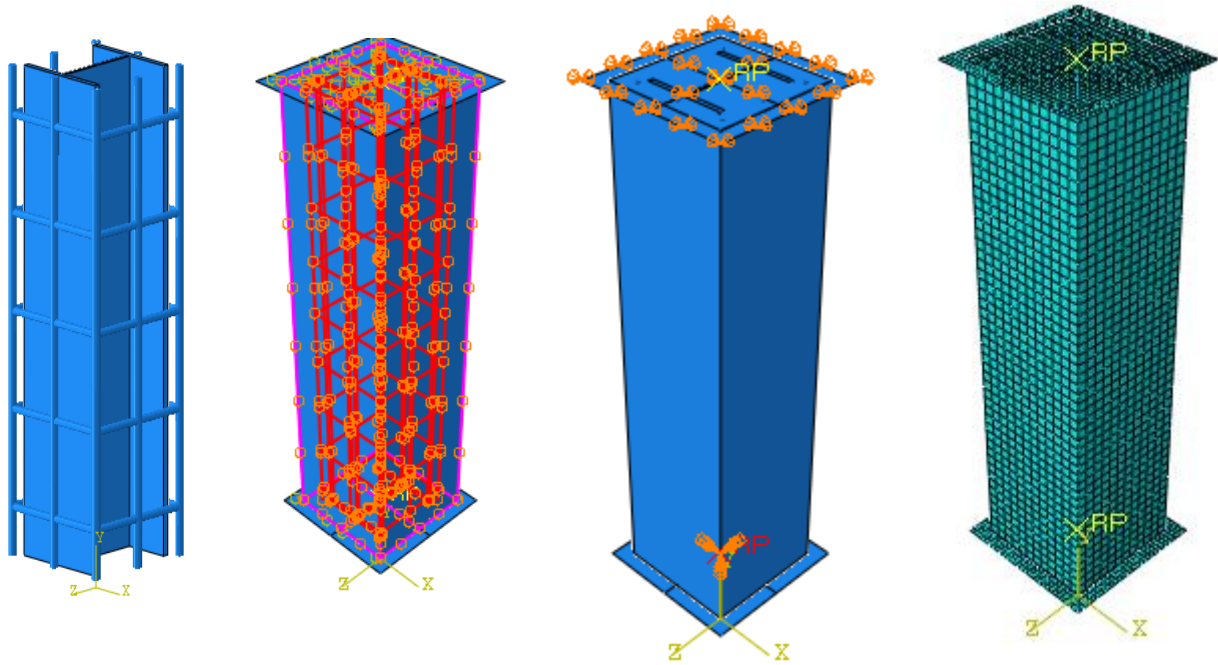
#. Parts



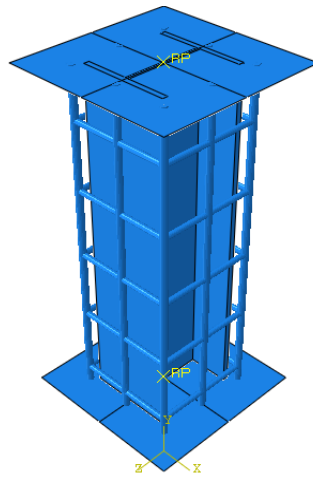


#.Different forms of composite column components

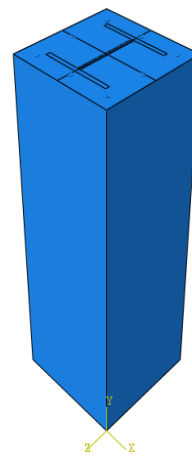




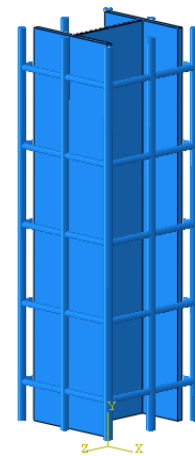
A.Assembled Model (All parts)



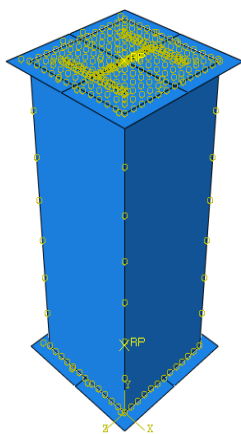
B.Steel, Reinforcements and plates model



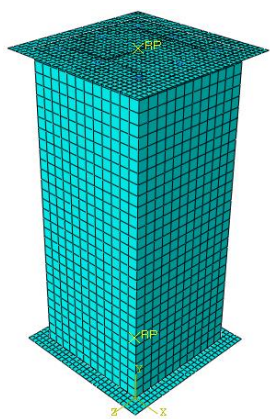
C.Concrete column with steel section



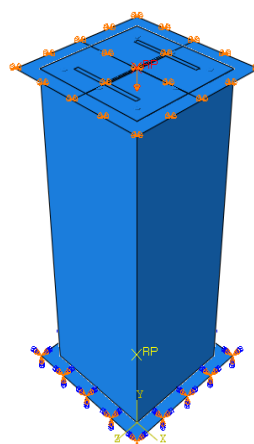
D.Steel and reinforcements



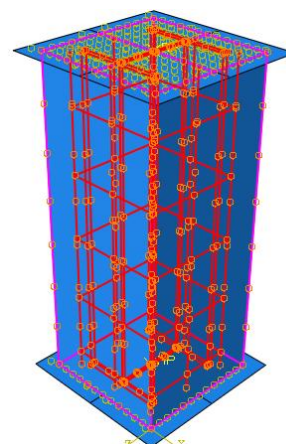
E.Interaction



F.Meshing



G.Load module

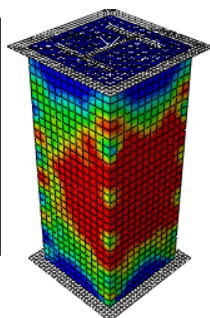
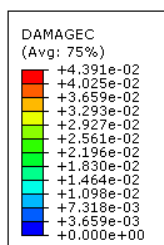


H.Embedment

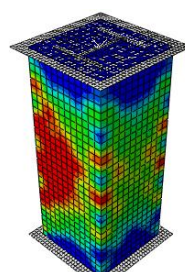
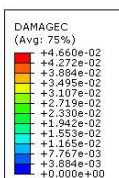
C. OUT PUT OF ANALYSIS

a) Concrete Strength

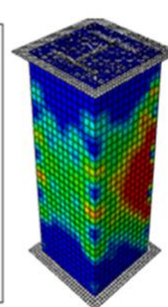
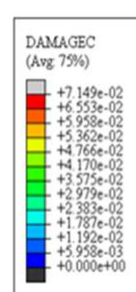
C25



C30

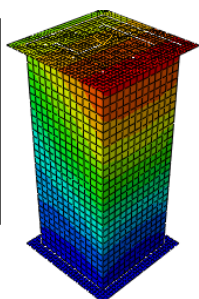
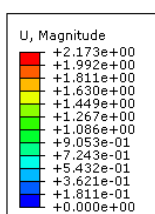


C35

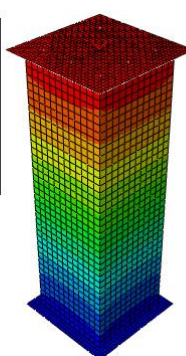
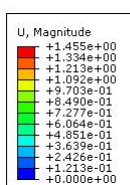


b) Length of column

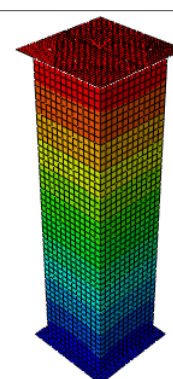
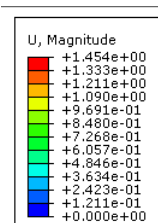
600mm



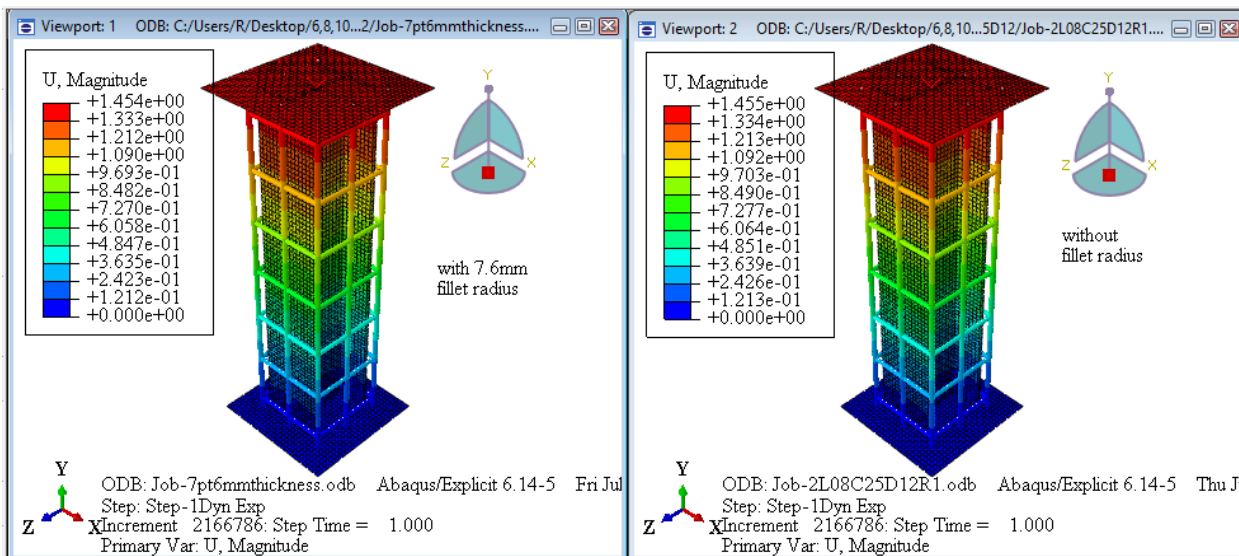
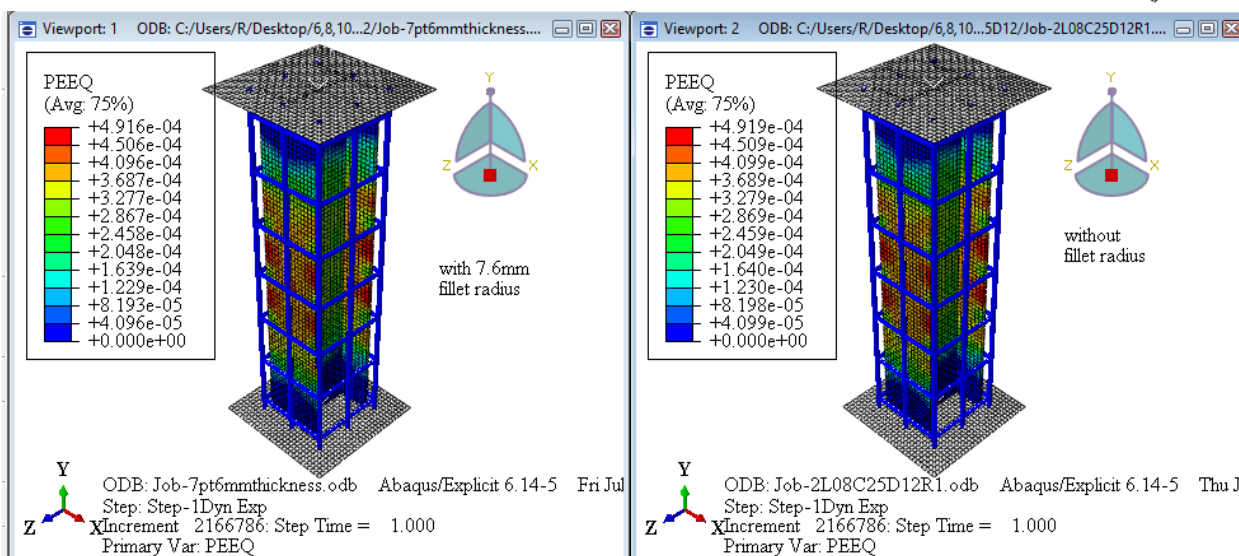
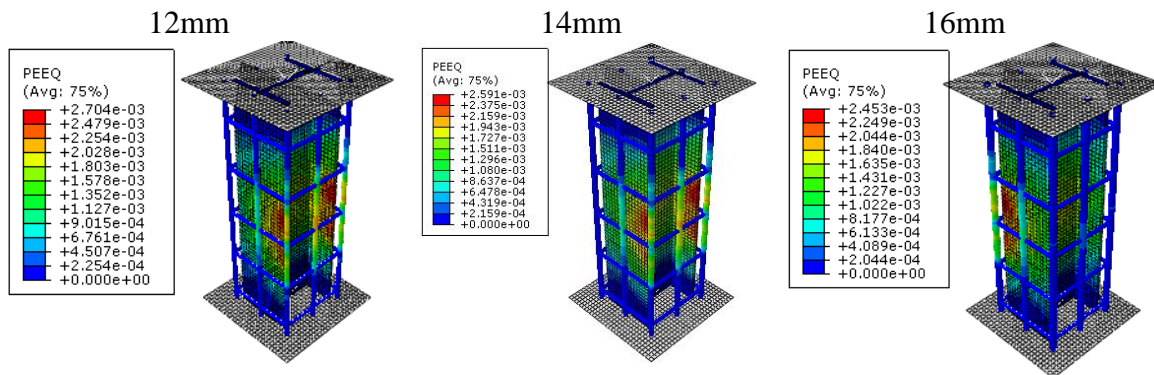
800mm



1000mm



c) Diameter of Longitudinal Bar



D. ANALYSIS OUT PUT FROM ABAQUS PROGRAM (SAMPLE)

Abaqus 6.14-5 Date 28-Jun-2021 Time 08:11:44
For use by Supplied by Team-SolidSQUAD under license from Dassault Systemes or its subsidiary.

The Abaqus Software is a product of:
Dassault Systemes SIMULIA Corp.
1301 Atwood Avenue, Suite 101W
Johnston, RI 02919, USA

The Abaqus Software is available only under license from Dassault Systemes or its subsidiary and may be used or reproduced only in accordance with the terms of such license.

On machine DESKTOP-8G8GHCL
you are authorized to run
Abaqus/Explicit until 31-Dec-2055

Your site id is:

For assistance or any other information you may obtain contact information for your local office from the world wide web at:

<http://www.3ds.com/products/simulia/locations/>

```
* * * * *
*
*          *****
*      * N O T I C E *
*          *****
*
*          Abaqus 6.14-5
*
*      BUILD ID: 2015_08_18-17.37.49 135153
*
*      Please make sure you are using release 6.14 manuals
*      plus the notes accompanying this release.
*
* * * * *
```

```
*Node
*Element, type=T3D2
*Nset, nset=ASSEMBLY_PART-2REBAR-1-LIN-1-2_SET-1
*Nset, nset=ASSEMBLY_PART-2REBAR-1-LIN-1-2__PICKEDSET11
*Elset, elset=ASSEMBLY_PART-2REBAR-1-LIN-1-2_SET-1
*Elset, elset=ASSEMBLY_PART-2REBAR-1-LIN-1-2__PICKEDSET11
*Node
*Element, type=T3D2
*Nset, nset=ASSEMBLY_PART-2REBAR-1-LIN-1-3_SET-1
*Nset, nset=ASSEMBLY_PART-2REBAR-1-LIN-1-3__PICKEDSET11
*Elset, elset=ASSEMBLY_PART-2REBAR-1-LIN-1-3_SET-1
*Elset, elset=ASSEMBLY_PART-2REBAR-1-LIN-1-3__PICKEDSET11
*Node
*Element, type=T3D2
*Nset, nset=ASSEMBLY_PART-2REBAR-1-LIN-2-1_SET-1
*Nset, nset=ASSEMBLY_PART-2REBAR-1-LIN-2-1__PICKEDSET11
*Elset, elset=ASSEMBLY_PART-2REBAR-1-LIN-2-1_SET-1
*Elset, elset=ASSEMBLY_PART-2REBAR-1-LIN-2-1__PICKEDSET11
*Node
*Element, type=T3D2
*Nset, nset=ASSEMBLY_PART-2REBAR-1-LIN-2-3_SET-1
*Nset, nset=ASSEMBLY_PART-2REBAR-1-LIN-2-3__PICKEDSET11
*Elset, elset=ASSEMBLY_PART-2REBAR-1-LIN-2-3_SET-1
*Elset, elset=ASSEMBLY_PART-2REBAR-1-LIN-2-3__PICKEDSET11
*Node
*Element, type=T3D2
*Nset, nset=ASSEMBLY_PART-2REBAR-1-LIN-3-1_SET-1
*Nset, nset=ASSEMBLY_PART-2REBAR-1-LIN-3-1__PICKEDSET11
*Elset, elset=ASSEMBLY_PART-2REBAR-1-LIN-3-1_SET-1
*Elset, elset=ASSEMBLY_PART-2REBAR-1-LIN-3-1__PICKEDSET11
*Node
*Element, type=T3D2
*Nset, nset=ASSEMBLY_PART-2REBAR-1-LIN-3-2_SET-1
*Nset, nset=ASSEMBLY_PART-2REBAR-1-LIN-3-2__PICKEDSET11
*Elset, elset=ASSEMBLY_PART-2REBAR-1-LIN-3-2_SET-1
*Elset, elset=ASSEMBLY_PART-2REBAR-1-LIN-3-2__PICKEDSET11
**
```

P R O B L E M S I Z E

```
NUMBER OF ELEMENTS IS                10560
NUMBER OF NODES IS                    14538
NUMBER OF NODES DEFINED BY THE USER   14538
TOTAL NUMBER OF VARIABLES IN THE MODEL 49386
(DEGREES OF FREEDOM PLUS MAX NO. OF ANY LAGRANGE MULTIPLIER
  VARIABLES. INCLUDE *PRINT,SOLVE=YES TO GET THE ACTUAL NUMBER.)
```

E N D O F U S E R I N P U T P R O C E S S I N G

```
JOB TIME SUMMARY
  USER TIME (SEC)      =    2.5000
  SYSTEM TIME (SEC)    =    0.30000
  TOTAL CPU TIME (SEC) =    2.8000
  WALLCLOCK TIME (SEC) =          4
```

INCREMENT	STEP TIME	TOTAL TIME	CPU TIME	STABLE INCREMENT	CRITICAL ELEMENT	KINETIC ENERGY	TOTAL ENERGY
1933948	8.890E-01	8.890E-01	09:05:37	4.486E-07	1003	6.362E-01	-4.448E+02
INSTANCE WITH CRITICAL ELEMENT: PART-5STEEL-1							
1941444	8.925E-01	8.925E-01	09:07:37	4.486E-07	1003	8.174E-01	-4.500E+02
INSTANCE WITH CRITICAL ELEMENT: PART-5STEEL-1							
1949174	8.962E-01	8.962E-01	09:09:37	4.486E-07	1003	1.032E+00	-4.558E+02
INSTANCE WITH CRITICAL ELEMENT: PART-5STEEL-1							
1956679	8.998E-01	8.998E-01	09:11:37	4.486E-07	1003	2.219E+00	-4.617E+02
INSTANCE WITH CRITICAL ELEMENT: PART-5STEEL-1							
1957069	9.000E-01	9.000E-01	09:11:44	4.486E-07	1003	2.253E+00	-4.620E+02
INSTANCE WITH CRITICAL ELEMENT: PART-5STEEL-1							
ODB Field Frame Number 18 of 20 requested intervals at						9.000000E-01	
1964900	9.037E-01	9.037E-01	09:13:44	4.486E-07	1003	1.182E+00	-4.680E+02
INSTANCE WITH CRITICAL ELEMENT: PART-5STEEL-1							
1972611	9.074E-01	9.074E-01	09:15:44	4.486E-07	1003	1.236E+00	-4.744E+02
INSTANCE WITH CRITICAL ELEMENT: PART-5STEEL-1							
1980245	9.111E-01	9.111E-01	09:17:44	4.486E-07	1003	1.822E+00	-4.809E+02
INSTANCE WITH CRITICAL ELEMENT: PART-5STEEL-1							
1987852	9.147E-01	9.147E-01	09:19:44	4.486E-07	1003	1.288E+00	-4.878E+02
INSTANCE WITH CRITICAL ELEMENT: PART-5STEEL-1							
1995388	9.183E-01	9.183E-01	09:21:44	4.486E-07	1003	1.248E+00	-4.945E+02
INSTANCE WITH CRITICAL ELEMENT: PART-5STEEL-1							
2002967	9.219E-01	9.219E-01	09:23:44	4.486E-07	1003	1.119E+00	-5.017E+02
INSTANCE WITH CRITICAL ELEMENT: PART-5STEEL-1							
2010580	9.255E-01	9.255E-01	09:25:44	4.486E-07	1003	1.197E+00	-5.088E+02
INSTANCE WITH CRITICAL ELEMENT: PART-5STEEL-1							
2017879	9.290E-01	9.290E-01	09:27:44	4.486E-07	1003	1.301E+00	-5.159E+02
INSTANCE WITH CRITICAL ELEMENT: PART-5STEEL-1							
2025512	9.326E-01	9.326E-01	09:29:44	4.486E-07	1003	1.454E+00	-5.232E+02
INSTANCE WITH CRITICAL ELEMENT: PART-5STEEL-1							
2033162	9.363E-01	9.363E-01	09:31:44	4.486E-07	1003	1.181E+00	-5.305E+02
INSTANCE WITH CRITICAL ELEMENT: PART-5STEEL-1							
2040490	9.398E-01	9.398E-01	09:33:44	4.486E-07	1003	1.122E+00	-5.379E+02
INSTANCE WITH CRITICAL ELEMENT: PART-5STEEL-1							
2047705	9.432E-01	9.432E-01	09:35:44	4.486E-07	1003	1.062E+00	-5.453E+02
INSTANCE WITH CRITICAL ELEMENT: PART-5STEEL-1							
2054877	9.466E-01	9.466E-01	09:37:44	4.486E-07	1003	5.031E-01	-5.524E+02
INSTANCE WITH CRITICAL ELEMENT: PART-5STEEL-1							

```

2061927  9.500E-01 9.500E-01 09:39:42 4.486E-07      1003  7.116E-01 -5.596E+02
INSTANCE WITH CRITICAL ELEMENT: PART-5STEEL-1
ODB Field Frame Number 19 of 20 requested intervals at 9.500002E-01
2068851  9.533E-01 9.533E-01 09:41:42 4.486E-07      1003  6.372E-01 -5.666E+02
INSTANCE WITH CRITICAL ELEMENT: PART-5STEEL-1
2075864  9.566E-01 9.566E-01 09:43:42 4.486E-07      1003  5.856E-01 -5.734E+02
INSTANCE WITH CRITICAL ELEMENT: PART-5STEEL-1
2082846  9.600E-01 9.600E-01 09:45:42 4.486E-07      1003  6.116E-01 -5.803E+02
INSTANCE WITH CRITICAL ELEMENT: PART-5STEEL-1
2089545  9.632E-01 9.632E-01 09:47:42 4.486E-07      1003  5.394E-01 -5.871E+02
INSTANCE WITH CRITICAL ELEMENT: PART-5STEEL-1
2096712  9.666E-01 9.666E-01 09:49:42 4.486E-07      1003  5.467E-01 -5.944E+02
INSTANCE WITH CRITICAL ELEMENT: PART-5STEEL-1
2103797  9.700E-01 9.700E-01 09:51:42 4.486E-07      1003  4.986E-01 -6.017E+02
INSTANCE WITH CRITICAL ELEMENT: PART-5STEEL-1
2110617  9.732E-01 9.732E-01 09:53:42 4.486E-07      1003  5.143E-01 -6.084E+02
INSTANCE WITH CRITICAL ELEMENT: PART-5STEEL-1
2117414  9.765E-01 9.765E-01 09:55:42 4.486E-07      1003  4.735E-01 -6.157E+02
INSTANCE WITH CRITICAL ELEMENT: PART-5STEEL-1
2124194  9.797E-01 9.797E-01 09:57:42 4.486E-07      1003  4.342E-01 -6.229E+02
INSTANCE WITH CRITICAL ELEMENT: PART-5STEEL-1
2131043  9.830E-01 9.830E-01 09:59:42 4.486E-07      1003  4.886E-01 -6.300E+02
INSTANCE WITH CRITICAL ELEMENT: PART-5STEEL-1
2138035  9.863E-01 9.863E-01 10:01:42 4.486E-07      1003  4.515E-01 -6.375E+02
INSTANCE WITH CRITICAL ELEMENT: PART-5STEEL-1
2145035  9.896E-01 9.896E-01 10:03:42 4.486E-07      1003  4.137E-01 -6.450E+02
INSTANCE WITH CRITICAL ELEMENT: PART-5STEEL-1
2152024  9.930E-01 9.930E-01 10:05:42 4.486E-07      1003  4.469E-01 -6.525E+02
INSTANCE WITH CRITICAL ELEMENT: PART-5STEEL-1
2159001  9.963E-01 9.963E-01 10:07:42 4.486E-07      1003  4.318E-01 -6.602E+02
INSTANCE WITH CRITICAL ELEMENT: PART-5STEEL-1
2165799  9.995E-01 9.995E-01 10:09:42 4.486E-07      1003  4.370E-01 -6.677E+02
INSTANCE WITH CRITICAL ELEMENT: PART-5STEEL-1
2166786  1.000E+00 1.000E+00 10:10:02 4.486E-07      1003  4.296E-01 -6.687E+02
INSTANCE WITH CRITICAL ELEMENT: PART-5STEEL-1
Restart Number 1 at 1.0000
ODB Field Frame Number 20 of 20 requested intervals at 1.000000E+00
THE ANALYSIS HAS COMPLETED SUCCESSFULLY

```